CZECH TECHNICAL UNIVERSITY IN PRAGUE
FACULTY OF BIOMEDICAL ENGINEERING
Department of Biomedical Technology

Master Thesis

2016 Dipl.-Ing. Lars I. Stumpp

ČESKÉ VYSOKÉ UČENÍ TECHNICKÉ V PRAZE

FAKULTA BIOMEDICÍNSKÉHO INŽENÝRSTVÍ

Katedra biomedicínské techniky

Manipulation of the rodent spatial representation via brain-computer interface

Master thesis

Study programme:	Biomedical and Clinical Technology
Field of study:	Biomedical Engineering

Author of master thesis:	Dipl. Ing. Lars I. Stumpp
Supervisor of master thesis:	MD. Ph.D. Marian Tsanov

Kladno 2016

Czech Technical University in Prague, Faculty of Biomedical Engineering

Department of Biomedical Technology

Academic year: 2015/2016

Diploma thesis assignment
(Master project thesis assignment)

Student:	Lars Stumpp
Study branch:	Biomedical Engineering (CEMACUBE)
Title:	Manipulation of the rodent spatial representation via brain-computer interface
Title in Czech:	Manipulace prostorové reprezentace hlodavců pomocí brain-computer interface (BCI)

Instructions for processing:

Create Matlab script to process neural and behavioural data generated in the open field recording experiment, including methods to confirm stability of measurement, methods to characterize the place field properties. Create method to evaluate symmetry of place fields and predict the preferred location in relation to a symmetry axis. Create method to calculate the spatial population vector which describes the behaviour and preferred firing location of place cells on a population level. Create Matlab script to process neural and behavioural data generated at the rectangular-shaped linear track experiment, including methods to confirm stability of measurement, methods to characterize the behaviour of the rat in the arena and methods to characterize the firing behaviour of the place cells on a population level. Create Matlab scripts to process neural and behavioural data generated in the continuous T-maze experiment, including methods to confirm stability of measurement, methods to characterize the behaviour of the rat in the arena, methods to characterize place field symmetry and methods to characterize the firing behaviour of the place cells on a population level. Evaluate and interpret results of the three experiments regarding the influence of dopaminergic projections on place cell firing behaviour and episodic-like memory characteristics of place cells.

References:

[1] De Lavilléon, G., Lacroix, M., Rondi-Reig, L., Benchenane, K., Explicit memory creation during sleep demonstrates a causal role of place cells in navigation, Nature neuroscience, ročník 18, číslo 4, 2015, 493–495 s.
[2] Georgopoulos, A.P., Schwartz, A.B., Kettner, R.E., Neuronal population coding of movement direction, Science, ročník 223, číslo 4771, 1986, 1416–1419 s.
[3] Wood, E.R., Place cells: a framework for episodic memory?, The Neurobiology of Spatial Behaviour, Jeffery, K.J., ed. ISBN-13: 9780198515241, 2003, Oxford

Validity of assignment until date: 20.08.2017

Supervisor of diploma thesis: Marian Tsanov, M.D., Ph.D.

.....
Head of Department

.....
Dean

In Kladno, 22.06.2016

DECLARATION

I hereby declare that I have completed this thesis with the topic "**Manipulation of the rodent spatial representation via brain-computer interface**" independently, and that I have attached an exhaustive list of citations of the employed sources to the Master thesis.

I do not have a compelling reason against the use of the thesis within the meaning of Section 60 of the Act No.121 / 2000 Coll., on copyright, rights related to copyright and amending some laws (Copyright Act).

In Kladno 15.09.2016 …..……..……...

Dipl. Ing. Lars I. Stumpp

ACKNOWLEDGEMENTS

Firstly, I would like to offer my thanks my supervisor Dr. Marian Tsanov of the Trinity College Institute of Neuroscience for his support during this work. The door to Dr. Tsanov's office was always open whenever I had questions. I also to thank Dr. Tsanov for giving me the opportunity to co-author an article in which results of my work will be published in an international journal.

I would also like to thank all the members of the Tsanov lab at the Trinity College Institute of Neuroscience for conducting all the experiments and providing the data which were used in this work

Finally, I must express my very profound gratitude to my parents and my aunt for providing me with unfailing support and continuous encouragement throughout my years of study and through the process of researching and writing this thesis. This accomplishment would not have been possible without them. Thank you.

Master's Thesis title:

Manipulation of the rodent spatial representation via brain-computer interface

Abstract:

The neuromodulation of dopaminergic neurons on the hippocampal activity is an important mechanism for the encoding of spatial information at Hippocampal place cells. For so-called misplace cells the location is a necessary but not sufficient condition for maximal firing, which is modulated by non-spatial stimuli. The fact that motivational or contextual factors influence the firing behaviour or even trigger complex remapping lead to the assumption that hippocampal place cells encode more than just spatial information. Motivational factor like reward and aversion are expressed by the mesolimbic system which is controlled by the ventral tegmental area (VTA) via its dopaminergic projections., which have modulatory effects on hippocampal functions like spatial learning and novelty detection. In this work, we used population analysis and a novel spatial symmetry method to examine the neuromodulation of hippocampal place cells, caused by dopaminergic projections of the VTA which were either artificially suppressed or excited by optogenetic stimulation or naturally modulated by trained preferences. As a result, we showed that dopamine-mediated synaptic plasticity is the underlying mechanism for spatial learning and memory, and demonstrated that hippocampal place cells encode the valence of location on a population level and thus show their episodic-memory-like characteristics.

Key words:

hippocampus, place cells, place preference, optogenetics, VTA

Table of Contents

.

List of symbols and abbreviations

µLED	micro LED
AP	anteroposterior
BSR	brain stimulation reward
CA1	Cornu ammonis 1 area of the hippocampus
ChR	channelrhodopsin
ChR2	channelrhodopsin2
CS	conditioned stimulus
DV	dorsal ventral
IR	infra-red
LED	light-emitting diodes
LTP	long term potentiation
MFB	medial forebrain bundle
ML	medial lateral
NAc	Nucleus accumbens
O	origin
TBS	theta-burst stimulation
TH	tyrosine Hydroxylase
TTL	transistor-transistor-logic
VTA	ventral tegmental area
YFP	yellow fluorescent protein

1 Introduction

Place cells are complex firing pyramidal neurons that can be found in all areas of the hippocampus (5). They were found to have firing characteristics that are heavily related to the animal's spatial location (6). This finding and the fact that spatial learning impairments can be consistently induced by hippocampal lesions led to the conclusion that the hippocampus with its place cells is the main centre for spatial memory (6). In a steady environment, its firing patterns are stable. Bostock et al. (7) showed that a manipulation of the environment can alter the spatial firing patterns of hippocampal place cells. Further research revealed that remapping of hippocampal place cell's spatial firing fields (place fields), which describes the shift of the place field location, the appearance of new place fields or the disappearance of existing place fields can be triggered in various ways. The most obvious trigger is the manipulation of environmental cues (7; 8; 9) and the shape of the environment (10; 11). But even with constant environmental cues and shapes, place fields can be influenced by motivational factors (12). The change of the reward location (13) (14), as well as the modification of a goal location (15; 16; 17) can trigger a dramatic place field reorganisation. It has also been shown that discrete learning events like contextual fear conditioning (18) can lead to place field remapping. The fact that motivational factors or learning events can alter the firing pattern of place cells give reasons to believe that place cells do not just store spatial information but also episodic-like memory providing us with information about the what, when and where of events (19). It was shown that place cell activity can reflect when/where (20; 21) and what/where (22) aspects. It still has to be figured out whether this is due to task dependent firing behaviour or actual memory. One of the primary hippocampal inputs that can regulate the goal-directed behaviour is the ventral tegmental area (VTA). The dopaminergic projection from the VTA has modulatory effects on hippocampal functions like spatial learning and novelty detection (23; 24). In this work, we show the effectiveness of direct optogenetic excitation and suppression of the VTA compared to conventional electrical stimulation of the medial forebrain bundle (MFB).

Using this method, we have examined the effect of artificially induced preferences and aversion on the formation of place fields. Also, we studied the population dynamics of hippocampal place cells to test the hypothesis that place cells encode spatial representation as well as goal-directed navigation for the preferred location.

2 Overview of the current state

2.1 Place cells

Place cells were first reported by O'Keefe and Dostrovsky (25) as complex spiking pyramidal neurons in the hippocampus which firing characteristics are related to a rodent's spatial location. Those cells can be found in the CA1 and CA3 regions of the Hippocampus (6). Place fields are specific areas where the place cell fires at high frequency. Stable place fields can be established within minutes (26). Once established the place field can remain stable for several weeks in a stable environment (27; 28). The spatial firing pattern of an ensemble of place cells cover the environment in an overlapping way and thus can be seen as a cognitive map of the environment. It has to be mentioned that the location of a place cell in the hippocampus is not related to the location of its firing field in an arena. This means that place cells that have overlapping firing fields are not necessarily neighbours in the hippocampus (6). However, for each environment just a small portion exhibit place fields, the majority is silent (29). It has been found that each place field can be modelled as the summation of two or more Gaussians (6; 30; 31). O'Keefe (32) reported a phase correlation between the spiking of hippocampal place cells and theta frequency band (7-12Hz). This correlation can be used to control the quality of single unit identification.

2.2 Place field remapping

It was found early that the spatial firing pattern of place cells can be modified by manipulating the environment (33; 34). This modification of firing pattern is commonly known as remapping and describes the disappearance of existing place fields, the appearance of new playfields, change of the place field location or change of the firing frequency of the place cells (35). Furthermore, different kinds of remapping can be distinguished. Rotational remapping, where the relations between the place fields stay the same but the orientation of the whole ensemble changes (7; 36) and complex remapping. Here the firing pattern change in an unpredictable way (7). Remapping can be triggered by different methods:

2.2.1 Change of environmental cues and shapes

Various studies examined the effect of manipulation of cues and arena shape. Bostock et al. (7), as well as Muller & Kubie (35) used a pellet chasing task to make the rodent sample a cylindrical arena randomly after a baseline recording session. Different changes to the environment were applied, which include rotation of a cue card along the arena wall (35; 7), cue card colour (7), change of the cue card size, arena size and arena shape (35). According to the different modifications, different types of remapping could be observed. Rotational remapping for the rotation of the cue card, where place fields rotate in an equal manner, or the removal of the cue card, which caused unpredictable rotation of the place fields. Change of the cue card colour, arena shape, and arena size resulted in complex remapping. While at the latter, a subpopulation of place cells remapped in a different way: 36% scaled, 52% remapped unpredictably. This lead to the conclusion that the behaviour of different subpopulations is driven by various features of a given stimulus. This finding was confirmed later when double rotation of proximal and distal cues in a plus maze was used to show that hippocampal place cells independently code specific subsets of cues in an environment (9).

2.2.2 Goal location

Hollup et al. (15) showed that place field remapping could be achieved even without visible manipulation of the environment. At their work, a water maze experiment was used, where a rat has to find a hidden platform in a circular water channel to examine the effect of the goal position on the firing pattern of place cells. He discovered an accumulation of place fields around the hidden platform. Later other goal related studies (17; 16) failed to reproduce such an abundance of place fields around goal areas and referred Hollup's result to other not goal-related factors. However, Hok et al. (37; 38) found in a place preference task (39) that place fields had a distinct secondary place field at the goal location (37). Since that cells just fire near the goal location when the hungry rat was waiting to receive a food reward and not at common passes the function of those signals are dubious. There is a hypothesis that it acts as an on-line feedback for identification of a goal location (37).

2.2.3 Fear conditioning

Another way to trigger place field remapping was found by Moita et al. (18). They managed to manipulate the spatial firing pattern by fear conditioning. In this work, they used a pellet chasing task in two different square arenas (training, control) to record baseline place fields. After baseline recording fear conditioning in the training arena was applied in a paired (electrical shocks to the eyelid were applied 300ms after the presentation of a tone) and an unpaired (no shock within 30seconds before or after the presentation of a tone) way. Succeeding the fear conditioning session, the place fields in the control and the training arena were recorded. It was found that partial remapping occurred in the training arena, where some place cells either lost their field, gained a new field or altered their field location, while place fields in the control arena just showed minor remapping. The experiments also demonstrated that contextual fear of the arena (unpaired group) led to higher level of remapping than when rats learn to fear a discrete auditory stimulus (paired group) (18). Similar results were found later when Donzis et al. (4) examined the effect of contextual fear on place field stability while the rat was navigating through an eight arm radial maze. There a rat was trained to visit all arms of the maze and collect a food reward at the end of each arm. Three baseline sessions were taken to ensure place field stability. Afterwards, auditory fear conditioning was applied where an audio stimulus (CS) were presented followed by a foot shock. In the succeeding stimulation session, the same audio stimulus was applied either when the rat was within the place field of a single unit (in-field) or far away from the place field (out-field). It was found that CS applied within a place field (in-field) led to remapping of the place field due to decreased stability, while CS applied outside of the playfield showed no effect (4).

2.2.4 Reward location

Different studies have shown that the spatial distribution of place field can be affected by the change of reward locations. Breese at al. (40) trained water deprived rats to collect a water reward from one of five cups evenly distributed over a square arena. By selectively baiting one of the cups it was managed to archive partial remapping, where a big portion of the place cells shift their place field toward the new reward location (40). Similar results have been produced by Dupret et al. (41) where they remapped the place fields repeatedly in a hidden reward test, where the rat had to find hidden food rewards and return to a start box.

In this experiment, most of the place cell shifted their playfield towards one of the three daily changing reward locations (41).

2.2.5 Artificially induced reward location

Similar to the use of food and water as a reward, the spatial firing pattern of place cells can be modified by directly applying electrical stimuli to specific brain regions (42; 1). Kobayashi et al. (42) trained a rat to trigger intracranial self-stimulation by visiting two unmarked reward zones in an alternating way. It was found that 71% of the place cells shifted their place fields towards the reward zones. Most of the remapped place cells were stable in subsequent random reward place search tasks (42). Analogue results have been found in mice. In a classic place preference task, De Lavilleon et al. (1) remapped the place fields of mice between two free exploration sessions in an open arena by applying electrical intracranial stimulation when the rat entered a predefined area (1). Intracranial stimulation in both studies was applied to the medial forebrain bundle which is a part of the reward system (see: 2.3 Medial forebrain bundle (MFB)).

The fact that motivational factors influence the stability and orientation of place field give rise to the assumption that place cells store not only spatial but also contextual or episodic information (see: 2.6 Episodic-like memory). In our experiments, we will use several of the aforementioned methods like real and artificial reward location and fear or aversion in a modified way to induce preferences and aversion to manipulate the spatial configuration of place fields (see: 4 Methods).

2.3 Medial forebrain bundle (MFB)

The medial forebrain bundle is part of the mesolimbic pathway and connects among others the nucleus accumbens (NAc) to the ventral tegmental area (VTA). Both are known to be involved in the generation of reward and pleasure (43; 44). Electrical stimulation of the MFB, also known as brain stimulation reward (BSR) is an effective and commonly used method to induce reward in rats and mice. Rodents will choose BSR over food or heat in subfreezing environments, even with lethal consequences (45; 46; 47). The MFB was the preferred site for stimulation to create pleasure/reward sensation since lower current intensities for sufficient stimulation is needed than in the ventral tegmental area, which reduces stimulation artefacts at recordings in nearby brain areas (47).

2.4 Ventral tegmental area (VTA)

As mentioned before (see: 2.3 Medial forebrain bundle (MFB)) the ventral tegmental area is part of the mesolimbic system, which is the primary system for reward and pleasure in the brain (43; 44). Besides the projection to the nucleus accumbens, which is the primary output nuclei of the VTA (48), via the mesolimbic pathway, the VTA projects dopaminergic to several other brain areas like the amygdala, cingulate gyrus, Olfactory bulb, prefrontal cortex, and hippocampus. Since the stimulation of the dopaminergic pathway from the ventral tegmental area to the nucleus accumbens results in the generation of reward and pleasure, it is evident that the stimulation of the VTA should lead to similar behaviour. The fact that stimulation of the MFB is more common than the stimulation of the VTA to create reward and preferences is due to the fact that, for reliable stimulation lower current intensities are needed in the MFB than in the VTA. Thus electrical stimulation of the VTA with a sufficient intensity would evoke motor side effects (47). Since the emerge of new stimulation methods like optogenetic stimulation (see: 2.5 Optogenetic stimulation), stimulation of the ventral tegmental area became more popular. Several studies examining the function of the VTA and its efferent on afferent projections have been conducted (49; 50; 24). Due to the scope of this work I will cover here just the function of VTA projections targeting the NAc and the hippocampus. As stated before, the VTA and NAc are part of the mesolimbic system which is responsible for the generation of reward and pleasure. The VTA's dopaminergic neurons are known to fire tonically at low frequencies in a resting state. In the present of motivationally relevant stimuli, these neurons will start firing in high-frequency bursts (44). According to that behaviour, excitatory stimulation of the VTA should result in the generation of reward signals. Lammel et al., (49) were able to create a place preference in mice by excitatory stimulation of the VTA, later Stamatakis et al. (50) reported reward-related behaviour in mice after excitatory VTA-stimulation. It has also been found that active suppression of the VTA can lead to aversive behaviour. Lammel et al. (49) managed to induce a place aversion via indirect VTA suppression by stimulation of the lateral hypothalamus which projects via GABAergic interneurons inhibitory towards the VTA. Confirmed were this results by Danjo et al. (48), as he managed to induce a significant place aversion at mice by actively suppressing the VTA. This preference and aversion related behaviour is controlled by the dopaminergic projection of the VTA to the NAc

(43; 44). The dopaminergic projection from the VTA to the hippocampus, however, seem to have a different function. Their function is not entirely understood, but it appears like the dopaminergic projection from the VTA to the hippocampus enhance memory stability and act as a novelty or prediction mismatch signal, which can promote the formation of memory. It is known that dopaminergic neurons projecting to the hippocampus responds with bursts of spikes to novel stimuli but does not show this behaviour at familiar Stimuli. Also, less than 100ms after the presentation of a novel stimulus a robust increase of hippocampal CA1 activity can be observed (51). Another fact that underlines the theory that dopaminergic VTA to hippocampus projections promote the formation of memory is that those projections are the main source of dopamine in the hippocampus. Long-time potentiation is mediated by dopamine (52), and it has been shown that injection of D1 antagonist in the hippocampus impairs memory (51). Stabilization of memory in the hippocampus is presumed to be supported by a reactivation of firing pattern experienced during exploration at sleep or rest periods during sharp wave/ripple (SWR) oscillatory events. It was found that pattern of familiar environments had a weaker reactivation than those of novel ones. This seems to be in relation with the findings that neurons that are projecting from VTA to hippocampus exhibit higher firing rates in new environments than in familiar ones (24). It was demonstrated by McNamara (24) that the reactivation of experienced firing pattern during SWR events could be increased by stimulation of the VTA during their formation. It is supposed that this enhances the stability of the newly formed memory.

2.5 Optogenetic stimulation

Optogenetic stimulation describes a recently developed, promising method to stimulate neurons. This method enables us to manipulate the activity of a neuron selectively with light. To enable a neuron to be optically stimulated, first it has to be genetically manipulated to express light-sensitive opsins. These opsins are ion channels, ion pumps or G protein-coupled receptors. The currently preferred way to genetically engineer specific cells is via Cre-recombinase based rodent lines, combined with a viral vector. The Cre-recombinase based rodent lines are engineered to express Cre-recombinase in specific cells. In our experiments, we used TH::Cre rat lines where Cre-recombinase is just expressed in neurons that also express tyrosine hydroxylase which can be found in dopaminergic neurons. This recombinase catalyses the recombination between two loxP-

sites that flank genetic material. In the viral vector, the gene that controls the opsin expression is typically inverted and flanked by two loxP-sites. The viral vector in then injected into the brain region of interest, there it infects all cells. But just in Cre-recombinase-expressing cells, the opsin expressing gene will be inverted and activated. This method has the significant advantage that existing rodent lines can be used with a variety of different opsins since the engineering of viral is easier and faster than breeding new rodent lines. Once a targeted neuron expresses the opsin it can be stimulated by shining light with a particular wavelength on the neuron. These opsins can be separated by their function into three major groups: opsins for excitatory stimulation, inhibitory stimulation and control of intracellular signalling. The latter group was not used in this work and thus will not be addressed here (53).

2.5.1 Opsins for excitatory stimulation

This group comprises channelrhodopsins, ultrafast opsins, step-function opsins and spectrally shifted opsins (53). Channelrhodopsins (ChRs) are light-gated ion channels which were found in unicellular algae (54; 55). In this work, channelrhodopsin 2 (ChR2) was used which is a nonspecific cation channel (55) this ion shows maximal excitation at 470nm (56). By manipulating ChRs, via targeted mutation or by creating chimeras, several different opsins have been created with very specific properties regarding kinetics, and excitation spectrum. Ultra-fast opsins exhibit very fast off-kinetic which allow the generation of very high spike frequencies in contrast step function opsins have very slow off-kinetics in the range of tens of seconds to minutes (53). Spectrally shifted opsins show a maximal excitation at longer wavelengths than ChR2 this can be of use at bidirectional stimulation or due to the higher wavelengths have a higher penetration through the tissue so those opsins can be utilized for a less invasive light application (53). All those opsins depolarise the neuron by allowing a passive inflow of cations, mainly Na+.

2.5.2 Opsins for inhibitory stimulation

This group consists of chloride pumps, proton pumps and spectrally shifted inhibitory opsins (53). Those opsins suppress the generation of action potentials by hyperpolarization, which is achieved by different methods. Chloride pumps like eNpHR actively transport negative chloride ions into the cell while protons pumps like eBR hyperpolarize the cell by actively transporting protons out of the cell. However, those ion

pumps are not very effective since they just transport one ion per used photon (53). Spectrally shifted inhibitory opsins like iC1C2 are more efficient since they allow passive inflow of chloride ions. IC1C2 was used in this work for optogenetic inhibition of the VTA. It operates on a blue light spectrum with a maximum excitation at 475 nm (57).

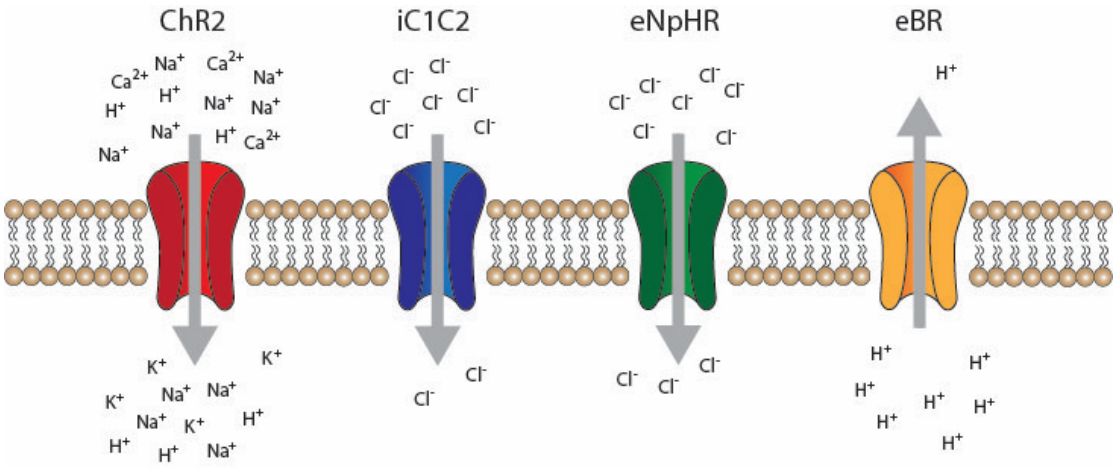

Figure 2-1: Function of different opsins

2.5.3 Application of light

Typically, the neurons are illuminated by light-emitting diodes (LED) or laser light sources. LEDs can either as a micro LED (µLED) directly be implanted at the stimulation area or coupled into an optical fibre. Both methods have disadvantages since implanted LEDs can generate heat and LED-optical fibre coupling exhibit a low efficiency. In contrast, Laser light sources can be efficiently coupled into optical fibres thus it is possible to deliver light with sufficient intensity even to deeper brain structures without the drawbacks of LEDs (53).

Optogenetic stimulation bears several advantages over conventional electrical stimulation of neurons. With this method, it is possible to stimulate brain regions and simultaneously record the same or close brain areas which is not possible with electrical stimulation, where the recording of single unit activity would be superimposed by high stimulation artefacts. The only ways to deal with stimulation artefacts at electrical stimulation would be either alternating stimulation and recording or offline artefact correction. Both methods will result in a loss of information. Only when µLED are directly implanted at the site of stimulation, minor artefacts have to be expected. Furthermore, optogenetic stimulation allows targeting specific types neurons e.g. dopaminergic neurons, cholinergic neurons, etc. with a high spatial and temporal resolution, while electric

stimulation will excite all neurons in a particular proximity given by stimulation intensity, tissue conductance and electrode shape. Recent works show that it is even possible to target a subgroup exclusively within a type of neurons with the help of multiple markers (58). By direct control of the ion-flow into or out of the cell, active suppression of specific neurons can be archived. Combining several opsins with different operating spectra e.g. the ion channel ChR2 (excitatory, peak excitation: 470 nm) and the chloride pump NpHR (inhibitory, peak excitation 580 nm) (53; 59) enables us for bimodal control over a neuron's behaviour.

2.6 Episodic-like memory

After Quillian had introduced the term semantic memory as a person's general knowledge, acquired during the life, Tulving (60) proposed the term episodic memory. To differentiate episodic from semantic memory he defined the difference between knowing (semantic memory) and remembering (episodic memory) something. Where knowing refers to recalling facts from a data collection, like reading it from a lexicon. While remembering relates to recalling specific past events and the ability to it live through again. According to that the term mental time travel was coined (60). The term episodic memory was then defined as the knowledge about past events that can be broken down into the questions: What happened? When did it happen? And where did it happen? And that three information have to be represented in a single memory (61; 62) There has been a long dispute whether animals possess episodic memory. Clayton & Dickinson (63) showed that food storing birds show behavioural elements of episodic-like memory. Later Babb & Crystal (64) were able to prove in their experiments that rats could store information about the what, where and when they encountered food and thus showed that rats possess an episodic-like memory. There is some evidence that links the formation, maintenance and recall of episodic memory to the hippocampus. Scoville & Mildner (65) reported an epilepsy patient who developed anterograde amnesia after removal of both his hippocampi. Similar symptoms have been found in a patient with bilateral lesions of the entire hippocampal CA1 area due to an ischemic episode (66). Not just the formation of new episodic memories is impaired by hippocampal lesions also the recall of episodic memory seems to be affected by hippocampal lesions. It is supposed that the episodic memory system, which enables us for mental time travels to the past also allows us to do mental time travels to the future to imagine upcoming events (67). The hippocampus

seems to be heavily involved in that task since it was shown that, during the imagination of future events the hippocampus was activated (68). The impairment of memory due to hippocampal lesions could also be shown in animals. Wood & Macdonald (69) demonstrated that hippocampal lesions can impair olfactory recognition. Other studies have shown that spatial memory (70) and the memory of temporal order (71) is impaired by damage to the hippocampus. The mechanisms how those memories are formed and maintained are yet not sufficiently clear. But since the memory of all the three conditions that defines episodic-like memory (what, when and where) can be impaired by damaging the hippocampus, it clearly shows that in animals the hippocampus can be linked to the formation and maintenance of episodic-like memories.

2.7 Misplace cells

As mentioned before (see: 2.2 Place field remapping) the distribution of the place cells firing fields can be influenced by different stimuli. Soon after the discovery of place cells, a subtype of place cells was found, which spiking behaviour was not entirely related to the location of the rat (72). It was found that so-called misplace cells had an elevated firing frequency when the rat was sniffing in a place where an object used to be or in a place where a new object was placed. Thus the firing of those cells was related to novelty (72). This theory was expanded by Wood (3). She stated that the behaviour of those cells not just reflect novelty but also is related to the rat's behaviour, the sampled stimuli as well as the importance of that stimuli for the ongoing task and even can represent the temporal order of events (3).

2.8 Place cells and episodic memory

As mentioned before (see: 2.2 Place field remapping; 2.7 Misplace cells) the place fields of hippocampal place cells can be affected by a variety of stimuli, which not necessarily have to be spatial. Eichenbaum et al. (73) proposed a theory where subpopulations of hippocampal place cell encode entirely spatial information while other subpopulations code for non-spatial features which repeatedly occur in an experiment. It was shown that hippocampal neurons develop place fields at locations where non-spatial features, like regularly performed actions or experiences, occur frequently. It is supposed that hippocampal place cells do not just reflect the spatial representation of an environment, but more represents a summary of the location of occurring regularities (73). Recalling

Tulving's definition of episodic-like memory as a memory that stores information about the what, where and when of a past event, there had been several studies, that tried to link those conditions to place cell activity.

2.8.1 What and where

There have been several studies that related firing pattern of place cells to spatial and contextual features of repeated stimuli. Gothart et al. (74) could identify in a spatial navigation task several subpopulations of place cells which reacted to different conditions of the task. In this study, the rat was trained to exit a pseudo-randomly positioned start box find a food reward which was placed in a fixed relation to two landmarks and returned to the start box which was in the meanwhile shifted to a different location. Four different subpopulations could be identified. Stable place cells which place fields related entirely to the extra-maze cues. Goal or landmark related cells which always fired in a fixed location in relation to the landmarks indication the reward position. Box related cells which exhibited place fields inside or at the entrance of the start box and place cells which firing patterns were influenced by a mixture of the before mentioned factors. It has to be said that the relation between the firing fields and the related factors were fixed even when landmarks and or the start box were moved within or between trials. Another study used a recognition memory task where a rat has to decide whether it encountered an odour in the preceding trial or not. One of the nine scents were pseudo-randomly presented at one of nine locations in the arena. Several place cells could be identified that showed distinct firing characteristics related to either the site of the presentation of the odour, to a particular scent, to the type of task or combination of the before mentioned (75). In a place navigation task Hok et al. (37) found that most of the place cells exhibit a secondary place field at a location where a particular action was carried out. In this experiment, the rat was trained to find an unmarked area with a 10 cm diameter where the rat has to wait for 2 seconds to receive a food reward, which was thrown randomly into the arena., The rat has to exit the goal area at least for 3 seconds to gain the next reward. It was remarkable that the place cells fired only at the goal location when the animal was waiting for a reward and not when the rat was randomly crossing the goal area. Those studies show that by analysing the firing pattern we can predict, not just the position in an arena, but also what kind of location it is, e.g. start box or reward location (74), what we can find in particular location e.g. which odour can be found in which location (75) and what kind of

action the rat is performing in a certain place e.g. waiting for a reward (37). To summarize this, it can be said that place cells can exhibit information about the context of a location or in short: provide us information about the what and where.

2.8.2 When & where

As mentioned before it could be shown that place cells can exhibit contextual information. To satisfy the definition of episodic-like memory (what, where, when) it was tested if place cells could provide temporal information. Essential proofs for a representation of temporal information in place cells has been provided by Wood et al. (20). In this work, rats were trained to navigate through a modified T-maze in an alternating way (Figure 2-2.)

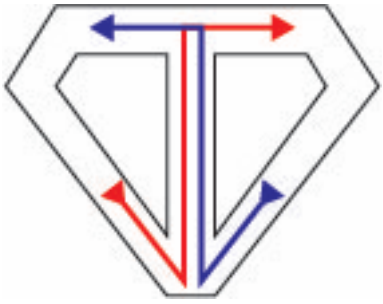

Figure 2-2: Modified T-maze used in Wood et al. (20)

The place cell activity in the stem of the T-maze was analysed, and it was found that more than 90% of the place fields in the stem showed a firing behaviour related to either one of the two conditions (right or left turn at the end of the stem). The behaviour of less than one-third of those cells could be explained by variations in behaviour (head direction, speed, etc.). The rest of the place fields, comprising two-thirds of all place fields in the stem of the T-maze, had significant different firing fields that could not be explained by the condition. Due to the design of the experiment, it could not be specified whether the behaviour was related to past events (coming from either left or right) or future intentions

(going either to the left or right). To find out whether the influence on the place fields is retrospective or prospective Frank et al. (21) used a W-maze (*Figure* 2-3),

)

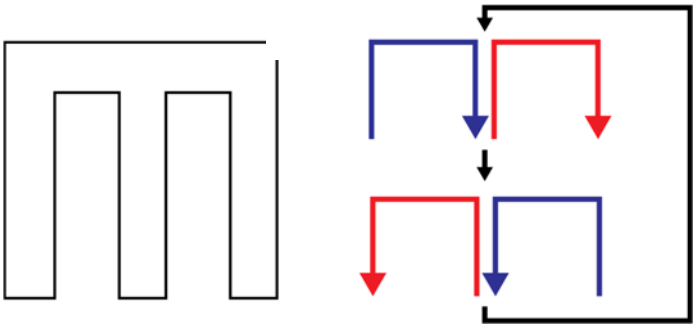

Figure 2-3: W-maze a) schematic of the arena, b) motion pattern used in Frank et al. (21)

where the rat has to move through the maze in an alternating pattern (e.g. left, centre, right, centre... see Figure 2-3). Just place fields in the centre arm were analysed. It was found that 36% of the place cells fired in relation the different conditions (inwards/outwards, left/right). Both, retrospective and prospective behaviour could be identified. Ainge et al. (76) showed that the destination of a rat in a maze could be predicted by the activity of some place cells.

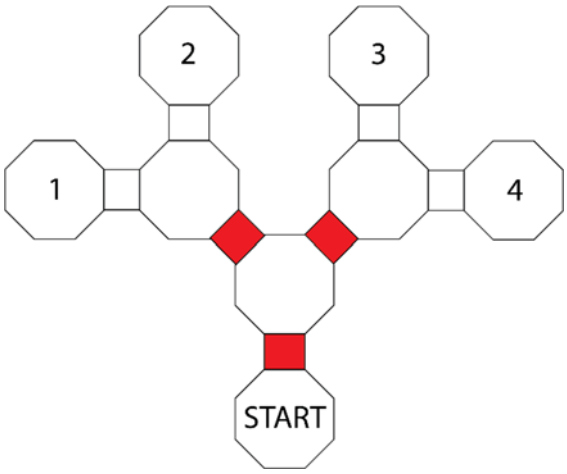

Figure 2-4: Y-Maze used in Ainge et al. (76)

In this task, the rat had to navigate repeatedly through a double Y-maze to collect a food reward at one of the reward sites (1-4). It was found that 44 – 46 % of the cells firing in the red marked areas (Figure 2-4) showed distinct firing characteristic related to the intended destination. In all three experiments, it has been demonstrated that a portion of the place cells carry information about the temporal context since past or future events could be predicted by analysing the firing pattern.

It has been shown that place cells can carry information about the three condition associated with episodic-like memory: what, where and when (61). However, it can be

argued whether the firing fields of the place cell represent real memory or can be seen as some kind of task-dependent behaviour, which can be for example a feedback signal during navigation to ensure that the intended destination was reached (37). Instead of analysing how the behaviour of the place cells is affected by an ongoing task we investigated how the training of a place preference, which can be seen as the creation of an episodic-like memory influence the distribution of place fields in a different succeeding task.

2.9 Manipulating memories by the help of place cells

Several studies have been conducted recently to find out if memories can be created or manipulated by stimulating hippocampal place cells. Ramierez et al. (77) labelled a hippocampal memory engram of a particular neutral context with ChR2 to enable that engram for optogenetic reactivation in a different context. By reactivation of that engram in a context where the animal was fear-conditioned by electrical foot-shocks, it was managed to increase significantly the fear reaction (freezing time) in the first context where foot-shocks were never applied. This results showed that it was possible to create an aversive memory by linking a memory engram to an aversive event and recalling that memory in an unrelated context (77). A more recent work showed that it was possible to change the valence of an existing memory (78). Here both, the switch from fear to reward as well as the switch from reward to fear could be achieved. In this experiment, hippocampal memory engrams created during either fear- (fear-to-reward group) or reward-conditioning (reward-to-fear group) were labelled with ChR2 for optogenetic stimulation. These engrams were reactivated during a place avoidance/place preference test. The comparison with a baseline test showed the effectiveness of the conditioning. Afterwards, the fear to reward group received a reward- and the reward to fear group a fear-conditioning. In both groups, the memory engrams were reactivated during the conditioning sessions. In the following place avoidance/place preference test an appetitive behaviour in the fear-to-reward and an aversive behaviour in the reward-to-fear group could be observed. This shows that it was possible to shift the valence of memories from negative to positive or vice versa. Those studies prove that episodic-like memories can be altered by manipulation of the hippocampal place cells and thus gives another proof that the hippocampus is involved in the formation and maintenance of episodic-like memories. It is unclear whether the valence of memories is stored by the

place cells or if those cells just provide a spatial framework for a complex system of different brain areas for memory storage (3). In contrast to the studies mentioned above in this work, we will not examine how memory can be influenced by manipulation of the place cells. Here we will analyse how the generation of long-term memories affect the firing behaviour of place cells.

2.10 Place cell firing analysis

Several methods to investigate the properties of the firing behaviour of place cells are known. In this work, we mainly focus on the classification of the spatial firing behaviour and the distribution of place fields. It is noticeable that one of the most crucial features of a place field is its location. Since place fields have an amorphous shape, there was the need of finding a universal, applicable description for a place field's position. Several methods to solve this problem have been suggested:

2.10.1 Distance-weighted centre

This method is inspired by the Shepard interpolation method (79) To find the inversed distance weighted centre a new averaged map of the place field is calculated. The values of the bins of those maps are the average of all other bins weighted by 1/distance. The bin with the highest value is the distance weighted centre (80).

2.10.2 Peak rate centre

This method also relies on average firing frequencies. Here for each bin, the mean frequency of the area surrounding that bin is calculated by dividing the number of spikes observed in the area of the bin and the next eight neighbours by the time spend in that area. The pixel with the highest average frequency is defined as the peak rate centre (80).

2.10.3 Centre of mass

This method relies on the calculation of geometrical centroid and calculated by a sum of the bins weighted by the position in X- and Y-direction (see: 4.14.1 Centre of mass (COM)).

Knowing that place fields are reproducible under constant conditions (35; 80) assumed that the best method would exhibit the smallest shift in the centre of the place field between different trials under constant conditions. It was found that the centre of mass showed the smallest displacement compared to the distance weighted centre and the peak rate centre and thus became the method of choice (80). Here we use the centre of mass (COM) in the classic way to describe the position of place fields in an open arena and in a modified way where we reduce the dimensionality to describe the spatial spiking distribution within a symmetric arena by a one-dimensional variable (see: 4.20 COM-distance).

2.11 Spatial coherence

Spatial coherence was first introduced by Muller & Kubie (81) as a measure of firing pattern quality. It estimates the local orderliness of a firing field since it assesses how good the value of a bin can be predicted by the values of its neighbours (82) (see: 4.13.3 Spatial coherence). Fenton et al. (80) used this method, in combination with other criteria, to distinguish place cells from other types of neurons. While Dupret et al. (41) used it in conjunction with spatial specificity to assess the spatial tuning of a place cell.

2.12 Information content (spatial specificity)

Skaggs et al. (83) introduced information-rate formula (see: 4.13.2 Information content (spatial specificity)) to provide an easy way to calculate the information content of a cell. It can be used to evaluate to which extent a cell provides information about a particular feature e.g. location vs. head direction (83). It is the method of choice to assess the quality of the place cells firing behaviour (80; 84; 11; 74; 21).

2.13 Autocorrelogram

The autocorrelogram is a histogram of the autocorrelation (the cross-correlation of a data series with itself) of a spike-train. This is a commonly used method to control the quality of single unit separation. The autocorrelogram is checked for spikes with an Interspike interval of less than 1.5-2 ms, which is the refractory period of a neuron. If spikes in this interval can be found, this is an indicator for insufficient single unit separation, since the spike train have to consist out of spikes from different cells (85; 76; 38).

2.14 Population vector

The principle of a population vector to describe the behaviour of an ensemble of cells was first introduced by Georgopoulos, et al. (2; 86). In this work, the signals of 224 neurons in the motor cortex of rhesus monkeys were used to predict the direction of the motion of the monkey's wrist to reach out for a button. The population vector P(M) which here represent the direction of a movement in direction M was calculated by the following formula:

$$P(M) = \sum_{i=1}^{N} w_i(M) C_i \quad (1)$$

Where C_i is the preferred direction of cell i (the direction of motion in which cell I exhibit the maximum firing frequency) and $w_i(M)$ is the contribution of cell i to the motion (M),

$$w_i(M) = d_i(M) - b_i \quad (2)$$

represented by the cells firing frequency $d_i(M)$ for the motion in direction M corrected by the baseline activity (b_i). Later the evaluation of the behaviour of a whole ensemble of simultaneously recorded neurons was introduced in studies regarding hippocampal place cells. Due to the different tasks of hippocampus and motor cortex, the application of the population vector was modified. The first use of the population vector at a collection of simultaneously recorded place cells was to predict the location of a rat by the help of the place cells firing behaviour (26). To do so, discrete rate maps (display of spatial firing behaviour represented by the mean firing frequency at a particular place, see: 4.13.1 Ratemaps / place fields) of hippocampal place cells were stacked, where the x-/y-axis represent the two spatial dimensions and z-axis represents the cell index. The population

vector describes the distribution of firing rates of a particular location (bin) across all cells (red arrow, Figure 2-5).

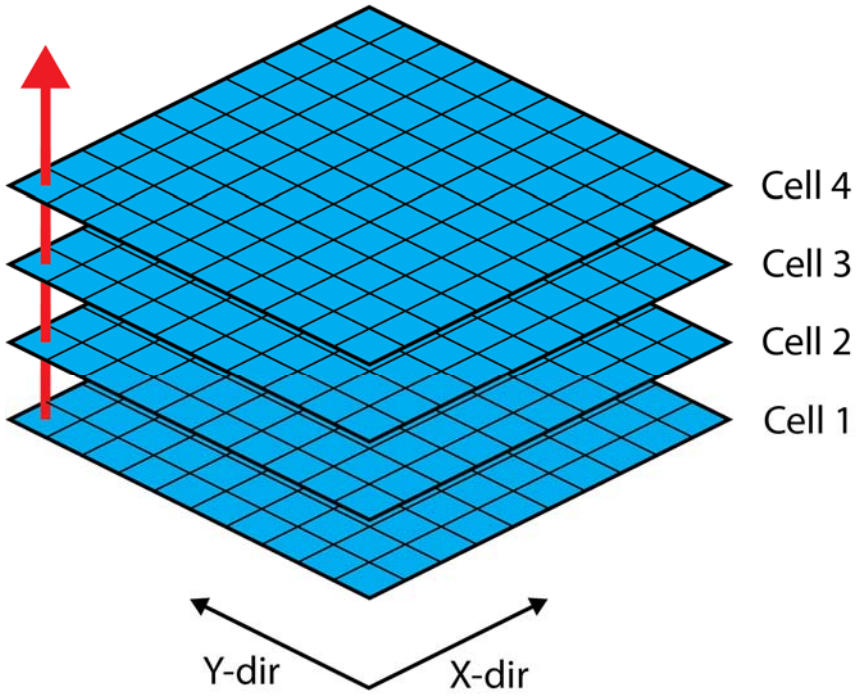

Figure 2-5: Schematic of a population vector

To predict the location of the rat, a rate vector is created by calculating the average firing frequency for every cell in a short interval of time (0.17 – 5 seconds) (84). That rate vector is now compared to the population vector of each bin. The one, showing the highest correlation to the rate vector is the best prediction of the rat's location (26; 84). Besides the prediction of the rat's position population vector analysis is a powerful tool for several applications. In several works, population vectors have been used to indicate remapping of place fields while gradually shifting from one to another arena size (e.g. square to circle). There for each arena ratemaps are calculated, from which population vectors for each location are derived. These population vectors are then compared between the arena shapes (87; 88; 85). Colgin et al. (85) calculated the cross-correlation coefficient between the population vectors for each location of two arena shapes while shifting one of the maps incrementally. Maps of the mean correlation coefficient indicated the absence of

remapping (high peak at the origin, Figure 2-6 a) or remapping (significantly decreased peak at the origin, Figure 2-6 b)

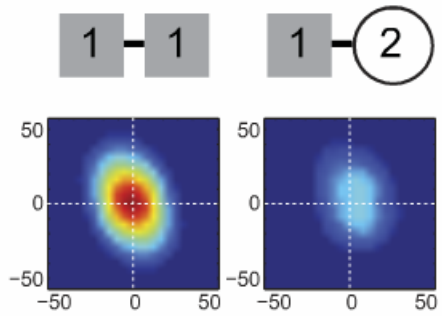

Figure 2-6: Mean correlation coefficients for a) similar and b) non-similar ratemaps (85)

Other works used population vector analysis to evaluate the influence of different conditions on the firing behaviour of place cells. There population vector analysis exhibit manifold applications from the evaluation how memory modulates journey-depended firing (89) to the study of the influence of motivational states on goal-directed navigation strategies (90). In those works, instead of comparing different recordings in various arenas, different trials or conditions within one recording are compared by the calculating of the correlation between population vectors. In this work, we used an approach close to the one of Georgopoulos, et al. (2) to examine the behaviour of an ensemble of simultaneously recorded hippocampal place cells. Instead of comparing different states, arenas or conditions we calculated a spatial population vector as a sum of one-dimensional variables, which describe the distribution of place fields, weighted by the average activity of the corresponding place cell (see: 4.21 Spatial population vector).

2.15Bhattacharyya distance

The Bhattacharya distance is a divergence type similarity measurement introduced by the Indian statistician A. Bhattacharyya (91). It was designed to calculate the pointwise overlap between two equally sized probability distributions, represented by the Bhattacharyya coefficients (see: 4.15.4 Influence of the stimulation location). To my knowledge, the Bhattacharyya distance is not a commonly used method to analyse firing behaviour of hippocampal place cells. However, Aherne et al. (92) showed the advantages of the Bhattacharyya distance over other similarity measurements like chi-squared metric and recommended its use for the comparison of frequency coded data. Nowadays the Bhattacharyya distance is a commonly used method for optical applications that requires a measurement of similarity such as tracking applications. In this work, the Bhattacharyya distance was used to evaluate the spatial shift of place fields in relation to the location of stimulation events. Figure 2-7 shows the general principle of use, where the upper row shows different distributions (A-F) while the lower row shows maps of the Bhattacharyya coefficients for the combination of 2 distributions (A-A, A-B, A-C, A-D, A-E, A-F) and its Bhattacharyya distance

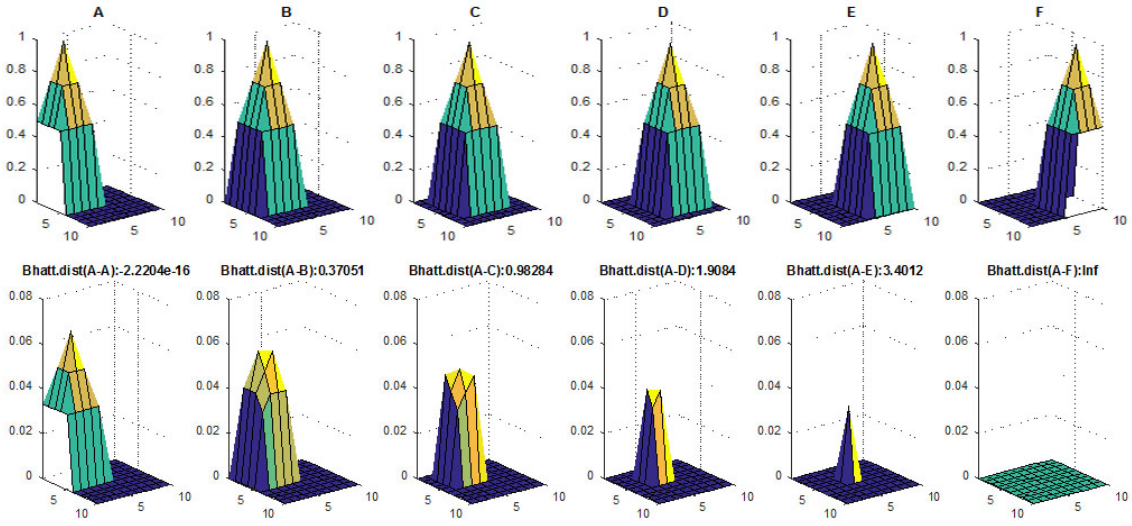

Figure 2-7***: Probability distribution A-F (top); Bhattacharyya coefficients for the comparison of two distribution (bottom)***

We can clearly see how the Bhattacharyya distance increases as the distributions drift apart.

2.16Symmetry

Recent studies showed that spatial firing pattern of place fields repeat in physically and contextual similar areas (93; 94). We assume that in a physically symmetric arena the induction of contextual differences, like a preference towards one-half will be reflected in a change of the symmetry of place cells' spatial firing pattern. To my knowledge, symmetry analysis was not used yet for describing the distribution of firing pattern of hippocampal place cells. Therefore, no commonly used method was available that suited the needs of this work. In this work, I created a method to evaluate the symmetry of the firing activity of place cells. This method was designed to be an alternative to common methods, like centre of mass based methods, to describe the spatial distribution of place fields for arena-shapes that impede the usage of common methods. A basic definition of symmetry was given by Cantwel (95):

> "An object is symmetrical if one can subject it to a certain operation and it appears exactly the same after the operation. The object is then said to be invariant with respect to the given operation."

This definition applies to reflectional as well as rotational symmetry. In the following, the term symmetry will refer to reflectional symmetry. Since just reflectional symmetry regarding a predefined symmetry axis will be considered. The complicated definition of two-dimensional symmetry Sθ{f} of the function f(t,s) (3) (96)

$$S_\theta\{f\} = \frac{\int S\{f(t,s)\}\|f(t,s)\|^2 dt}{\int \|f(t,s)\|^2 dt};\ S_\theta\{f\} \epsilon [0,1] \quad (3)$$

Where t represents the position on a symmetry axis tilted by an angle θ in relation to the x-axis

$$t = x \cdot cos\theta + y \cdot sin\theta \quad (4)$$

And s represents the distance perpendicular to the before mentioned symmetry axis

$$s = x \cdot sin\theta - y \cdot cos\theta \quad (5)$$

By modifying the coordinate system and separating the map into rows perpendicular to the symmetry axis, we can express the symmetry S{f} as an average of linear symmetries S_n(f(x)) weighted by a weighting function w_n.

$$S\{f\} = \frac{\sum_{n=1}^{N} w_n S_n\{f(x)\}}{\sum_{n=1}^{N} w_n} S\{f\} \epsilon [0,1] \quad (6)$$

Where each linear symmetry is given by (96):

$$S_n\{f(x)\} = \frac{\|f_s(x)\|^2}{\|f(x)\|^2};\ S\{f(x)\} \epsilon [0,1] \quad (7)$$

And the symmetry function is given by (96):

$$f_s(x) = \frac{f(x) + f(-x)}{2} \quad (8)$$

Given that f (x) is discrete and just can take positive values the linear symmetry $S_n\{f_n(m)\}$ can be expressed as an average of the pointwise symmetry $S_m\{f(m)\}$:

$$S_n\big(f_n(m)\big) = \frac{\sum_{m=1}^{M} S_m\{f(m)\}}{M} \quad (9)$$

Where:

$$S_m\{f(m)\} \widehat{=} \frac{f(-m)}{f(m)} \quad (10)$$

So I started creating the symmetry measuring method from the idea of an averaged bin-wise comparison of bins symmetric to the symmetry axis (see: 4.19 Symmetry method).

3 Aims of thesis

As mentioned before (see 2.2 Place cell remapping) place fields of hippocampal place cells can be remapped by non-location stimuli or have firing behaviour related to not purely locational inputs (see 2.7 Misplace cells, 2.8 Place cells and episodic memory). However, there are various theories describing this behaviour is purely task dependent (3), might represent some kind of decision or feedback signal (37) or if it represents places of frequent performed actions (73). The hypothesis in this thesis is that the firing behaviour of hippocampal place cells on a population level represent an episodic like memory which is coding for preferences and is controlled by dopaminergic projections from the VTA. To confirm this hypothesis several points have to be investigated:

- To verify the dopaminergic control of hippocampal place cell's firing pattern, the direction of the place field shift in relation to the site of stimulation has to be investigated (see: 4.8 open field recording).

- To verify the relation between aversion and low activity of the dopaminergic projection from the VTA to the hippocampus, the behaviour of the rat while actively suppressing the Dopaminergic activity of the VTA has to be analysed (see: 4.9 Rectangular-shaped linear track).

- To verify the hypothesis that place cell activity can reflect non-locational properties in an arena, the symmetry of the placefield distribution of a physically but not contextual symmetric arena has to be analysed (see: 4.10 Continuous T-maze task).

- To verify the hypothesis that the activity of hippocampal place cells exhibit characteristics of episodic like memory and reflects the valence of a location on a population level the population vector of place cell activity, recorded in an arena with locations of special preference or aversion, has to be analysed. (see: 4.9 Rectangular-shaped linear track; 4.10 Continuous T-maze task).

In order to investigate the before mentioned points, methods to quantify symmetry and the behaviour of place cells on a population level have to be created (see: 4.19 Symmetry method; 4.21 Spatial Population vector). These methods have to be, in combination with commonly used methods to describe place cell activity and the quality of recording (see: 4.12 Spike-specific data; 4.13 Spike and path dependent data; 4.14 Place field properties; 4.15 Comparative analysis) as well as the behaviour (see: 4.17 Behavioural data), implemented into single Matlab (The MathWorks, Inc.) scripts for each experiment (see: 5.1 Stimcomp_open_opto_V3; 5.2 Stimcomp_tmaze_V3; 5.3 Stimcomp_linrec)

4 Methods

4.1 Subjects

5 male (250-350g) Lister-Hooded rats (Harlan UK) have been used as the MFB group in the open field recording (see: 4.3 Electrical MFB-stimulation), and 16 male (250-350g) Lister-Hooded TH::Cre rats (Rat Resource & Research Center P40OD011062, US) have been used for the VTA-on (n = 3), VTA-off (n = 7) and VTA-control (n = 7) group (see: 4.2 Optogenetic VTA-stimulation). The animals were housed at a 12:12 hour light/dark cycle with ad libitum access to water, but restricted access to food the diet was set to keep the rats at 90% of the average body weight. (97). All experiments have been conducted in accordance with DIRECTIVE 2010/63/EU OF THE EUROPEAN PARLIAMENT AND OF THE COUNCIL of 22 September 2010 on the protection of animals used for scientific purposes and the S.I. No. 543 of 2012, and followed Bioresources Ethics Committee, Trinity College Dublin, Ireland, and international guidelines of good practice.

4.2 Optogenetic VTA-stimulation

For optogenetic excitation and suppression of the VTA Cre-inducible ChR2 / iC1C2 viral constructs have been used (98; 99; 97). This viral vector target tyrosine hydroxylase expressing cells in TH::Cre rat lines. Tyrosine hydroxylase is a catalyst for the conversion of L-tyrosine to L-3,4-dihydroxyphenylalanine (L-DOPA), which is a precursor of the neurotransmitter dopamine and thus can be found in dopaminergic neurons.

4.2.1 Virus construction: VTA-on group (excitatory)

The viral construct pAAV-Ef1a-DIO-hChR2(E123T/T159C)-EYFP-WPRE-pA was serotyped with AAV5 coat proteins and packaged by Vector Core at the University of North Carolina. Viral titers ranged from 1.5-8 x 10^{12} particles per mL (98; 97). This viral vector makes targeted cells express channelrhodopsin-2 (ChR2), which is a light-gated ion channel that allows nonspecific cation transfer between intra- and extra-cellular spaces. ChR2 is activated by blue light and allows the generation of action potentials by depolarization due to the influx of sodium ions (53).

4.2.2 Virus construction: VTA-off group (inhibitory)

The viral construct AAV8-EF1a-DIO-iC++-TS-EYFP was serotyped with AAV8 coat proteins, in titer of 4.3 x 10^{12} particles per mL and provided by Karl Deisseroth, Stanford University (97). This viral vector makes targeted cells express the channelrhodopsin hybrid iC1C2 which acts as a light-gated ion channel specific to chlorides. By allowing chlorides the passage into the intracellular space along a concentration gradient, the cell can be hyperpolarized when iC1C2 is activated by blue light (53).

4.2.3 Virus construction YFP group (control)

A viral vector bearing only the YFP reporter was used as a control (97). Rats injected with the control viral vector showed no effect of laser light on the recorded neurons (98).

4.2.4 Virus Application

The virus was injected unilateral to the ventral tegmental area (5.7 AP, 1.9 ML, angle 10^{o} medially). 1µl each were applied to 2 different levels (8.0 and 9.0 mm dorsoventral to dura) (97).

4.2.5 Optical activation

Following the virus injection, an optical fibre (200 µm core diameter, Thorlabs Inc.) was chronically implanted (5.7 AP, 1.9 ML, 8.0 DV, angle 10^{o} medially) (97). For stimulation, the optical fibre is connected to a 473nm, 50mW fibre coupled laser source (Thorlabs S1FC473MM).

4.3 Electrical MFB-stimulation

For the electrical stimulation of the MFB one electrode (SNEX-300, Kopf Instruments) were implanted (AP 1.7 ML 1.7, DV 8). The stimulation followed the theta-burst stimulation (TBS) protocol which consists of four bursts, containing 3 pulses at 10 ms (100 Hz) each, with an inter-train interval of 125 ms (8 Hz) and a current amplitude of 50-200µA (100; 97; 101; 102). The amplitude was tuned with respect of the test pulse stimulus artefact. The bursts are generated by a constant current bipolar stimulus isolator (A365D, World Precision Instruments, Inc.). The stimulus isolator was controlled by the recording system (dacq, Axona, Ltd.) via the TTL output signal and was synchronized

with the motion-tracking system (dacq-Track, Axona). Rats without electrodes implanted in the MFB were used as controls.

4.4 Surgical implantation of electrodes

To record the single unit activity of place cells or dopaminergic neurons (for verifying optogenetic stimulation), eight tetrodes has been implanted either to the hippocampus (-3.8 AP, 2.3 ML and 1.8 mm dorsoventral to dura) or the ventral tegmental area (5.7 AP, 1.9 ML, angle 10° medially and 8.0 mm dorsoventral to dura) (Figure 4-1). Each tetrode consists out of four twisted 25µm-diameter platinum-iridium wire (90% platinum, 10% iridium, California Fine Wire) each wire is insulated by polyimide (103).

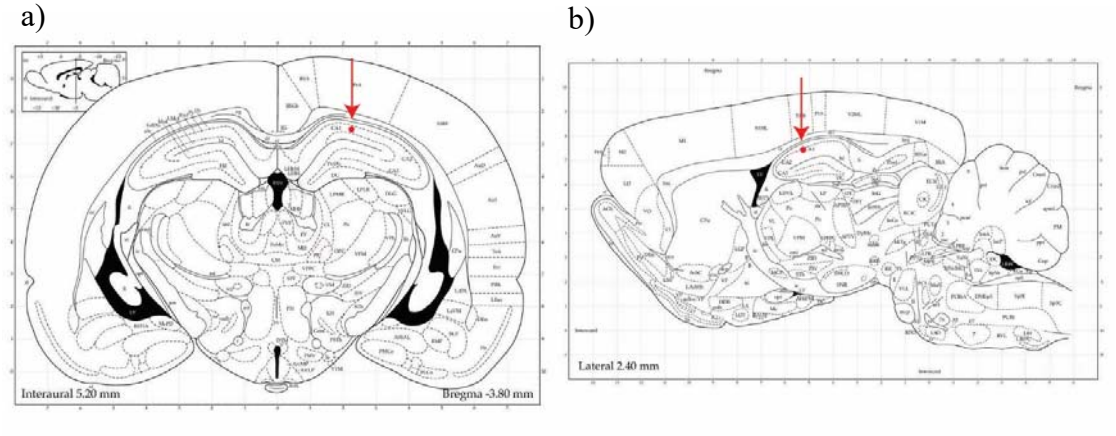

Figure 4-1: Location of the tetrode tips, a) coronal plane, b) sagittal plane

4.5 Motion tracking

The motion of the rat in the maze is tracked by following the trajectory of an IR-LED attached to the head stage by a monochrome IR camera (Bosch LTC0355) connected to the dacqTrack video tracking system (Axona Ltd.)

4.6 Single unit recording

The Implanted tetrodes were connected to a dacq recording system (Axona Ltd.) via a 32 channel head stage (Axona Ltd.) For single unit detection, the signal, sampled at 44.1kHz, was amplified (Gain: 10000 - 30000) and bandpass filtered (passband: 380 Hz - 6 kHz) (97).

4.7 Single unit identification

Different units were separated off-line by k-mean clustering method using the Tint graphical cluster-cutting software (Axona Ltd.). Only waveforms of an amplitude bigger than three times the noise threshold were used. Suitable waveforms were then separated based on spike amplitude, spike duration, maximum/minimum spike voltages and the duration of those peak values. Following the separation, autocorrelation histograms were calculated for each unit. Spikes within the first 2 ms (refractory period) were used as an indicator for insufficient unit isolation, and the unit was eliminated from further analysis. Similarity comparison of spike clusters and cross-correlation of spike amplitudes between training sessions have been used to evaluate the stability of the signal. Units that did not show sufficient stability over succeeding days were also eliminated

4.8 Open field recordings

The open field recordings conducted by Mamad et al. (97) took place in an arena, which was made from a 60cm x 60cm square piece of plywood which was painted black and elevated 30 cm above the floor. It was surrounded by black curtains. After the rat was placed into the arena 20mg food pellets (TestDiet, Formula 5TUL) were thrown into the arena in 20-second intervals to random locations within the arena (pellet-chasing task) to keep the animal in permanent locomotion. This allows the complete sampling of the arena. The experiment was separated into a baseline and a stimulation session with a duration of 12 min each. This duration was chosen to enable the rat to sample the whole arena evenly. Durations shorter than 10 minutes resulted in an insufficient exploration of the arena while durations longer than 15 minutes at baseline sessions reduced the sampling of the arena in subsequent stimulation sessions to an insufficient level. During both sessions, the path of the rat in the arena and the single unit activity of pyramidal neurons of the CA1 area in the hippocampus were recorded. Additionally, in the stimulation session either the VTA or the medial forebrain bundle (MFB) was stimulated each time the rat entered a predefined quadrant of the arena. The stimulation at each entry of the quadrant in contrast to the stimulation while the rat is in the quadrant was chosen to prevent the rat from excessive self-stimulation and thus keep the rat in constant motion. The VTA was excitatory stimulated by a single train of optical 12 pulses, 5ms pulse duration, 50 Hz, 473nm. For the optogenetic stimulation, eleven test subjects (ChR2-YFP) and eight controls (YFP) have been used (see: 4.2 Optogenetic VTA-stimulation).

The MFB was stimulated by four electrical bursts, each burst containing three pulses at 10ms (100 Hz), with an inter-train interval of 125ms (8Hz) and an amplitude of 50-200µA (see 4.3 Electrical MFB-stimulation). For the electrical stimulation, 18 test subjects and 13 controls have been used. Before the recording, the rats were habituated to the arena. In this experiment the influence of dopaminergic activity on place field properties and its remapping was tested. To evaluate the effect of repeated augmented dopaminergic activity the trials have been carried out daily for up to five days.

4.9 Rectangular-shaped linear track

The third experiment done by Mamad et al. (97), uses a rectangular-shaped linear 10cm wide track made of plywood with a length of 85cm (Figure 4-2) was used. The arena was painted black, elevated 30cm above the floor and surrounded by black curtains.

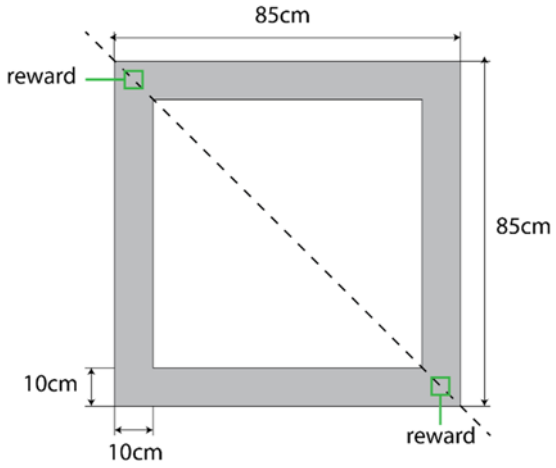

Figure 4-2: Rectangular-shaped linear track

During the trials, two food pellets (TestDiet, Formula 5TUL) were continuously placed at the northwest (NW) and the southeast (SE) corner (green squares, Figure 4-2). Eight test subjects (VTA-off) and five controls (YFP) (see: 4.2 Optogenetic VTA-stimulation), were trained to move continuously between the two reward zones. The animals were allowed to move in clockwise and counter clockwise direction through the arena. The duration of each session was 12 minutes. In the probe sessions, continuous optical stimulation was applied while the rat remains the west or south arm of the track (Figure 4-3).

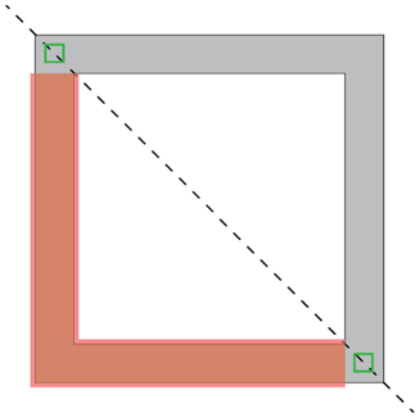

Figure 4-3: Stimulation zone in the rectangular shaped linear track

To stimulate the VTA continuous photo-stimulation trains, containing 12 pulses per train, at 50Hz with 5ms pulse duration and 1 sec inter-train interval, at 473nm were applied. This experiment was designed to analyse the behaviour of place fields while actively inducing a place aversion (49), and allows us to study the effect of suppression of dopaminergic projection from the VTA to the hippocampus on the formation and stability of place cell firing pattern.

4.10Continuous T-maze task

In the second experiment of Mamad et al. (97), a continuous T-maze arena with 10cm track-width and 85cm length of leg arms was used (Figure 4-4). The arena was made of plywood, which was painted black and set in a room with four cue cards (distal cues) attached to the curtains surrounding the arena. The illuminance was set in the range of 10-15lux and kept constant between the sessions. The purpose of this experiment was to generate a reward driven place-preference and evaluate its effect on the spatial firing distribution of hippocampal place cells.

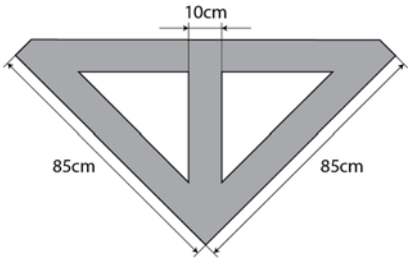

Figure 4-4: Dimensions of the T-maze

Proximal (choice point shape) and distal (cue-cards) allocentric cues were available for the rat navigating the maze. However, the presentation of the distal cues was designed in a way that they could be identified and used for navigation by just about 50% of the rats. Egocentric learning was prevented by allowing the rat to navigate in all directions

(clockwise / counter-clockwise) so opposite head turns at the choice points were needed. As a result of that rat has to learn to navigate with the help of proximal or distal cues (97). The experiment was separated into a training phase and a probe phase. The training phase consisted of three daily trials with a duration of 12 minutes each over three days. In the training phase, south-east half of the maze was disconnected but visible. At the beginning of each trial the rat was set at choice point 2 (Figure 4-5 a) and were allowed to explore the maze. To train the rat a reward-driven place preference two food pellets (TestDiet, Formula 5TUL) were positioned in the southwest (SW) corner (reward zone, Figure 4-5 a) while no food reward was placed in the north-east (NE) corner. The food reward was replaced each time the rat passed directly through the two choice points. In the case of direct passes between SW corner and NE corner no reward was given. To keep the rat in constant locomotion in a loop pattern through the choice points at 33% of the passes a food pellet was placed at choice point 1 and at 33% of the passes a food pellet has been put at choice point 2. In the rest of the passes, no pellet was placed in either choice point 1 or choice point 2. (97).

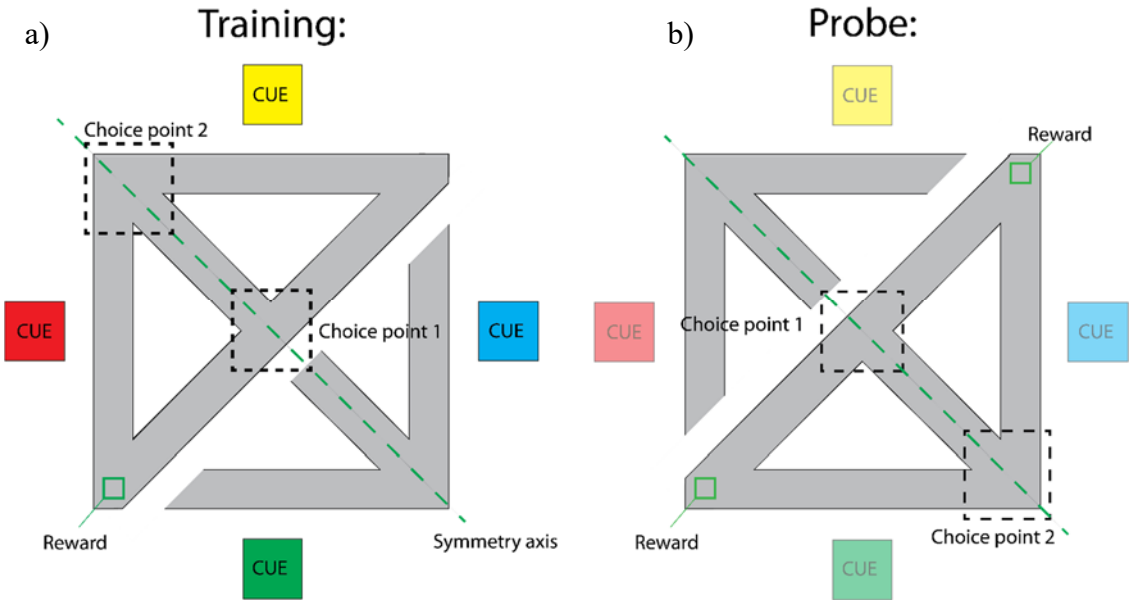

Figure 4-5: T-maze for a) training and b) probe sessions

After finishing the training phase, the rat was given a probe trial on day 4. During the probe trial, the north-west half of the maze was disconnected but visible, so the rats were exposed to opposite distal cues. In probe trials, the illumination was set to a level at which the probability for the rat to rely on navigation dependent on distal cues was approximately 50% (104; 105). Like in the training trials the rat started at the choice point 2. In contrast to the training phase 2 food pellets were positioned at two reward zones at the SW corner and the NE corner (Figure 4-5 b). The level of illumination defines the

strategy for navigation in this task. At high illumination levels, the rat can identify distant cues and use them for navigation. A 180° shift of the distal cues leads to a conflict between proximal and distal cues. This will result in a split navigation strategy towards the two arena halves. At low levels of illumination below 5 lux, it is hard for the rat to identify the distal cues and will rely primarily on proximal cues for navigation through the maze. In this case, the rat will navigate in more than 50% towards the NE corner. (97). Based on the distribution of passes we can now identify if the allocentrically-guided navigation strategy of the rat is relying predominantly on proximal (conflict free) or proximal and distal (conflict-affected) cues. In this experiment conflict free navigation is considered preferential navigation since the rat's behaviour exhibit the trained place preference and conflict-affected navigation is considered non-preferential navigation. This experiment gives us the opportunity to examine the behaviour of place cells in relation to place preferences with a sufficient number of passes in the non-preferential section of the arena. Insufficient number of passes results in incomplete experience for the formation of place fields (106) and invalidates the evaluation of their properties (82).

4.11 Data evaluation

To evaluate the data generated during the experiments (see: 4.8 Open field recordings; 4.9 Rectangular-shaped linear track; 4.10 Continuous T-maze) three Matlab (The MathWorks, Inc.) scripts had to be written. To produce this scripts was the primary task in this thesis. These scripts were designed to read the datasets provided by the dacq recording system (Axona, Ltd.) and store the quantitative results of the analysis into Excel files (Microsoft Corporation) and plots into postscript files.

4.12 Spike-specific data

4.12.1 Spike waveform

For calculation of the spike waveform, first, all spikes identified as belonging to the cell under examination have to be averaged. The Axona dacq output dataset includes a collection of all identified spikes. Each spike is stored as a series of 50 sample points. The spike waveform is calculated as an average across all spikes of one channel and is displayed with +/- standard deviation. The spike waveforms were used to ensure constancy between the recordings. Significant changes in the waveform between the recordings indicates a displacement of the tetrode. This would make the different

recording sessions not comparable since it cannot be ensured if the same cell was observed across all recording sessions.

4.12.2 Spike properties

The spike properties, spike width, spike amplitude and spike height, are now calculated from those mean waveforms. To do so, the peaks of the waveforms have to be calculated. The peaks are defined as the sample point at which the slope equals zero and the slope changes from positive to negative or vice versa. The positive peak of the waveform is the global maximum that satisfies the before mentioned condition. The negative peak is defined as the local minimum of the interval from the start till the positive peak that satisfies the before mentioned condition. If no negative peak can be found the local minimum of the interval from the positive peak till the end that meets the before mentioned condition was defined the negative peak. If no peak can be found, the negative peak is defined the last sample point in the series. The spike properties are calculated as follows:

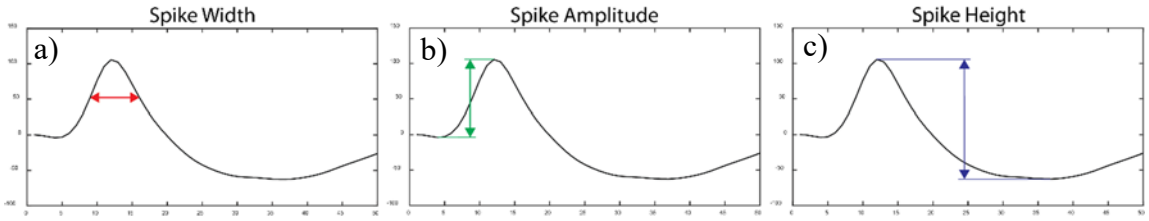

Figure 4-6: Definition of the spike properties: a) spike width, b) spike amplitude, c) spike height

Spike width: the spike width is the duration in which the amplitude of the wave is above 50% of the peak amplitude (red arrow, Figure 4-6 a).

Spike amplitude: The spike amplitude is defined as the difference between the positive peak and the negative peak (green arrow, Figure 4-6 b).

Spike height: The spike height is defined as the difference between the global maximum and the global minimum (blue arrow, Figure 4-6 c).

The spike properties were like the spike waveform used to ensure constancy between the recording sessions. Here significant changes in the spike width, amplitude and high indicate a displacement of the tetrode

4.12.3 Autocorrelogramm

As mentioned before the autocorrelogram is a standard method to control the quality of the single unit separation (see: 2.13 Autocorrelogram). The autocorrelation $\rho_f(t)$ of the

function f(τ) is the cross correlation of f(τ) with itself. The autocorrelation is defined as follows (Bracewell, 1965.):

$$\rho_f(t) = f(\tau) * f(\tau) = \int_{-\infty}^{\infty} f(\tau)\bar{f}(\tau - t)\, d\tau \quad (11)$$

Where $\bar{f}$ is the complex conjugate of f. Since the spike trains are discrete and real the autocorrelation can be calculated as:

$$\rho_f(l) = \sum_{n=-\infty}^{\infty} f(n)f(n-l) \quad (12)$$

Two histograms in different resolutions were used in the scripts. One in a high resolution (0.1ms) over a small interval around zero (-10ms – 10ms) and one with a low resolution (10ms) and a big interval around zero (-1000ms – 1000ms).

4.12.4 Spike cluster

To plot the spike cluster, the spike height (see: 4.12.1 Spike waveforms; 4.12.2 Spike properties) of every spike recorded at each channel of the current tetrode, which was identified as a spike of a place cell, has to be calculated. The spike height of one channel is now plotted against the spike height of another channel for each spike and all combinations of channels, where different cells are indicated by different colours.

Table 4-1: Presentation of the spike cluster in the output files

X-axis: Spike height channel 2 Y-axis: Spike height channel 1	X-axis: Spike height channel 3 Y-axis: Spike height channel1	X-axis: Spike height channel 4 Y-axis: Spike height channel 1
X-axis: Spike height channel 3 Y-axis: Spike height channel 2	X-axis: Spike height channel 4 Y-axis: Spike height channel 2	X-axis: Spike height channel 4 Y-axis: Spike height channel 3

The spike cluster is used to control the single unit separation. If no defined patches of spikes can be identified, this indicates incorrect single unit separation. It also enables us to observe the generation of new or the vanishing of existing place fields.

4.12.5 Mean frequency

The mean frequency is calculated as follows:

$$f_{mean} = \frac{n_{total}}{t_{total}} \quad (13)$$

Where n_{total} is the number of all spikes of the cell under examination during the recording session and t_{total} is the duration of the recording session. This the mean frequency was used below to calculate the spatial population vector.

4.13 Spike and path dependent data

4.13.1 Ratemaps / place fields

As mentioned before (see: 2.10 Place cell firing analysis) the analysis of spatial firing pattern start with the motion tracking data of the rat and the timestamps of the spikes of the place cell under examination from this data we can plot a path and spike map (Figure 4-7). To plot this map each motion data sample point was plotted connected in the order its timestamp. The spike coordinates were obtained by comparing the spike timestamp with motion data timestamps.

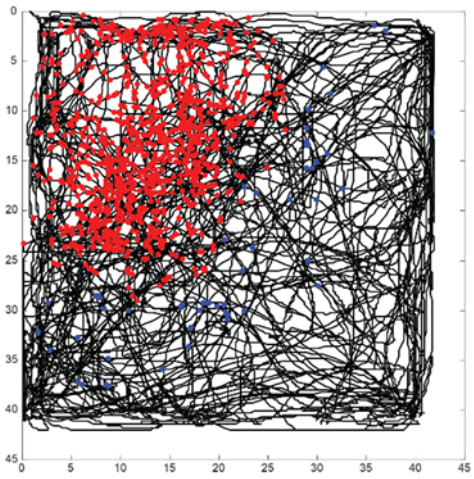

Figure 4-7: Exemplary path and spike map from open field recordings

For further analysis, firing rate maps, which represent the average firing frequency in Hertz for each bin, have to be calculated. For the calculation of the firing rate maps (short: ratemaps), the arena is divided into single bins, with a bin size of 2.5 cm x 2.5 cm. This was found to be a suiting size to prevent outlier and under-sampling but still offers a good resolution. This size lies within the commonly used range of 2 cm – 3 cm (8; 38; 24). For each bin, the dwell-time t_d, calculated from the number of sample points n and the

sampling frequency f_s, was calculated. The dwell time and the number of spikes were stored in time- and firing-maps.

$$t_d = n \cdot \frac{1}{f_s} \quad (14)$$

From this two maps, two different kinds of rate maps can be calculated. The raw ratemap is calculated by a bin-wise division of the firing- and the dwell-time-map (Figure 4-8) (8)This ratemap is used to calculate the quality of the recording of the place cell activity (see 2.10 Place cell firing analysis).

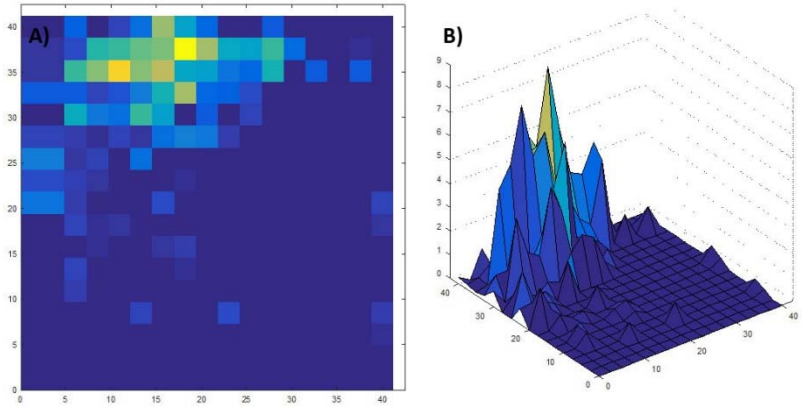

Figure 4-8: Raw ratemaps, a) two-dimensional, b) three-dimensional

As mentioned before place fields can be modelled as a Gaussian or the summation of multiple Gaussians (see: 2.1 Place cells). Therefore, a more accurate representation of the place fields can be obtained from a smoothed ratemap. For the calculation of the smoothed ratemap, the dwell-time and firing map is low pass filtered by replacing each bin by the average of that bin and its eight closest neighbours and afterwards correcting for edge effects (15; 13). The smoothed ratemap is then calculated by bin-wise division of smoothed firingmap and timemap (Figure 4-9). The same method was used at the stimcomp_open_opto_v3 script to create the artefact maps. Here the spike location was replaced by the location of the onset of a stimulation event.

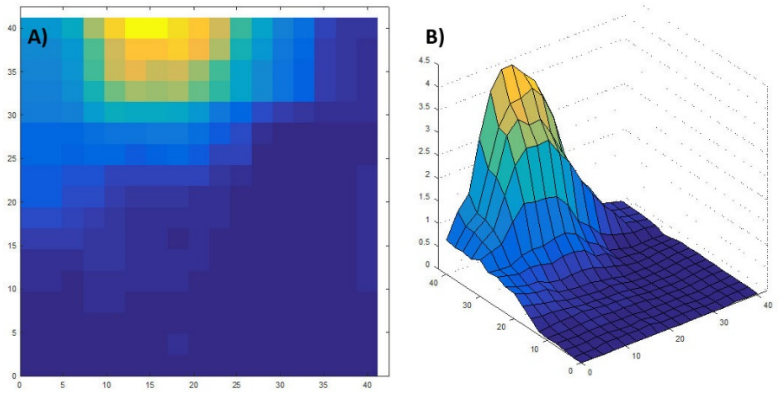

Figure 4-9: Smoothed ratemaps, a) two-dimensional, b) three-dimensional

To describe the spatial firing behaviour of the place cells we needed to define place fields. Two different kinds of place fields were used, raw place fields were derived from raw ratemap and smoothed place fields were derived from smoothed ratemaps. We defined a place field as a cluster of nine or more (80; 17) adjacent bins, sharing at least one edge (17; 84) and having a mean firing rate above 0 Hz for the raw place field (80). And 20% of the maximum firing rate for the smoothed place field (107; 11; 15). Since not all place cells have multiple or sub place fields, at the open field recording just the biggest place field was considered, while at the T-maze and the linear rectangular track all fields larger than eight bins were considered to increase the sensitivity of the symmetry measurement. To make the ratemaps more easy to read they were usually displayed as a levelled ratemap were the frequency were grouped in different level (0 - 16.7%; 16.7 – 33.3%; 33.3 – 50%, 50 – 66.7%; 66.7 – 83.3%; 83.3 – 100%) (Figure 4-10).

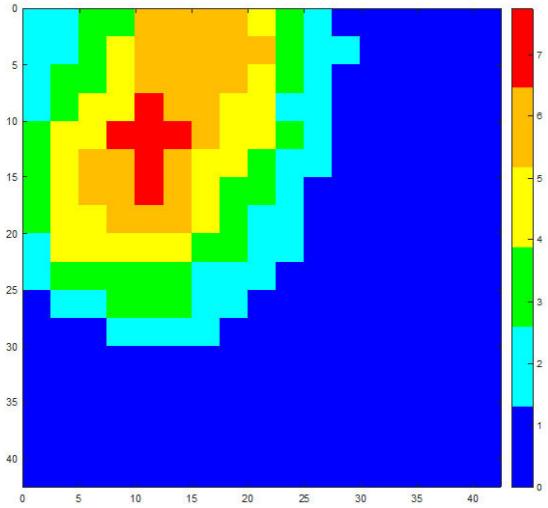

Figure 4-10: Exemplary leveled presentation of a smoothed ratemap of an open field recording

4.13.2 Spatial specificity / spatial information content (Skaggs)

The spatial information content is a commonly used property to describe the spiking activity of a place cell (see: 2.12 Information content) calculates as follows:

$$I = \sum_i P_i(\lambda_i/\lambda)\log_2(\lambda_i/\lambda) \quad (15)$$

Where P_i is the occupancy probability in bin i, λ_i is the average spiking rate in bin I and λ is the global average firing rate of the place cell (83). This value gives a measure how much location related information can be gathered by single action potential of a place cell, expressed in bits per spike.

4.13.3 Spatial coherence:

It is calculated by as the Pearson's correlation coefficient r_{AB} between all bins of the ratemap A and a corresponding map of averaged firing rates of the eight nearest neighbours of each bin B (81; 108; 109). The Pearson's correlation coefficient is calculated as follows (110):

$$r_{AB} = \frac{1}{N-1}\sum_{i=1}^{N}\left(\frac{A_i - \mu_A}{\sigma_A}\right)\left(\frac{B_i - \mu_B}{\sigma_B}\right) \quad (16)$$

Where μ is the mean:

$$\mu_A = \frac{1}{N}\sum_{i=1}^{N} A_i \quad (17)$$

And σ is the standard deviation:

$$\sigma = \sqrt{\frac{1}{N-1}\sum_{i=1}^{N}(A_i - \mu_A)^2} \quad (18)$$

This property describes the evenness of the firing distribution of a place cell and can be used as a measure to quantify the quality of the recording

4.14 Place field properties

To characterize the place field several properties regarding the location, size and frequency distribution have been calculated.

4.14.1 Centre of mass (COM)

The calculation of the centre of mass of a place field is based on the calculation of the centroid of an area, which is defined as (111):

$$x_s = \frac{\int x\, dA}{\int dA};\ y_s = \frac{\int y\, dA}{\int dA} \quad (19)$$

Which for areas made up from subareas is defined as:

$$x_s = \frac{\sum_{i=-\infty}^{\infty} x_i A_{x,i}}{\sum_{i=-\infty}^{\infty} A_{x,i}};\ y_s = \frac{\sum_{j=-\infty}^{\infty} y_j A_{y,j}}{\sum_{j=-\infty}^{\infty} A_{y,j}}; \quad (20)$$

Where x_i is the x-coordinate of the centroid of subarea A_{xi}, y_j is the y-coordinate of the centroid of subarea A_{yj}. The subareas A_{xi} and A_{yj} can be further divided and expressed as a sum of smaller subareas:

$$A_{x,i} = \sum_{j=-\infty}^{\infty} A_{i,j};\ A_{y,i} = \sum_{i=-\infty}^{\infty} A_{i,j} \quad (21)$$

Which results in:

$$x_s = \frac{\sum_i \sum_j x_i A_{i,j}}{\sum_i \sum_j A_{i,j}};\ y_s = \frac{\sum_i \sum_j y_j A_{i,j}}{\sum_i \sum_j A_{i,j}} \quad (22)$$

This, however, does not consider the frequency distribution of the ratemap. To make it sensitive to the frequency distribution we weight substitute the subarea $A_{i,j}$ by a constant size A and frequency $f_{i,j}$:

$$A_{i,i} = f_{i,j} \cdot A \quad (23)$$

Since size A is constant it can be reduced, the centre of mass can be calculated as follows:

$$x_s = \frac{\sum_i \sum_j x_i f_{i,j}}{\sum_i \sum_j f_{i,j}};\ y_s = \frac{\sum_i \sum_j y_j f_{i,j}}{\sum_i \sum_j f_{i,j}} \quad (24)$$

The centroids $c_{i,j}$ of the subarea $A_{i,j}$ are defined as follows:

$$c_{i,j} = \left(i \cdot l_{bin} - \frac{l_{bin}}{2} \quad j \cdot l_{bin} - \frac{l_{bin}}{2}\right) \quad (25)$$

Where l_{bin} is the length of the edge of the bin. Thus the centroids of the subareas are defined as:

$$x_i = i \cdot l_{bin} - \frac{l_{bin}}{2};\ y_j = j \cdot l_{bin} - \frac{l_{bin}}{2} \quad (26)$$

So the absolute coordinates of the centre of mass (x_s y_s) are:

$$x_s = \frac{\sum_i \sum_j i \cdot f_{i,j}}{\sum_i \sum_j f_{i,j}} \cdot l_{bin} - \frac{l_{bin}}{2};\ y_s = \frac{\sum_i \sum_j j \cdot f_{i,j}}{\sum_i \sum_j f_{i,j}} \cdot l_{bin} - \frac{l_{bin}}{2} \quad (27)$$

As mentioned before (see: 2.10 Place cell firing analysis) the centre of mass is a commonly used and reliable method to describe the spatial location of place fields. It was also used to calculate the COM-distance (see: 4.20 COM-distance).

4.14.2 Centre rate / Centre rate location (CR)

As mentioned before (see: 2.10.2 Peak rate centre) the centre rate is another method to describe the place field location. The CR is calculated by creating a map of the place field, where each bin of the place field was replaced by the average frequency of that bin and its eight closest neighbours. The centre rate is now defined as the global maximum of that map and the centre rate location is the centroid of the bin exhibiting the centroid rate. However, it has been proven to be less reliable as the COM method, but it still can give us information about the place field shape. This method calculates the centre rate of the place field and its location. It is more reliable to show the peak rates of place fields of raw ratemaps since it is, due to the averaging, less prone to outliers than just looking for the global maximum.

4.14.3 Place field size

The place field size is defined as the number of bins belonging to a place field. It was calculated for the place field of the smoothed ratemap.

4.14.4 Grand rate

The grand rate is defined as the average firing frequency of a cell within its place field it is calculated by the number of spikes occurring within the place field n_{pf} and the time spent in the place field t_{pf}.

$$f_{grand} = \frac{n_{pf}}{t_{pf}} \quad (28)$$

4.15 Comparative analysis

The open field recording experiment's aim was to evaluate the influence the effect of stimulation events on the firing pattern of hippocampal place cells. The stimcop_open_opto_v3 script was designed to evaluate differences between the baseline

and stimulation sessions of the same or different recording sessions. Therefore, the script provides in the output the shift of the centre of mass as well as the change in the skewness of the pass dependent firing for passes through the place field either close to the COM or the centre rate. It also provides the change in the spatial coherence and the change in the spatial information content.

4.15.1 COM-shift

The shift of the COM (see: 4.14.1 Centre of mass(COM)) is presented as the direction vector,

$$\overrightarrow{COM_{base}COM_{sstim}} = \left(COM_{stim,x} - COM_{base,x}, COM_{stim,y} - COM_{base,y}\right) \quad (29)$$

pointing from the COM of the baseline session (COM_{base}) towards the COM of the stimulation session (COM_{stim}). And the distance of the COM-shift calculated as the norm of the direction vector.

4.15.2 Change of spatial coherence

The change in the spatial coherence Δr (see: 4.13.3 Spatial coherence) was calculated analogue to the shift of pass dependant firing:

$$\Delta r = r_{stim} - r_{base} \quad (30)$$

4.15.3 Change of spatial information content

The change spatial information content ΔI (see: 4.13.2 Spatial specificity / spatial information content) was calculated analogue to the shift of pass dependant firing:

$$\Delta I = I_{stim} - I_{base} \quad (31)$$

4.15.4 Influence of the stimulation location

To analyse the impact of the stimulation location on the place field location, the place fields have to be compared in respect to the stimulation location. Therefore, a ratemap of the stimulation events was created by the same means as for common rate maps (see: 4.13.1 Ratemaps/place fields) with the difference, that instead of the locations of the place cell spikes the location of the onset of an electrical MFB- or an optogenetic VTA-stimulation-event was used. Below this ratemap of the stimulation location is named “artefact map”. To evaluate the influence of the stimulation location both the firing

pattern of the baseline session and the firing pattern of the stimulation session has to be compared to the stimulation pattern. As mentioned before (see: 2.15 Bhattacharyya distance) the Bhattacharyya distance is a measurement of the similarity of two different distributions, where absolute similarity is represented by a Bhattacharyya distance of 0 and no overlap is represented by an infinite distance. In this work, the Bhattacharyya distance was used to determine to which extent optogenetic VTA-stimulation or electrical MFB-stimulation shift the place field of a hippocampal place cell towards the stimulation location. The Bhattacharyya distance B is defined as (112).

$$B = -log \int \sqrt{g(x)f(x)}dx \quad (32)$$

Where g(x) f(x) are the two compared distributions. Since the distributions in this work are discrete and two-dimensional we can use this formula:

$$B = -log \sum_{x \in X} \sum_{y \in Y} \sqrt{g(x,y)f(x,y)} \quad (33)$$

The two distributions compared by the Bhattacharyya distance in this work were the ratemap of the cell under examination (f(x,y)), which was named basemap for the baseline session and stimmap for the stimulation session in the output file of the script, and the artefact map(g(x,y)). For both, baseline and stimulation session the Bhattacharyya distance was calculated for raw base-/stim-map and raw artefact-map as well as for smoothed base-/stim-map and smoothed artefact-map (smoothing: see: 4.13.1 Ratemaps/place fields). Smoothing was applied to make the measurement more sensitive to the spatial distance between the two distributions since smoothed ratemaps are more spread, which will increase the overlap. Using smoothed ratemaps also minimize the influence of noise and the shape of the place field/stimulation event distribution. Since a difference in the magnitude of the two distributions will affect the distance each ratemap were normalized by the sum of all mean frequencies within that ratemap before the Bhattacharyya distance was calculated. For visual inspection cross-maps of the bin-wise overlap between basemap or stimmap and the artefact map was plotted. The overlap o_{xy} was defined as:

$$o_{xy} = \sqrt{g(x,y)f(x,y)} \quad (34)$$

4.16 Arena fitting

To apply the symmetry measure, it is important to have a sufficient fit of the motion data to the arena. Several factors impede fitting. Since the linear rectangular track and the T-maze consist of narrow, elevated walkways without walls the rat is not entirely constricted to the arena and can cut corners and peek outside of the arena. Because of the rat's position is being tracked by an IR-LED positioned at the head-stage above the head there can be tracking samples outside of the arena, especially at corners (Figure 4-11). Another factor impeding the fitting is the lack of a referencing system between the arena and the motion tracking system.

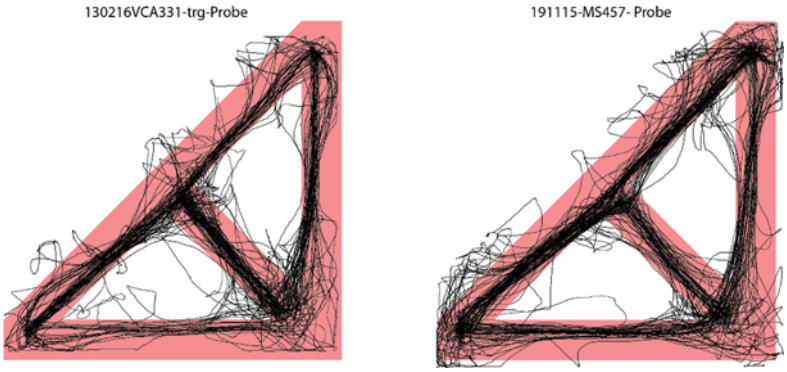

Figure 4-11: Rat's trajectory compared to the real arena shape for two sessions

As it can be seen in Figure 4-11, the motion data sample points cannot be directly fitted into an arena shaped stencil. To fit the motion data, a referencing system has to be created. Such a referencing system needs specific points which can be identified in the motion data and are linked to some landmarks in the arena. Figure 4-12 a/b shows the expected passes through the choice points, where passes from or towards the stem (red arrows, Figure 4-12) are supposed to be more frequent than direct passes between the east and south quadrants of the arena (green arrows, Figure 4-12). Since the real passes will be somehow distributed around that theoretical passes, it is to be expected that an accumulation of motion data sample points can be found in the area enclosed of the theoretical paths. A second assumption is that direct passes (green arrows, Figure 4-12) are faster than passes from or toward the stem since the rat has to turn less, and thus contribute fewer motion data sample points. As a result of this, the most motion data sample points are expected to be found at the borders of the stem (dashed lines, Figure 4-12 c).

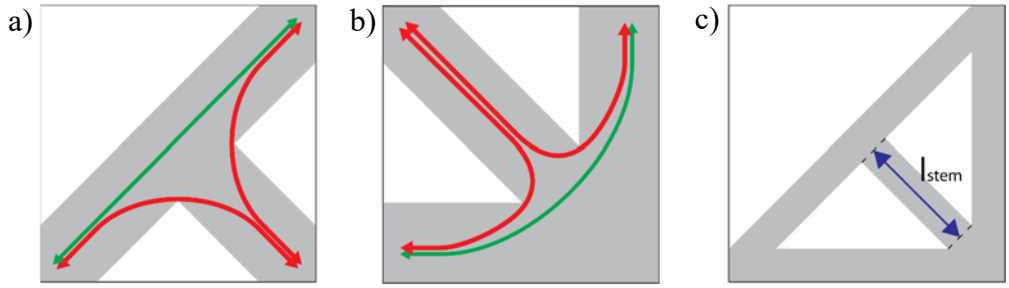

Figure 4-12: Schematic of T-maze: a) passes through choice point 1, b) passes through choice point 2, c) schematic of the T-maze arena

To find the accumulation of motion data sample points, the arena was divided into 1cm x 1cm bins and the number of sample points per bin was counted. Afterwards, the map was convolved with a 5 x 5 array of ones and normalized by the convolution of the same array with a map-sized array of ones. The smoothed motion sample map was divided into nine equal parts, the middle and the south-east section (purple rectangles, Figure 4-13 a) were searched for a local maximum. These maxima (red squares /red arrows, Figure 4-13) were now defined as reference points. The mean distance of the reference points for the T-maze was 33,2 cm ±2,4cm, which matches the length of the stem l_{stem} = 33,1cm. This confirms the assumptions about the position reference points, made before.

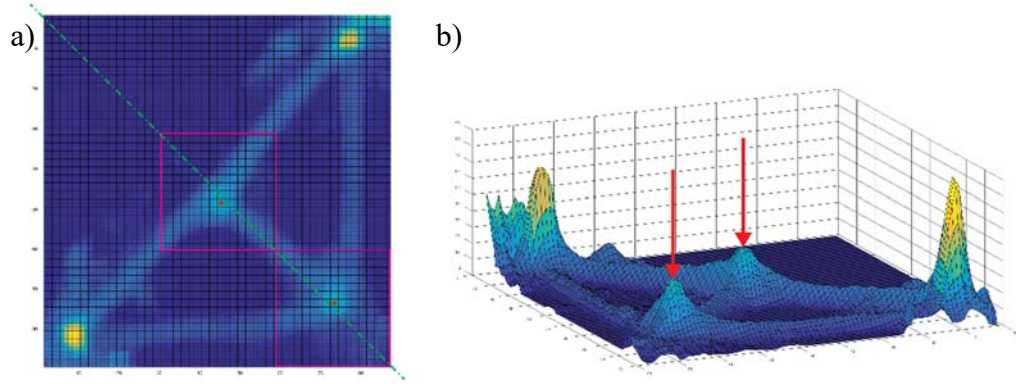

Figure 4-13: Motion sample point map T-Maze, a) 2D map with symmetry axis (green dashed line) and expected locations of the choice points (purple squares), b) 3D map with indicated reference points (red arrows)

Analogue to the T-maze, the reference points for the linear rectangular track, were defined. Here the locations of the food reward were expected to show the biggest accumulation of motion data sample points. To find these sites, the arena was divided into 16 equally sized sections and the most north-west and the south-east sections (purple rectangles, Figure 4-14 a) were searched for local maxima, which then were defined as reference points (red squares/ red arrows, Figure 4-14)

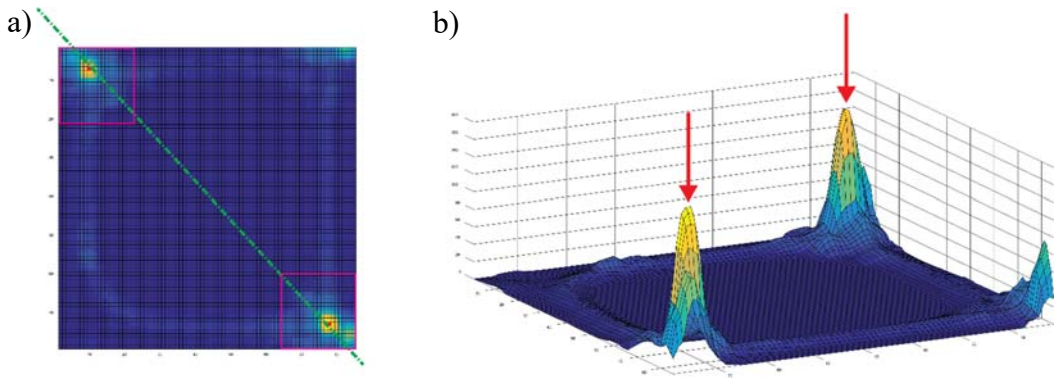

Figure 4-14: Motion sample point map rectangular-shaped linear track, a) 2D map with symmetry axis (green dashed line) and expected locations of the reward sites (purple squares), b) 3D map with indicated reference points (red arrows)

To fit the symmetry axis, which has to meet the criteria x = y, to the reference points r_1, r_2 an offset in y-direction o_y was calculated:

$$o_y = \frac{(r_{1,y} - r_{1,x}) + (r_{2,y} - r_{2,x})}{2} \quad (35)$$

The offset was then added to the y-coordinate of all motion data sample points.

4.17 Behavioural data (pass sorting)

The rat's path through the arena was analysed to calculate the number of passes through different quadrants of the arena and to investigate the behaviour of the rat in the choice points (T-maze) and the number of passes and the time spent in each half of the arena (linear rectangular track). The same factors that impede the arena fitting (see: 4.16Arena-fitting) obstruct the pass sorting. To overcome those problems, two adaptive systems using the reference points (see: 4.16Arena-fitting) have been created.

4.17.1 T-maze

The primary task at the T-maze was to describe how the rat behaves at the choice points (Figure 4-5), meaning how often the rat turns in which direction. Since the movement of the animal is not entirely restricted to the arena, for each recording session the area around the choice points has to be set individually, to catch every pass through the choice point and allow the definition of entry-/exit-zones. To do so, an iterative method was used. This method uses an unsmoothed map representing the number of motion samples per 1 cm x 1 cm bin and the reference points defined before (see: 4.16 Arena-fitting). For choice point 1 the area around the reference point (red square, Figure 4-15) was incrementally increased by 2 cm each step. After each step the direct divider between east and south

quadrant, sitting in the top left corner of the choice point area (purple area, Figure 4-15 a) was checked if it contains motion sample points. This was repeated till no motion sample points could be found within the direct divider area. That divider was defined to have a width of 2 cm and a leg length of one-quarter of the edge length of the choice point area.

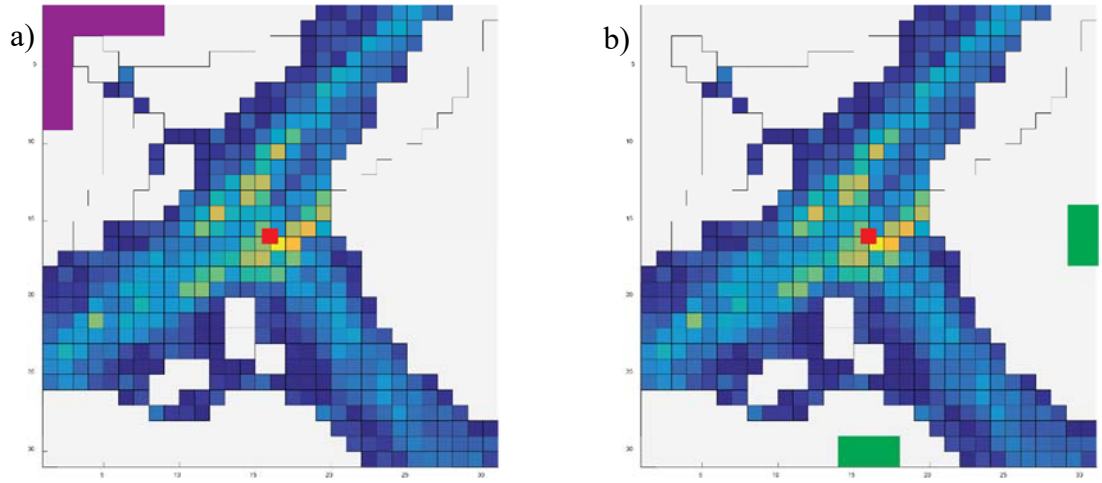

Figure 4-15: Definition of the choice point 1 area and divider, a) direct exit zone divider (purple area), b) indirect exit zone divider (green areas)

After defining the choice poin1 area-size that cover all passes through the choice point 1 it was checked if the choice point area was big enough to separate motion data samples on the stem from samples on the hypotenuses of the surrounding triangular track. Therefore, the indirect divider (green rectangles, Figure 4-15) checked for motion data sample points. If motion data sample points were found within one of the areas of the indirect divider the choice point area was further increased till no motion sample points were found in the area of the indirect divider. The indirect divider was defined as a rectangle with 2 cm width and a length of 10 % of the edge length of the choice point area and sits in the middle of the lower respectively the right edge of the choice point area. Due to the different geometry of choice point 2, a different method was needed. Here the choice point area size was defined as by the reference point and the maximal values of the motion data sample points in x- and y- direction:

$$S_{CP2} = \begin{cases} 2 \cdot dist_x + 1cm & ; dist_x > dist_y \\ 2 \cdot dist_y + 1cm & ; dist_x < dist_y \end{cases} \quad (36)$$

Where S_{CP2} is the size of the choice point 2 area and $dist_x$, $dist_y$ is the distance of the reference point to the maximum value in x- and y- direction (yellow arrows, Figure 4-16 a)

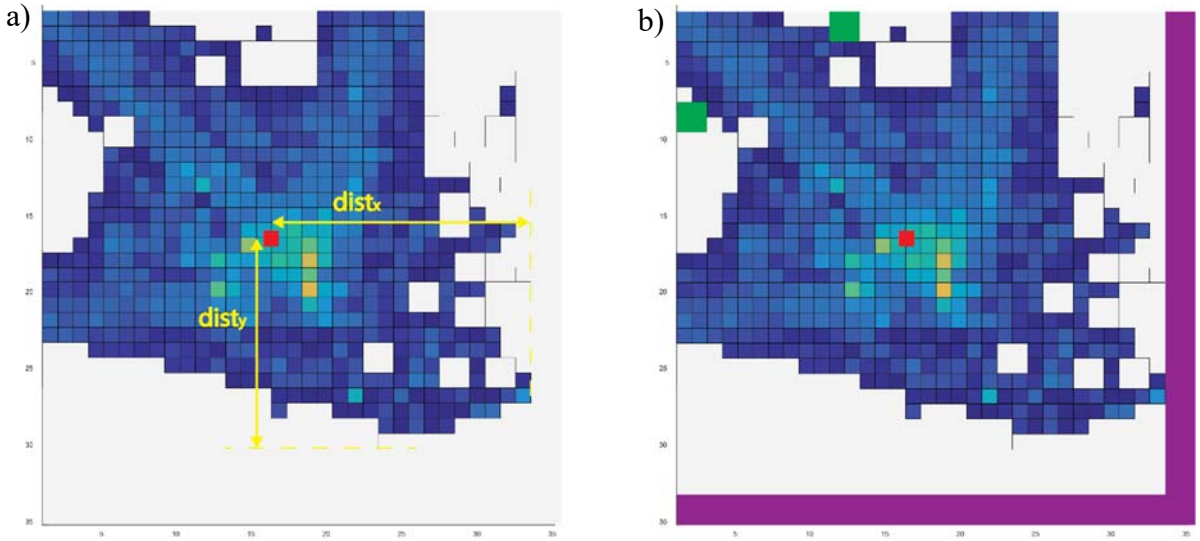

Figure 4-16: Definition of the choice point 2 area and divider a) distance of reference point to maxima, b) definition of direct (purple area) and indirect (green areas) exit zone dividers

The direct divider (purple area, Figure 4-16 b) is defined by the geometry of the arena. The indirect divider, a 2 cm x 2 cm rectangle, (green squares, Figure 4-16 b) were slid from the top left corner along the left, respectively the top edge till a position was reached, where no motion sample points could be found within the indirect divider area. Based on the defined dividers and the choice-point-size entry-/exit-zones were defined as 2 cm wide areas, lying inwards on the edge of the choice point area between the dividers.

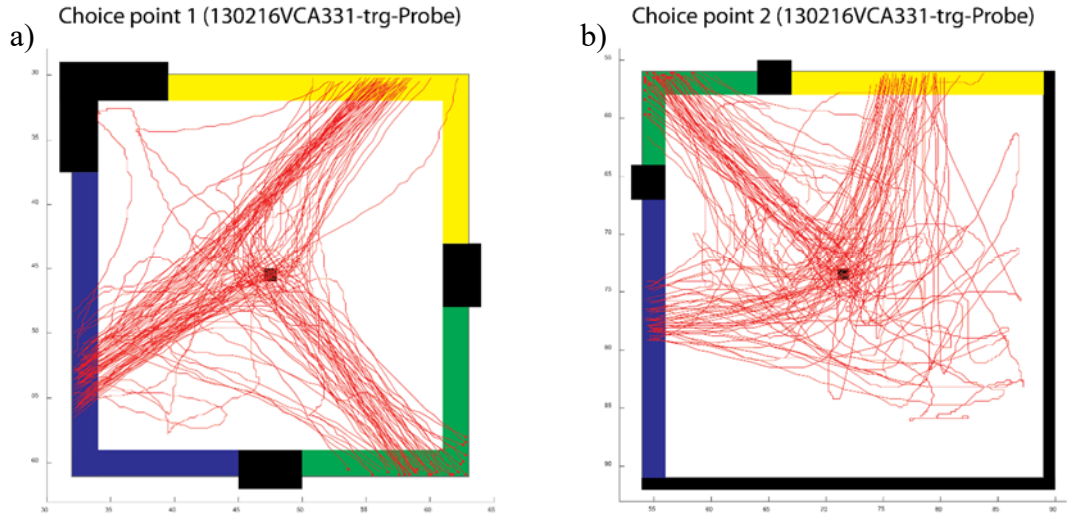

Figure 4-17: Passes through the choice points a) Choice point 1, b) choice point 2

Illustrated in Figure 4-17 are the passes (red) through choice-point 1 (left) and choice-point 2 of the session: 130216VCA331-trg-Probe. Between the dividers (black) the entry-/exit-zones for the south quadrant (blue), the east quadrant (yellow) and the stem (green) were defined. To analyse the passes each motion data sample point was were checked whether it lies within one of the choice point areas or not. Consecutive series of sample points within one of the choice points were defined as a pass and the timestamps of start

and endpoint of those passes were saved. The start and endpoints were now checked for the entry-/exit-zone they lie in. The first and the last pass through a choice-point at the recording was dismissed if the recording started or ended within the choice point and thus were missing an entry or an exit timestamp. Also passes, consisting of just one data point were dismissed. Knowing where the rat entered and exited the choice point area, the behaviour of the rat at the junctions could be described. Three categories were evaluated: coming from the stem and either leaving to the south or east quadrant, coming from either the south or the east quadrant and leaving to the stem and direct passes towards the south or the east quadrant.

4.17.2 Linear-rectangular track

Here the behavioural analysis was easier to realize than at the T-Maze since at the linear rectangular track just the time spent in each half and the number of passes through each half of the arena as to be calculated. To do so, the arena was separated into four zones (Figure 4-18).

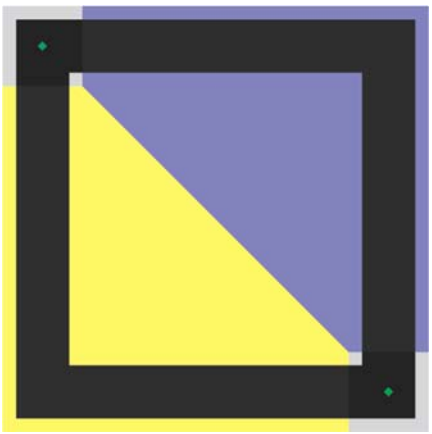

Figure 4-18: Linear rectangular track divided into neutral zones (grey squares), north-east half (blue area) and south-west half (yellow area)

These zones were north-east half (blue) south-west half (yellow) and two neutral zones around the reward position (green rhombi). The neutral zones where needed to differentiate reliably between passes toward one-half of the arena and the rat scurrying around while picking up the food reward. To determine the size of the neutral zones the corrected motion data sample points (see: 4.16 Arena-fitting) were again separated into 1 cm x 1 cm bins and the bins along the symmetry axis (x=y) were copied into a vector. This vector was used to find the start and the length of the longest connected group of bins containing no motion sample points (red bins, Figure 4-19).

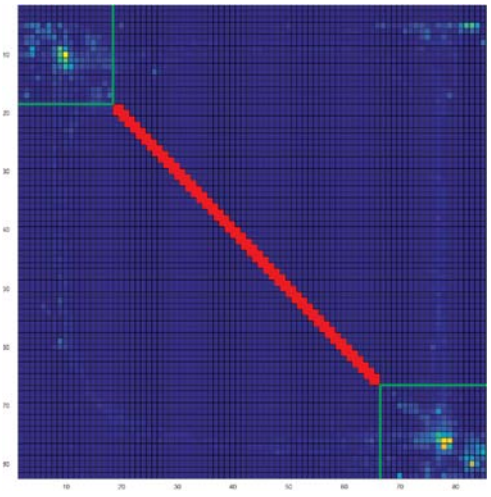

Figure 4-19: Definition of neutral zone size

The borders of the neutral zones (green rectangles) were then set to include all motion sample data points along the symmetry axis. Each data point was now checked whether it lies in one of the neutral zones or in the north-east (N-E) respectively the south-west (S-W) half of the arena. The timestamps of the entry into and exit from the N-E / S-W halves were saved to define a pass. Only complete passes were considered, so the first and the last pass were dismissed when it started/ended within the N-E or S-W half. Also, the neutral zone from which the rat entered one-half of the arena and to which it left were saved to describe the direction of movement. Since the rat moved directly between the neutral zones, without turning around somewhere in-between, all passes starting and ending at the same neutral zone were considered scurrying and thus dismissed. For each half, the total number of passes were count as well as the number of passes in each direction (north-west to south-east/south-east to north-west). To calculate the time, spend in each half, the number of data points per pass have been computed and added up for each half and each direction and multiplied by the sampling interval (0.02 seconds).

4.18Symmetry method evolution

As mentioned before the evaluation of symmetry was intended to be a measure for the evenness of the distribution of firing pattern in arenas that are symmetric and impede the use of COM-based methods, which are suitable for open arenas but have a limited suitability for describing the firing patterns over a whole arena consisting of just small tracks like the linear rectangular track or the T-maze. To my knowledge, no method to calculate the symmetry of place fields was used before. As mentioned before the symmetry can be expressed as an average of the bin-wise comparison of bins in symmetric locations (see: 2.16 Symmetry), where a symmetry value of 1 means full symmetry and a value of 0 means total non-symmetric. Since in this work, the coordinate system was set, so the symmetry axis meets the condition: x = y, the symmetry can also be expressed as the similarity between a ratemap and its transposed copy. So the first idea was to use standard similarity measures like the 2D-correlation. The 2D-correlation was found to be not a suitable method as the correlation can be negative, which would represent anti-symmetry. However, the idea of calculating the similarity of two distributions as a sum of a bin-wise overlap was kept for later use. To design a method to compute the symmetry, different approaches were taken. To start the development, a method was searched to quantify the fundamental symmetry of the firing pattern based purely on the spike location. The two basic ideas were either to compare the ratemap bin-wise or to calculate the overlap between the place fields. The direct bin-wise comparison was considered not entirely reliable since the position of the symmetry axis could not be determined with full confidence this was shown as the average distance of the reference points at the T-maze showed a standard deviation in the range of the bin size (see: 4.16 Arena-fitting). To compensate for that, the bin-wise method was designed to search for each bin containing a firing frequency above zero a bin either at the symmetric location or at the next neighbours of the symmetric location. The method for place field wise comparison measured the overlaps between each place field and each other transposed place field, normalized by the place field size. To evaluate the effectivity of each method. For an ensemble of 10 place cells, desired values for the symmetry of the place fields were subjectively assigned (Table 4-2).

Table 4-2: Comparison of bin- and place field-wise methods

	Desired values	Best bin-wise method	Best place field wise method
Cell 1	0	0.1695	0
Cell 2	0	0.1176	0.0965
Cell 2	0-0.25	0.6914	0
Cell 4	0-0.25	0.4819	0.2428
Cell 5	0.3	0.375	0.5801
Cell 6	0.3-0.4	0.4179	0.4316
Cell 7	0.5-1	0.6413	0.6186
Cell 8	0.9-1	0.7288	0.7436
Cell 9	0.9-1	0.625	0.78
Cell 10	1	0.898	0.8333
	Mean error:	0.05051	-0.00349
	Error rating:	1.2	0.5

To quantify the effectivity, the mean error and the error rating was calculated. The mean error was defined as the average distance of the calculated value to the desired value range, a small mean error represents a small systematic error. The mean error was the sum of the absolute distance of the calculated value to the desired value range rounded down to the first decimal place, to allow small errors since the desired values were defined subjectively. Small error rating represents a small statistical error. For each method several factors were varied, like the number of next neighbours or different extensions for the place fields to make the method more sensitive. Table 4-2 presents just the values of the best method for bin- and place field-wise calculation. As we can see the place field dependent method exhibit a better mean error and a better error rating than the bin-wise method. So the bin-wise method was discarded. To make the method frequency sensitive, the overlap between the place fields were weighted by the average firing frequency.

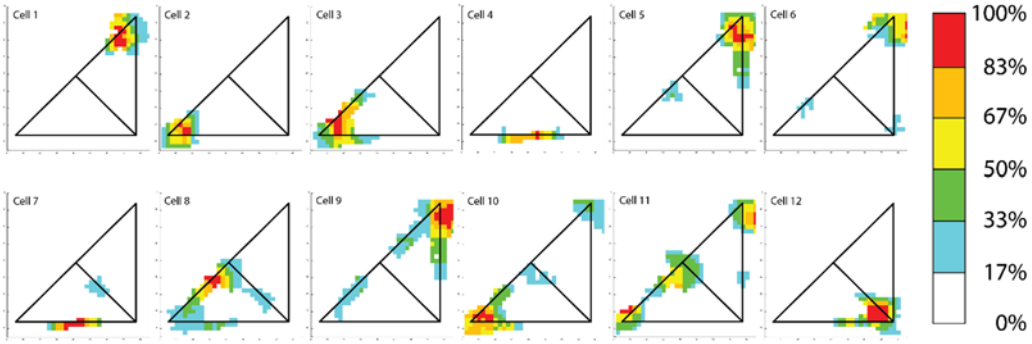

Figure 4-20: Exemplary place fields of a place cell ensemble subjectively ordered for symmetry

The place fields off an ensemble of 12 cells shown in Figure 4-20 subjectively ordered for symmetry was used to verify the method. Calculated symmetry values are given in Table 4-3.

Table 4-3: Calculated symmetry values

Cell number	Symmetry value	Cell number	Symmetry value
1	0	7	0.05255134
2	0	8	0.14876938
3	0	9	0.18852306
4	0	10	0.28320216
5	0	11	0.48576703
6	0.00287435	12	0.6512057

It can be seen that the calculated symmetry values follow the subjective order. However, since this method just considers average frequencies, it is not sensitive to the frequency distribution within the place field, which can lead to wrong results. Given the example in Figure 4-21, which has a high overlap at low frequencies but no overlap at the high frequencies.

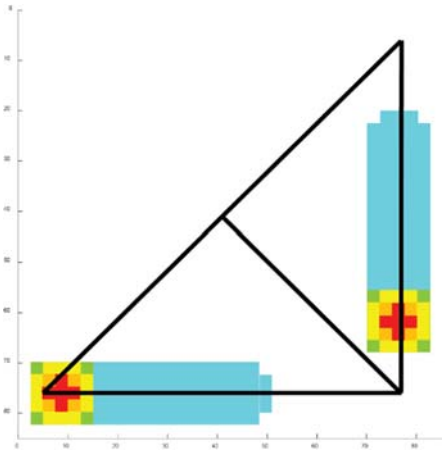

Figure 4-21: Exemplary low-symmetry place fields

The method concerning just average frequencies would have resulted in a high symmetry value. To fight this error and make the method more sensitive to symmetries of peaks the place fields were separated into several frequency levels (see: 4.19 Symmetry method), which were then checked for overlap which each place field for the same or lower level. The symmetry values for the frequency distribution sensitive method (Table 4-4) show now increased symmetry values for overlapping peaks (e.g. cell 10, 12) and decreased values general overlap in place fields but with less symmetric peaks (cell 11).

Table 4-4: Calculated symmetry values final method

Cell number	Symmetry value	Cell number	Symmetry value
1	0	7	0.10784314
2	0	8	0.12030075
3	0	9	0.17608889
4	0	10	0.39931574
5	0	11	0.46447811
6	0.00537634	12	0.73368495

For an exact description of the method, see 4.19 Symmetry method.

4.19Symmetry method

As mentioned before, this method senses the symmetry of the symmetry of the place fields and its frequency distribution over the place fields. The basic principle is to calculate the symmetry of the distribution of one or more place fields adding up the overlap between place fields and weighting it by the fraction of the frequency levels at the point of overlap. The symmetry of a place cell's firing distribution is calculated from its smoothed ratemap with the size [M bins x M bins] and its corresponding thresholded place field-map containing N place fields, consisting of nine or more bins (see: 4.13.1 Ratemaps/place fields). The resulting ratemap of the place fields is created by setting all bins that are not part of a place field to zero.

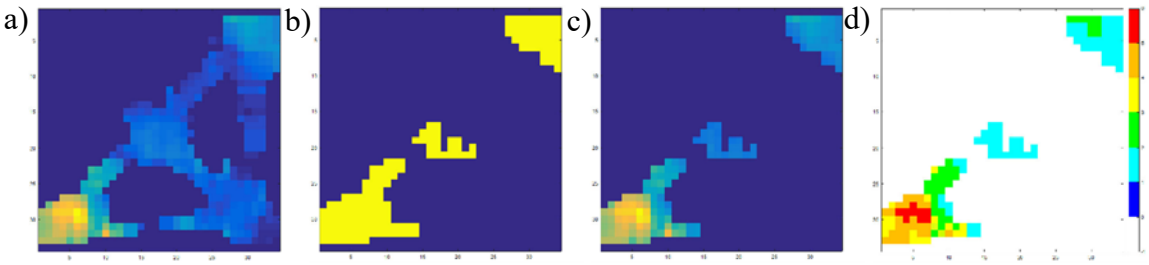

Figure 4-22: Ratemaps and place fields for symmetry analysis, a) smoothed ratemap, b) thresholded place fields, c) resulting ratemap for the place field, d) resulting leveled ratemap for the place fields

The resulting map is grouped into six levels (>0, >1/6 f_{max}, >2/6 f_{max}, >3/6 f_{max}, >4/6 f_{max}, >5/6 f_{max}) according to the maximum firing frequency of the ratemap (f_{max}) and separated into the single place fields. Because of the threshold at the calculation of the place field, the 0- 1/6 f_{max} level does not contribute to the place field shape and its symmetry, so it was ignored. The maps presented in Figure 4-23 are considered binary.

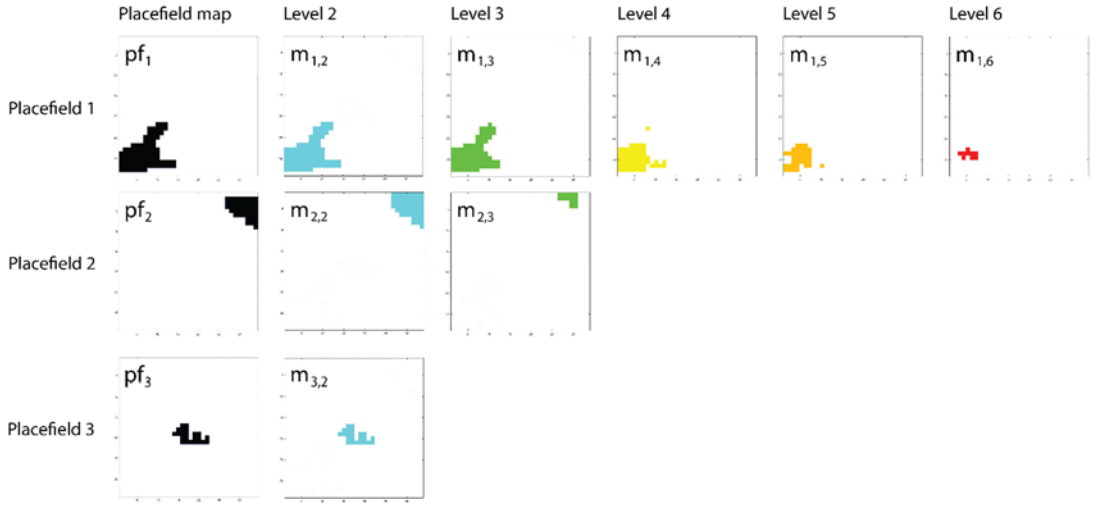

Figure 4-23: Maps of each place field separated into levels

For each level l $\{l \in \mathbb{N} | \ 2 \leq l \leq 6\}$ a [N x N] relation matrix is created by counting the overlap between each map ($m_{n,l}$) and each transposed map ($m^t_{m,k}$) of the same or lower level and the transposed placefield map (pf^t_p)

$$R_l = \begin{bmatrix} r_{1,1,l} & r_{1,m,l} & \cdots & r_{1,N,l} \\ r_{n,1,l} & r_{n,m,l} & \cdots & r_{n,N,l} \\ \vdots & \vdots & \ddots & \vdots \\ r_{N,1,l} & r_{N,m,l} & \cdots & r_{N,N,l} \end{bmatrix} \quad (37)$$

The N x N sized relation matrix displays the relations between place field n at level l and place field m

$$r_{n,m,l} = A_{n,l}^{-1} \cdot o_{n,m,l} \quad (38)$$

The relation between place field n at level l and place field m ($r_{n,m,l}$) is the overlap between placefield n at level l and placefield m ($o_{n,m,l}$) normalized by the area of placefield n at level l($A_{n,l}$).

$$o_{n,m,l} = \sum_{i=1}^{M}\sum_{j=1}^{M} m_{n,l}(i,j) \cdot \left(pf_m^t(i,j) + \sum_{k=2}^{l} m_{m,k}^t(i,j) \right) \quad (39)$$

The overlap between place field n at level l and place field m is the sum of the multiplication of the value of bin (i,j) of the map of place field n at level l ($m_{n,l}(i,j)$) and the value of the bin(i,j) transposed placefield map ($pf_m^t(i,j)$) of placefield m and the value of the bins(i,j) transposed maps of placefield m at all levels equal and smaller l ($m_{m,k}^t(i,j)$).

$$A_{n,l} = l \cdot \sum_{i=1}^{M}\sum_{j=1}^{M} m_{n,l}(i,j) \quad (40)$$

Where $A_{n,l}$ is the area, expressed by the number of bins, of place field n at level l weighted by the level l.

From the relation matrix, we can calculate the spatial symmetry (SS_l) for each level by adding up the rows of the relation matrices and weight it by the ratio of the area of place field n at level l divided by the sum of the areas of all place fields in level l (w_{nl}).

$$SS_l = \sum_{n=1}^{N} w_{n,l} \sum_{m=1}^{N} r_{n,m,l} \quad (41)$$

$$w_{n,l} = \frac{A_{n,l}}{\sum_{n=1}^{N} A_{n,l}} \quad (42)$$

The spatial symmetry of the firing characteristics of the cell is an average of the spatial symmetries of each level weighted by the ratio of the area of all place fields in level l divided by the sum of the area of all place fields in all levels (A_{total}).

$$S_{spat=} \sum_{l=2}^{6} SS_l \cdot \frac{\sum_{n=1}^{N} A_{n,l}}{A_{total}} \quad (43)$$

$$A_{total} = \sum_{l=2}^{6}\sum_{n=1}^{N} A_{n,l} \quad (44)$$

4.19.1 Symmetry angle θ_{SS}

To present the symmetry in a more intelligible way and make it comparable to the COM distance it was expressed in the form of an angle. There, in the case of an arena symmetric to an axis in the direction from the north-west to the south-east corner, a symmetry angle of 0° represents a total non-symmetric distribution, weighted towards the south-west half of the arena. A symmetry angle of 45° represents a total symmetric firing distribution, and a symmetry angle of 90° represents a total non-symmetric distribution weighted towards the north-west half of the arena. The symmetry angle Θ_{ss} was calculated as follows:

$$\theta_{SS} = \begin{cases} s_{spat} * 45°, COM_x < COM_y \\ 90° - s_{spat} * 45°, COM_x > COM_y \end{cases} \quad (45)$$

Where S_{spat} is the spatial symmetry value and COM_x, COM_y is the X-, Y- coordinate of COM.

4.20 COM-distance

The calculation of the COM is a commonly used method to describe the firing distribution of a place cell (see: 4.14.1 Centre of mass COM). However here the calculation of the COM in the form of two-dimensional coordinates is not suitable since the firing distribution was needed to be described in the form of a one-dimensional variable, with respect to the symmetry axis. Therefore, I created the normalized COM-distance (short: COM-distance) measure, which describes to which extent the COM deviates from the symmetry axis. To reliably calculate the COM-distance the motion data sample points have to be fitted to virtual arena borders (Figure 4-24) to ensure correct normalization. The virtual arena borders are a square surrounding all motion data sample points. The fitting was done by sliding all motion data sample points along the symmetry axis and adjusting the arena border size till d_1 (distance between reference points and arena border) was equal for both reference points, or the d_2 (distance between middle point of the arena borders and middle point between the two reference points) was 24,5cm (defined by arena geometry).

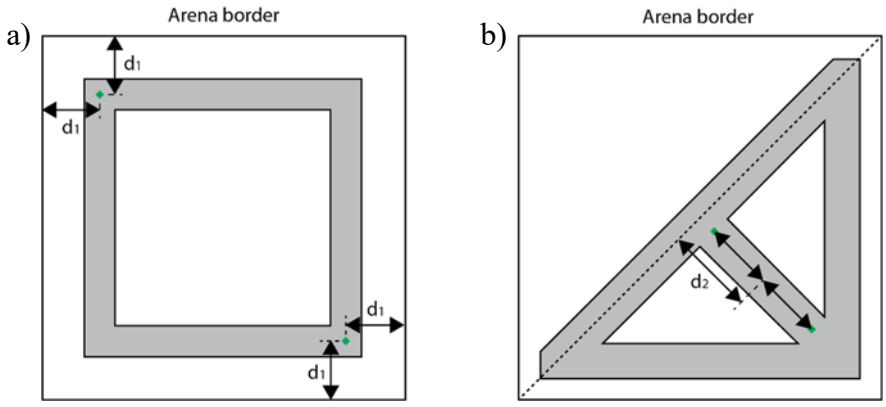

Figure 4-24: Fitting to virtual arena border, a) rectangular-shaped linear track, b) continuous T-maze

The symmetry axis was defined by its origin O (O_x,O_y) and its direction D (D_x,D_y). The distance between the COM (COM_x,COM_y) and the symmetry axis was calculated as follows

$$dist_{COM/sym} = \frac{\left|det\begin{bmatrix} D_x - O_x & D_y - O_y \\ COM_x - O_x & COM_y - O_y \end{bmatrix}\right|}{\sqrt{(P_x - O_x)^2 + \left(D_y - O_y\right)^2}} \quad (46)$$

Since the arena borders are defined as a square surrounding all motion tracking sample points with an equal distance to the real limits of the arena at all sides, the normalized COM distance could be calculated according to the following scheme (Figure 4-25).

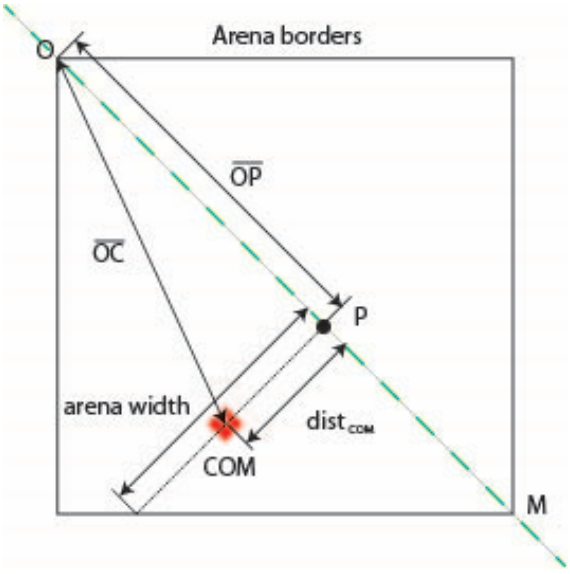

Figure 4-25: Calculation scheme for COM-distance

Knowing $dist_{COM}$ we can calculate the distance OP (distance between the origin and the COM-projection on the symmetry axis) as follows:

$$\overline{OP} = \sqrt{({COM_x}^2 + {COM_y}^2) - {dist_{COM}}^2} \quad (47)$$

According to the Pythagorean theorem the distance of the COM to the symmetry axis normalized by the arena-width $dist_{norm}$ could be calculated as follows:

$$dist_{norm} = \left\{ \begin{array}{c} \frac{dist_{COM}}{\overline{OP} \cdot C}, \overline{OP} < \frac{\overline{OM}}{2} \\ \frac{dist_{COM}}{(\overline{OM} - \overline{OP}) \cdot C}, \overline{OP} > \frac{\overline{OM}}{2} \end{array} \right\} \quad (48)$$

Where $\overline{OM}$ is the diagonal through the arena border between the origin O and the point M and C is a correction factor to compensate outliner in the motion tracking data and is set to 0.95 for the T-Maze and 0.85 for the linear rectangular track

4.20.1 COM-angle

The COM-distance was analogue to the spatial symmetry, presented as an angle where 0° represent a distribution totally weighted towards the south-west half of the arena, 45° an even distribution and 90° a distribution totally weighted towards the northeast half of the arena. The COM –angle is now calculated:

$$\theta_{COM} = \begin{Bmatrix} 45° \cdot (1 - dist_{norm}), COM_x < COM_y \\ 45° \cdot (1 + dist_{norm}), COM_x > COM_y \end{Bmatrix} \quad (49)$$

4.21 Spatial Population vector

In this work, we used the population vector of the place field distribution D as well as the grand rate population vector F to describe the collective behaviour of the whole population of place cells recorded. To calculate the spatial population vector, a cell collection was created in the form of a *.mat file where the cell identifier (tetrode number, cell number) the COM- and symmetry-angle and the mean firing frequency of the cell was stored. The population vector of place field distribution consists of the COM-angle of each cell $\theta_{COM,n}$ where n indicates the cell index

$$D_n = \theta_{COM,n} \quad (50)$$

$$F_n = \frac{s_n}{\Delta t_{tot}} \quad (51)$$

s_n: number of spikes of cell n; Δt_{tot}: duration of the measurement

The spatial population vector is not a population vector which is commonly used in relation with hippocampal place cells. Here the spatial population vector refers to the use of population vector like Georgopoulos, et al. (1986) introduced the term to describe the intended motion of a population of motor neurons (see: 2.14 Population vector). According to that, the spatial population vector represents the behavior of the firing distribution of all place cells within a population. The spatial population vector weighted by the mean firing frequency of the cells $SPV_{weighted}$ is calculated as the dot-product of the grand rate population vector F and the population vector of place field distribution D normalized by the 1-norm of the grand rate population vector.

$$SPV_{weighted} = \frac{F \cdot D}{\|F\|_1} \quad (52)$$

And the average spatial population vector SPV_{avg} is defined as the 1-norm of the population vector of place field distribution D, normalised by the number of place cells N in the population:

$$SPV_{avg} = \frac{\|D\|_1}{\mathrm{N}} \quad (53)$$

The 1-norm of a vector is defined as the sum of its elements:

$$\|F\|_1 = \sum_{n=1}^{N} |F_n| \; ; \; \|D\|_1 = \sum_{n=1}^{N} |D_n| \quad (54)$$

4.21.1 Frequency percentage

The frequency percentage p_f is the place cell's mean firing frequency normalized by the sum of the average firing frequency f_i of all N cells in the collection

$$p_f = \frac{f_i}{\sum_{i=1}^{N} f_i} \quad (55)$$

5 Results

5.1 Stimcomp_open_opto_V3

This script was designed to analyse the open arena recording. It was capable of analysing different baseline and stimulation sessions for the same place cell and compare the results. This script creates cell specific output files for the particular baseline-/stimulation-session pairs. To execute the script full path and filename of the baseline session *.set-file, of the stimulation session *.set-file and of the Stimulation session *.log-file as well as the desired tetrode and cell number has to be defined.

Command:

stimcomp_open_opto_v3('[baseline *.set-file]', '[stimulation *.set-file]', '[stimulation *.log-file]', [tetrode number], [cell number])

The main tasks of the script were:

- *Analysis of spike specific data:* Plot spike shape, autocorrelogram, and spike cluster. Calculate spike width, spike amplitude, spike height, mean firing frequency (see: 4.12 Spike-specific data).
- *Analysis of path and spike dependent data:* Plot spike/path map, calculate and plot raw and smoothed ratemaps, calculate raw / smoothed place field, calculate map correlation, Skaggs, and spatial coherence (see: 4.13 Path and spike dependent data).
- *Analysis of place field properties:* Calculation of centre rate, centre rate, COM (see 4.14.1 Centre of mass), grand rate and field size (see: 4.14 Place field properties).
- Comparative analysis: calculation of COM- and Skaggs-shift between baseline and stimulation session. Calculation and comparison of the Bhattacharyya distance between the artefact map (ratemap of the simulation events) and the ratemap for the baseline and the stimulation session (see: 4.15 Comparative analysis)

5.2 Stimcomp_tmaze_V3

This script was designed to analyse and display the results of the continuous T-maze task training and probe sessions combined. It is capable of creating output files for each recorded cell (cell specific results) as well as an ensemble of simultaneously recorded cells (population specific results). To execute the script, the full path- and filename of the *.set-file of the probe session and of the training session, the full pathname of the output folder, the tetrode and cell number as well as a save flag has to be defined. The save flag was a flag set to either 0, 1 or 2 and indicates if the current cell should be added to [1] or removed from [2] the cell collection for calculating the population vector or if just cell-specific tasks should be executed [0].

Command:

stimcomp_tmaze_v3('[probe *.set-file]', '[training *.set-file]', '[output folder]', [tetrode number], [cell number], [save flag])

The main tasks of this script were:

- *Analysis of spike specific data:* Plot spike shape, autocorrelogram and spike cluster Calculate spike width, spike amplitude, spike height and mean firing frequency of the cell (training + probe session). (see: 4.12 Spike-specific data).
- *Arena fitting:* correction of the motion data points to fit the arena / symmetry axis (probe session) (see: 4.16 Arena fitting).
- *Analysis of path and spike dependent data:* Plot spike/path map, calculate and plot smoothed ratemaps, calculate smoothed place field (see: 4.13.1 Ratemaps/place fields) (training + probe session).
- *Analysis of behavioural data:* separation of the trajectory of the rat in the arena into passes through the choice points and analyse the behaviour at the choice points and plot the behaviour at the choice points (see: 4.17 Behavioural data (pass sorting)) (probe session).
- *Analysis of place field distribution:* Calculate and plot the COM-distance (see: 4.14.1 Centre of mass(COM); 4.20 COM-distance) calculate and plot the symmetry (see: 4.19 Symmetry method) (probe session).
- *Population analysis*: Calculate and plot population vector (see: 4.21 Spatial population vector), save population data into a collection for simultaneous recorded cells. (probe session).

5.3 Stimcomp_linrec

This script was designed to analyse and display the results of the linear rectangular track. It is capable of creating output files for each recorded cell (cell specific results) as well as an ensemble of simultaneously recorded cells (population specific results). To execute the script, the full path, and filename of the probe session *.set file, the full pathname of the output folder, the tetrode and cell number, as well as the save flag (see: 5.2 stimcomp_tmaze_v3), has to be defined.

Command:

stimcomp_linrec(' [probe *.set-file]', '[output folder]', [tetrode number], [cell number], [save flag])

The main tasks of this script were:

- *Analysis of spike specific data:* Plot spike shape, autocorrelogram, and spike cluster. Calculate spike width, spike amplitude, spike height and mean firing frequency of the cell. (see: 4.12 Spike-specific data).
- *Arena fitting:* correction of the motion data points to fit the arena / symmetry axis (see: 4.16 Arena fitting).
- *Analysis of path and spike dependent data:* Plot spike/path map, calculate and plot smoothed ratemaps, calculate smoothed place field (see: 4.13.1 Ratemaps/place fields).
- *Analysis of behavioural data:* separation of the trajectory of the rat in the arena into passes through the north-east / south-west half of the arena and plot the different types of paths (see: 4.17 Behavioural data (pass sorting)).
- *Analysis of place field distribution:* Calculate and plot the COM-distance (see: 4.14.1 Centre of mass(COM); 4.20 COM-distance) calculate and plot the symmetry (see: 4.19 Symmetry method).
- *Population analysis*: Calculate and plot population vector (see: 4.21 Spatial population vector), save population data into a collection for simultaneously recorded cells.

5.4 Control of recording quality

By the help of those scripts the data from the three experiments (see: 4.8 Open field recordings; 4.9 Rectangular shaped Linear track; 4.10 Continuous T-maze) were analysed. The spike specific data has not been used to perform specific analysis related to the experiment, but was used to ensure consistency between different recording sessions as well as to check the quality of single unit isolation and single unit identification.

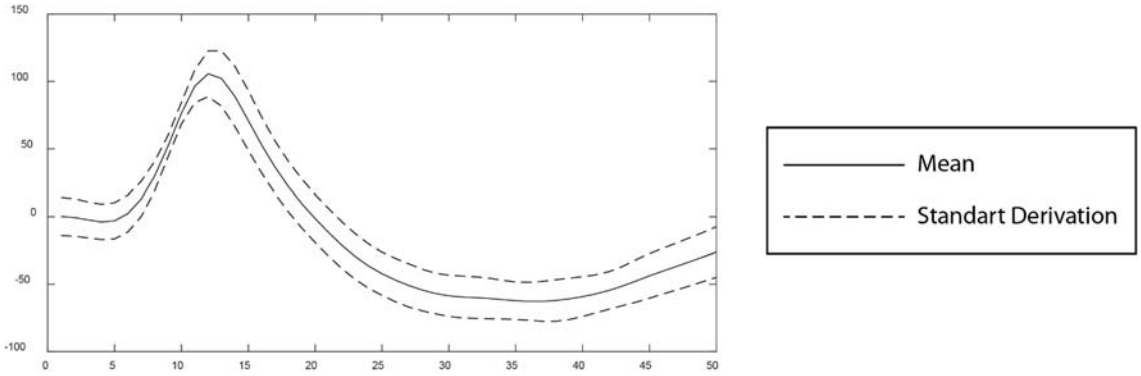

Figure 5-1: Exemplary display of spike waveform

The spike waveforms (see: 4.12.1 Spike waveforms) (Figure 5-1) and the spike properties (spike width, spike amplitude, spike height) (see: 4.12.2 Spike properties) have been compared be between the different recording sessions of one rat for each cell (spike waveform, spike properties). Substantial deviations between different recording sessions indicate a displacement of the tetrode. In the case of a tetrode displacement, it could not be ensured that the same place cell was observed across all recording sessions. As a result, the cells recorded from this tetrode has to be removed from further analysis. The spike cluster (see: 4.12.4 Spike cluster) (Figure 5-10 b) was used for two purposes. First, it can be used as a rough indicator of the quality of single unit separation. If no different patches can be identified this indicates that the spike sorting software failed in reliably separating the spikes and correctly assigning them to individual cells. Second, it is an easy indicator for the appearance of place fields of formerly silent place cells or the disappearance of existing place fields and silencing of place cells in later sessions(Figure 5-10 b).

Autocorrelogramms (see: 4.12.3 Autocorrelogramm) have been calculated for different tasks, the high-resolution autocorrelogram can be used to control the single unit separation. Here spikes within the refractory period 0-2ms (red area, Figure 5-2 a) indicate inadequate separation since the spike train consists obviously of spikes from different neurons. The low-resolution autocorrelogram can be used to control the single unit

identification. As mentioned before (see: 2.1 Place cells) the spiking activity of hippocampal place cells shows a phase correlation with the theta-band activity (7-12Hz). The exhibition of a periodicity in the range of ~83 - ~142ms (green arrows, Figure 5-2 b) in the low-resolution autocorrelogram indicates a good single unit identification. If no periodicity in that range can be identified, this would be a strong indicator that the cell under examination is not a hippocampal place cell.

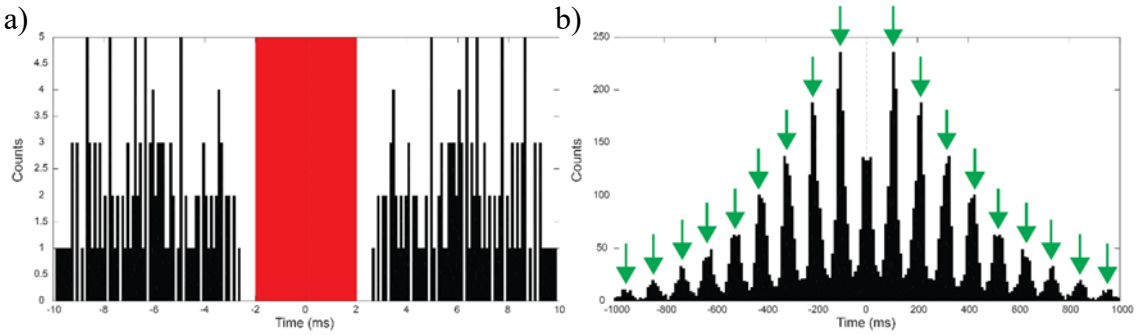

Figure 5-2: Exemplary autocorrelograms a) high resolution, b) low resolution

5.5 Spatial Symmetry:

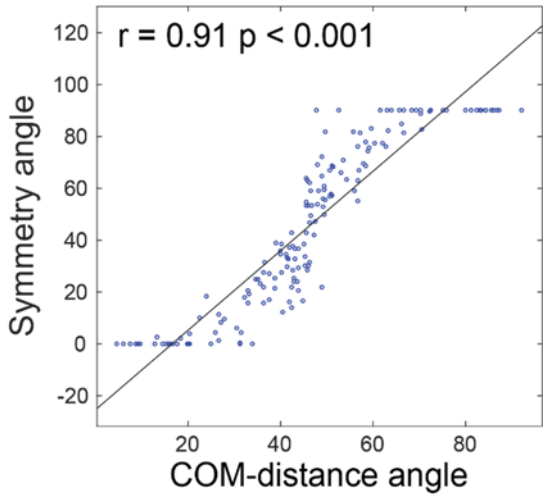

Figure 5-3: Correlation plot between Symmetry angle and COM-distance angle

Comparison of the symmetry angle with the COM-distance angle shows a high correlation (Pearson's r = 0.91) (Figure 5-3).

5.6 Open field recording:

To evaluate the effect of electrical MFB stimulation and optogenetic VTA stimulation on the firing distribution in the open field recording (see: 4.8 Open field recording) several parameters have been analysed (see: 4.14 Place field properties) for comparability all

values have been displayed as ratios between the 1st baseline session and 1st stimulation session / 2nd baseline session / 2nd stimulation session.

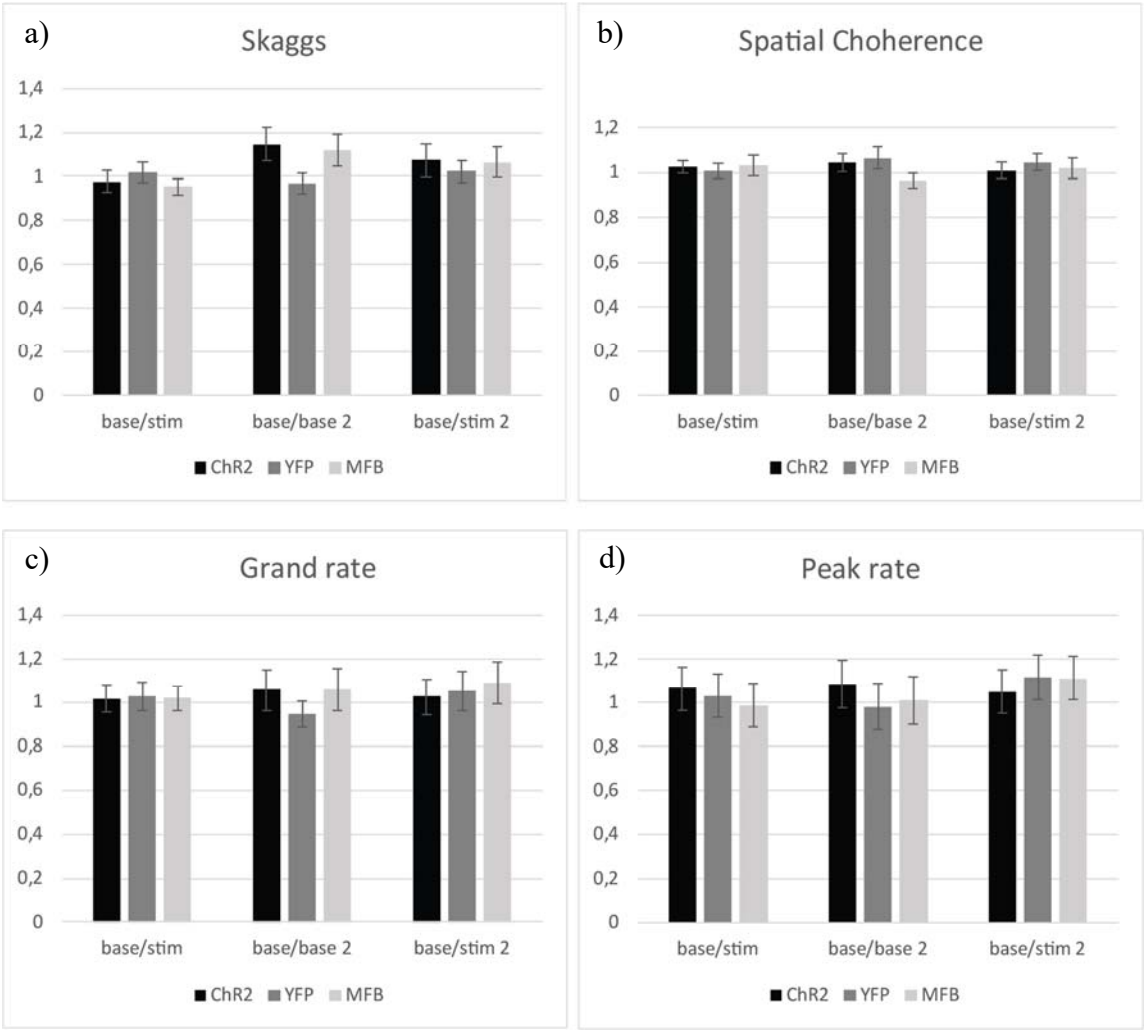

Figure 5-4: Non-location dependent place field properties: ratio of mean a) Skaggs, b) spatial coherence, c) grand rate and d) peak rate between baseline session and stimulation / 2nd baseline / 2nd stimulation session

At none of the non-location dependent place field properties, spatial coherence, Skaggs, peak rate, grand rate (see: 4.13.3 Spatial coherence; 4.13.2 Spatial specificity; 4.14.2 Centre rate; 4.14.4 Gand rate) a significant change between baseline and one of the other sessions could be found.

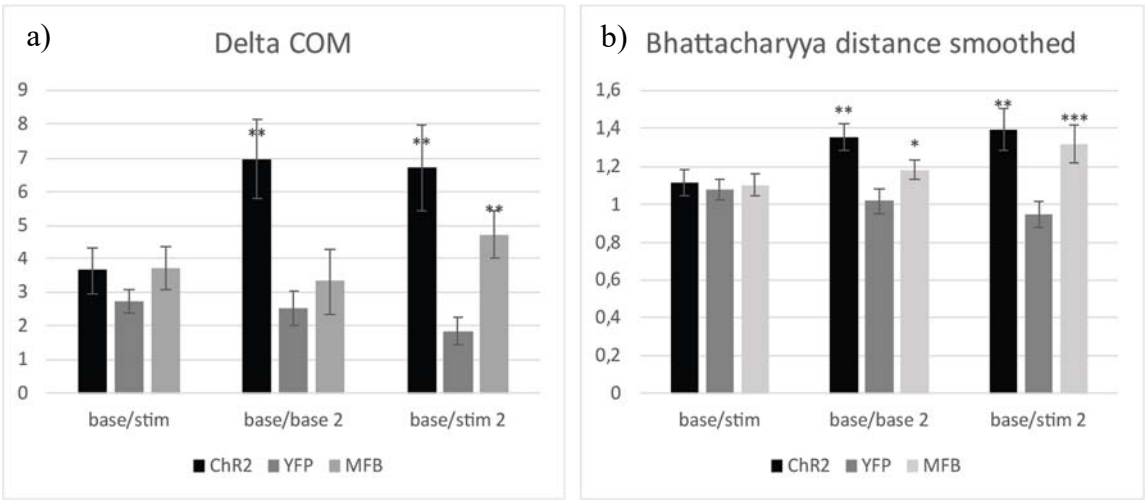

Figure 5-5: Location dependent place field properties: mean a) COM shift, b) ratio of the Bhattacharyya distance for smoothed ratemaps

Location dependent place field properties like the difference in the Bhattacharyya distances and the shift of the COM between the sessions show significant differences (Figure 5-5).

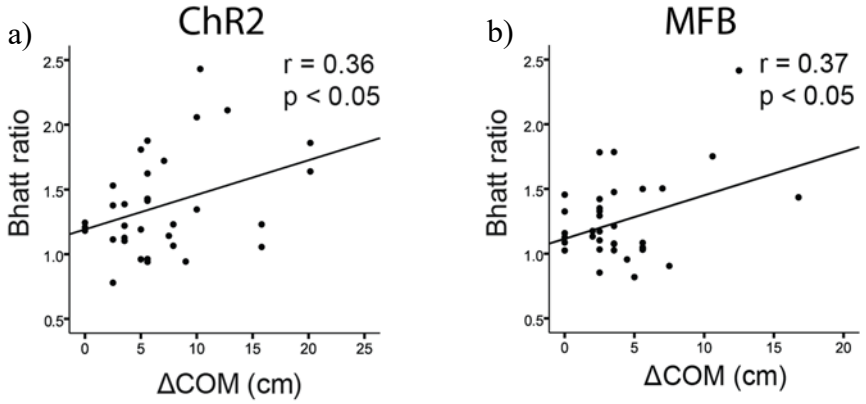

Figure 5-6: Correlation plots between Bhatt ratio and COM-shift for a) VTA-stimulation and b) MFB-stimulation

A significant correlation between the ratio of Bhattacharyya distances and the COM-shift could be found for both cases, MFB and VTA stimulation (Figure 5-6).

5.7 Rectangular-shaped linear track

To describe the behaviour of the rat in the arena the number of passes through each half was compared. (Figure 5-7).

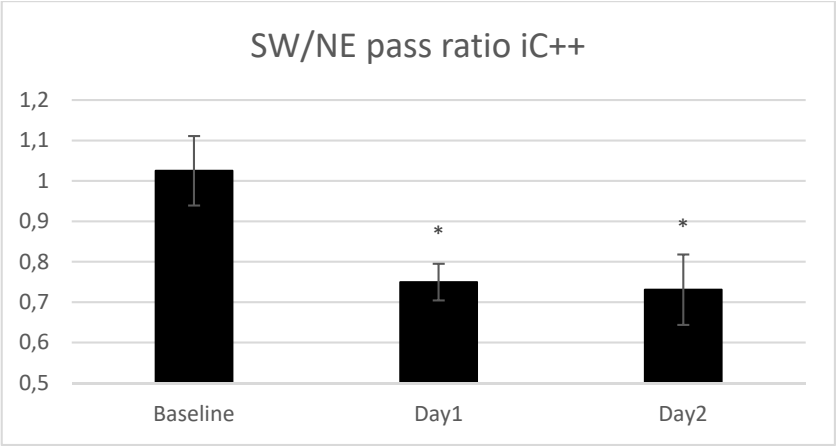

Figure 5-7: SW/NE pass ratio iC++

To investigate the effect of the absence of reward signal, behavioural data and the SPV of the VTA-suppression group (iC++, n=6) and the control group (YFP, n=7) were compared (Table 5-1).

Table 5-1: SW/NE pass ratio and spatial population vector values

	SW/NE pass ratio			SPV weighted			SPV average		
Animal	Base-line	Day1	Day2	Base-line	Day1	Day2	Base-line	Day1	Day2
iC++_1	1.333	0.709	0.583	41.857	49.099	48.490	42.198	53.573	43.135
iC++_2	0.923	0.812	0.500	42.337	45.675	58.280	44.539	46.615	49.906
iC++_3	0.800	0.652	0.869	43.071	45.636	59.888	42.797	46.764	59.106
iC++_4	1.058	0.968	0.911	50.595	67.103	76.875	51.053	63.318	71.369
iC++_5	1.250	0.676	1.028	44.757	42.027	48.606	45.221	45.609	42.919
iC++_6	0.785	0.678	0.491	43.194	50.580	51.147	42.113	47.235	48.225
YFP_1	1.182	1.275	1.070	55.825	58.907	58.578	56.138	57.947	58.624
YFP_2	0.875	1.079	1.044	44.700	43.533	45.205	39.928	39.485	39.746
YFP_3	0.802	0.593	0.744	38.703	31.963	28.773	51.142	42.095	43.818
YFP_4	0.855	0.847	0.581	42.461	41.646	43.504	43.557	45.209	47.019
YFP_5	1.000	1.000	0.265	47.306	51.678	44.439	50.232	50.898	47.736
YFP_6	1.013	1.326	0.883	46.589	43.945	46.031	44.173	39.788	41.998
YFP_7	1.432	0.942	1.289	42.739	53.331	56.227	39.478	42.782	47.698

5.8 Continuous T-maze:

The behaviour of the rat in the arena can be described regarding the number of turns the rat took in each direction at the choice points (Table 5-2/ Figure 5-8).

Table 5-2: Behavioural data continuous T-maze

# rat	South quadrant passes	East quadrant passes	South / East Passes ratio	binomial p
Rat 1	14	8	1.750	0.0762
Rat 2	17	44	0.386	0.0002
Rat 3	33	28	1.179	0.0831
Rat 4	10	13	0.769	0.1363
Rat 5	23	33	0.697	0.0439
Rat 6	0	23	0.000	0.0001
Rat 7	5	33	0.152	0.0000
Rat 8	21	46	0.457	0.0008
Rat 9	25	25	1.000	0.1122
Rat 10	18	32	0.563	0.0160
Rat 11	18	19	0.947	0.1285
Rat 12	19	51	0.373	0.0001
Rat 13	20	16	1.250	0.1063

By calculation of the binomial p-value for passes through the east quadrant two groups of rats could be identified due to their navigation behaviour (Figure 5-8). The two groups were separated by a 5% significance level into preference group ($p < 0.05$, $n=7$) and non-preference group ($p > 0.05$, $n=6$)

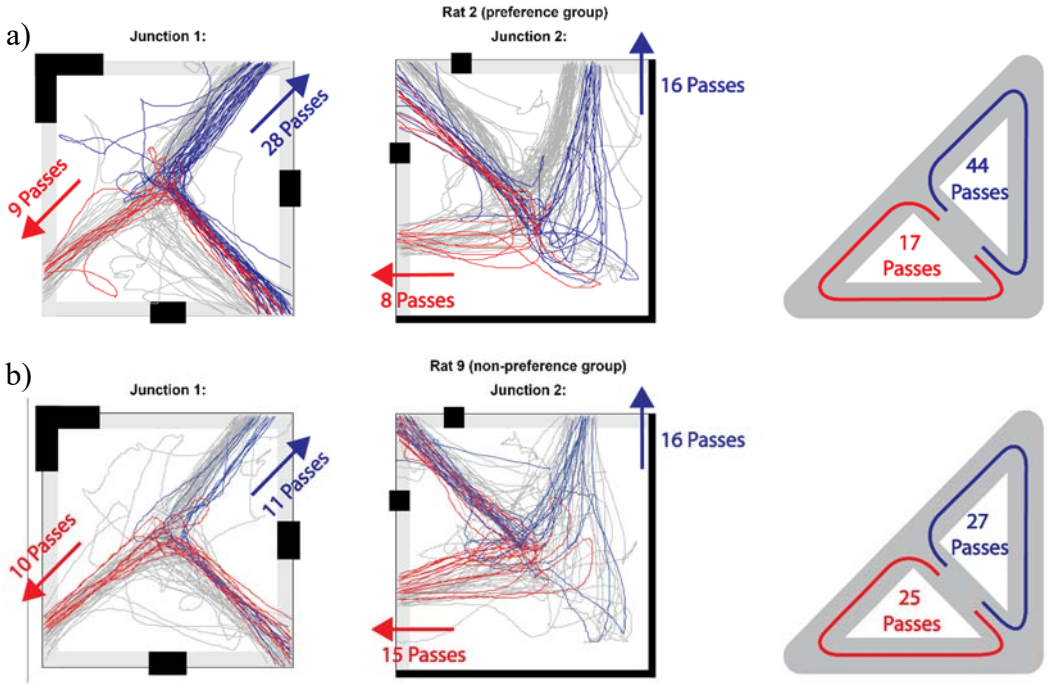

Figure 5-8: Exemplary passes for a) preference group (rat 4) and b) non-preference (rat 5) group

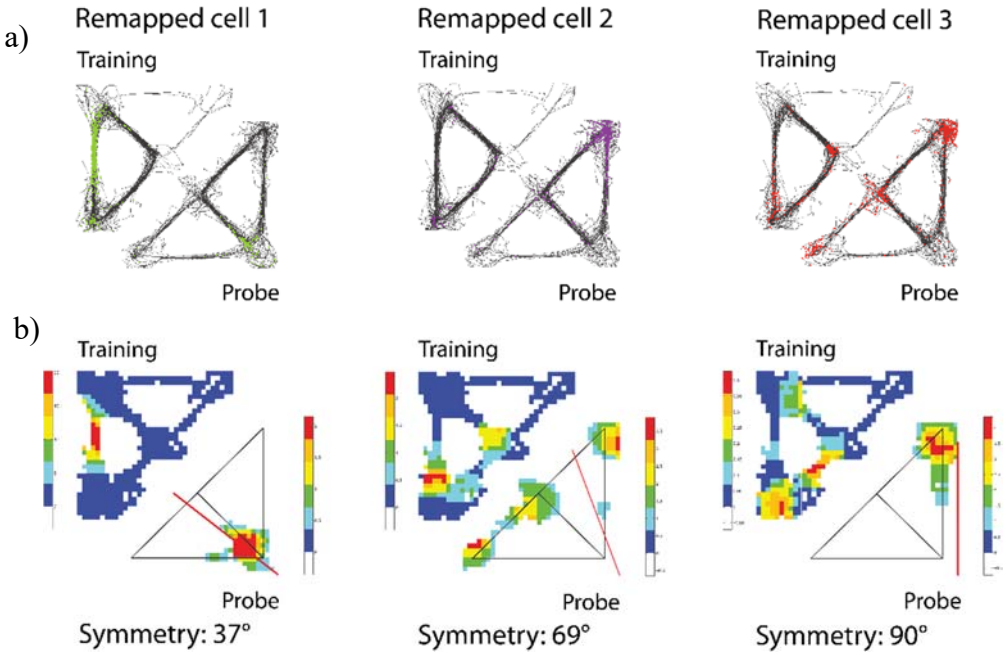

Figure 5-9: Remapped cells a) path/spike maps, b) ratemaps / place fields for training and probe session

169 cells could be identified that exhibit a place field in the west quadrant of the training arena, which was related to reward driven preference (see: 4.10 Continuous T-maze). 48 (28.4%) of those cells lost their place field in the probe arena while 121 (71.6%) remapped their place field exemplary displayed for three cells (Figure 5-9). 47 new cells exhibit a place field in the probe arena but not in the training arena exemplary shown in Figure

5-10 a, two new patches can be observed in the spike cluster at the probe run (Figure 5-10 b) total 216 cells from 13 rats have been recorded.

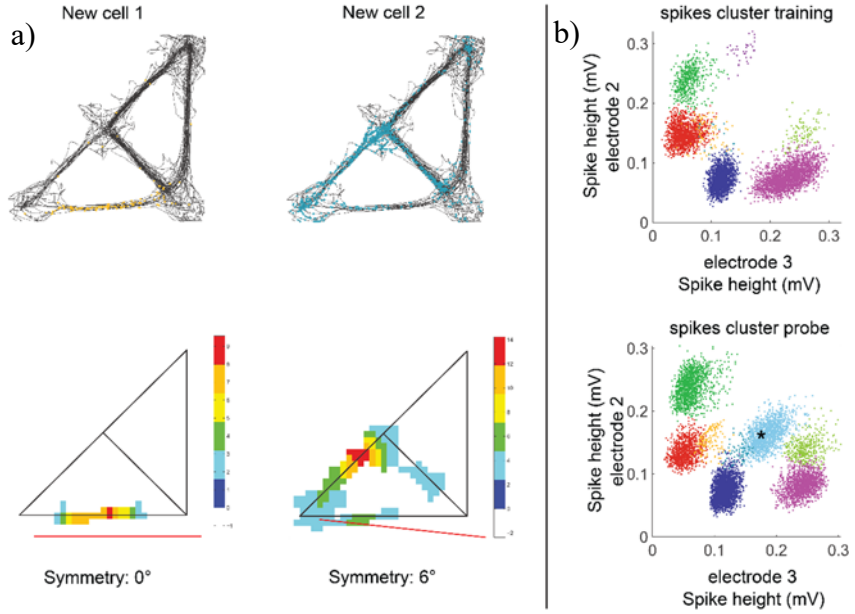

Figure 5-10: Cells with new place field in the probe-arena, a) path/spike maps and place fields, b) spike cluster training/probe

The symmetry-angle (see: 4.19.1 Symmetry angle) was evaluated for all place cells that exhibit a place field in the training as well as in the probe arena, and for the cells that exhibit a place field just in the probe arena. The symmetry values were grouped according to the preference or non-preference behaviour of the rat. The remapped place cells had a mean symmetry angle of 60 ±3.6° for the preference, 36.5 ±3.9° for the non-preference group. Cells that exhibit just new place fields in the probe arena had a mean symmetry angle of 26.3 ± 5.9° for the preference and 53.2 ± 6.9° for the non-preference group. The mean symmetry angel for both types of cells together was 49.9 ± 3.5° for the preference and 40.6 ± 3.4° for the non-preference group. For all three groups, remapped cells, cells with new place fields and combined, the difference between preference a non-preference group was significant (Wilcoxon rank sum test, remapped place fields: $p < 0.001$; new place fields: $p=0.029$; combined: $p=0.0477$).

To describe the place cell's spike distribution for each cell, the COM-distance expressed as the COM-angle (see: 4.20 COM-distance) was calculated. The distributions for all cells of each rat were represented by the spatial population vector in an averaged form, and weighted by the average spiking frequency of the correspondent neuron (see: 4.21 Spatial population vector). The population vector was grouped regarding the behaviour and the cell type. Mean SPV is presented in Table 5-3

Table 5-3: Mean SPV values;

Group	Remapped cells		All cells	
	Weighted SPV	Averaged SPV	Weighted SPV	Averaged SPV
Preference group	54.6 ± 1.6°	54.8 ± 1.8°	50.9 ± 1.4°	48.8 ± 0.7°
Non-preference group	39.7 ± 3.3°	39.9 ± 2.6°	43.2 ± 2.4°	43.3 ± 1.5°

To measure the connection between behaviour and the distribution of the SPV the correlation between the south/east pass ratio and the SPV, presented in Figure 5-11 was calculated.

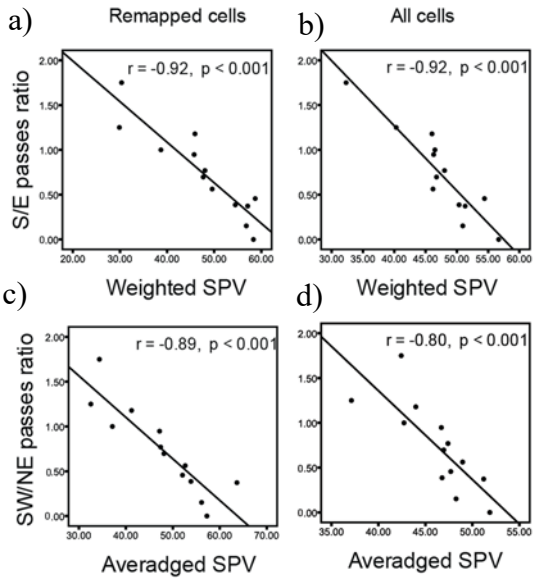

Figure 5-11: Correlation between S/E pass ratio and, a) weighted SPV, remapped cells, b) weighted SPV, all cells, c) averaged SPV, remapped cells, d) averaged SPV, all cells

It can be seen that all cases show a high correlation. For both SPV, weighted and unweighted, the addition of the cells exhibiting a new place field in the probe arena show either no (weighted) or just little (averaged) difference in the correlation values.

In general, the weighted SPV exhibit a higher correlation (Pearson's r = 0.92, fig) than the averaged SPV (Pearson's r = 0.89, fig)

6 DISCUSSION

6.1 Symmetry Method

As it has been shown that place fields can repeat in physically and contextual similar areas (93; 94). The symmetry method (see: 4.19 Symmetry method), created in this work has been demonstrated to be an excellent tool to measure contextual changes within a physical symmetric arena by describing the evenness of place field distributions. This method can also be applied when it is needed to describe the preferred location of place fields in terms of weights toward one half of the arena. A comparison with a COM-based measure (COM-distance) (Figure 5-3) showed a high correlation ($r = 0.91$, $p < 0.001$). Being backed up by a well-established method like the centre of mass (80)(see: 2.10 Place cell firing analysis) shows the reliability of this method. However, COM-based methods show better results for open arenas. But for complex arenas, consisting out of narrow tracks along the borders of the arena, like the rectangular-shaped linear track, the symmetry method describes the distribution in terms of being weighted to one-half of the arena better (Figure 6-1), since the geometry of the arena does not play a role as long as it is symmetric.

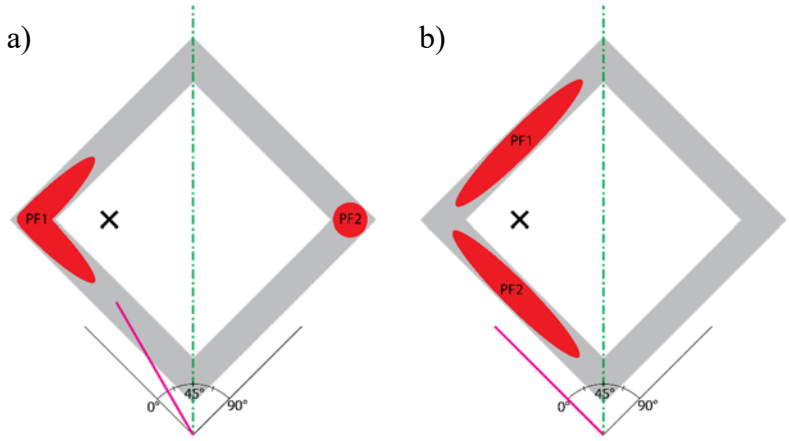

Figure 6-1: COM versus symmetry in a rectangular shaped track for two place fields in a) symmetric distribution b) non-symmetric distribution

At example in Figure 6-1 where the distribution of the two place fields (PF1, PF2, Figure 6-1) should be described as being distributed towards one-half where 0°/90° represents totally asymmetric distributions toward left/right half, and 45 ° represent a total even distribution. COM-related methods (x, Figure 6-1) for example the COM-distance (see: 4.20 COM-distance) are not able to distinguish between the two cases, while the symmetry method will give the right result.

6.2 Open field recording:

It is known that reward and pleasure sensation can be evoked by the stimulation of the MFB (47) or the VTA (113; 99). Here we used both types of stimulation to evaluate the direction of place field remapping by applying discrete stimulation events at specific locations in the proximity of the place field. We can observe a significant shift of the centre of mass (COM) between the first and the second baseline session for VTA stimulation (6.96 ±1.21 cm, n=3 rats, 17 cells) (Figure 5-4) and a significant shift of COM between the first baseline and the second stimulation session for MFB stimulation (4.72 ± 2.94 cm, n = 5 rats, 18 cells) while no significant shift could be observed for the control group (2.51 ± 0.5 cm, n = 3 rats, 16 cells) (Figure 5-5 a). Since none of the non-location dependent properties show any significant difference between the sessions, it is clear that the remapping purely affects the location of the place field and no other property. The COM-shift is paralleled by a significant increase of the ratio Bhattacharyya distance between baseline and sessions succeeding the first stimulation session for both, VTA and MFB stimulation but not for the control (Figure 5-5 b). Those two properties showed a significant correlation (ChR2: Pearson's r = 0.36, $p < 0.05$; MFB: Pearson's r = 0.37, $p < 0.05$) (Figure 5-6). An increase in the ratio of Bhattacharyya distances is equivalent to an increase of overlap between the ratemap and artefact map. This implies a shift of the place field towards the stimulation location (Figure 6-2).

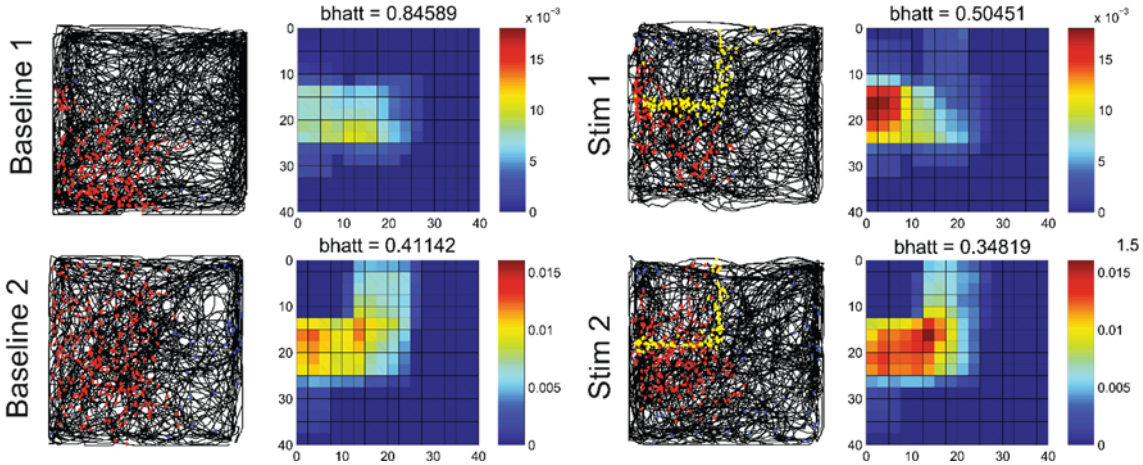

Figure 6-2: Spike/path map (red dots: spikes within the place field, blue dots: spike outside place field, yellow dots: stimulation events) and map of the overlay between rate and artefact map for baseline 1, stimulation1 (VTA), baseline 2, stimulation 2 (VTA) session

We can see that unselective stimulation of the medial forebrain bundle, which contains dopaminergic neurons from the VTA, show the same effect, but with a lower magnitude. This decrease in magnitude could be explained by the unselective nature of electrical stimulation. Since stimulation of non-dopaminergic neurons in the MFB might lead to

parasitic effects. The MFB consists of 30% GABAergic neurons, which have been found to modulate the associative learning via cholinergic interneurons, or locally inhibit dopaminergic projections (114). Several works reported a remapping of place fields towards a goal location (11; 42), where the remapping towards the goal location is a result of the reverse replay of the trajectory while resting at the reward location (115; 116). This, however, does not apply here since, due to the pellet chasing task, no fixed goal location can be identified, and the rat did not rest during the recording. Also, directional plasticity cannot account for the COM shift since at random locomotion in an open arena the firing of hippocampal place cells is statistically directionally independent (106). It is shown that optogenetic or electric activation of the dopaminergic projections of the VTA reliably can induce significant remapping of a place field and that the direction of remapping is significantly biased toward the location of increased dopaminergic activity (stimulation location) when the stimulation is frequently applied and close to the place field location. This implies that dopamine is the main driving force behind place field remapping. It seems like this dopamine-mediated remapping of place cell firing behaviour is the basis of long-term synaptic plasticity. This is backed by the widespread believe that long-term potentiation (LTP) is the physiological mechanism for memory and learning (117; 118), since dopamine is known to mediate LTP (51; 52; 119) and the blockade of D1 receptor inhibit LTP (120).

6.3 Rectangular-shaped linear track

Place aversive behaviour in rats can be induced by the stimulation of inhibitory projections to the VTA (49) or direct optogenetic suppression (48). We managed to induce a significant place aversion within two stimulation sessions by photo-inhibition of the dopaminergic neurons in the VTA.

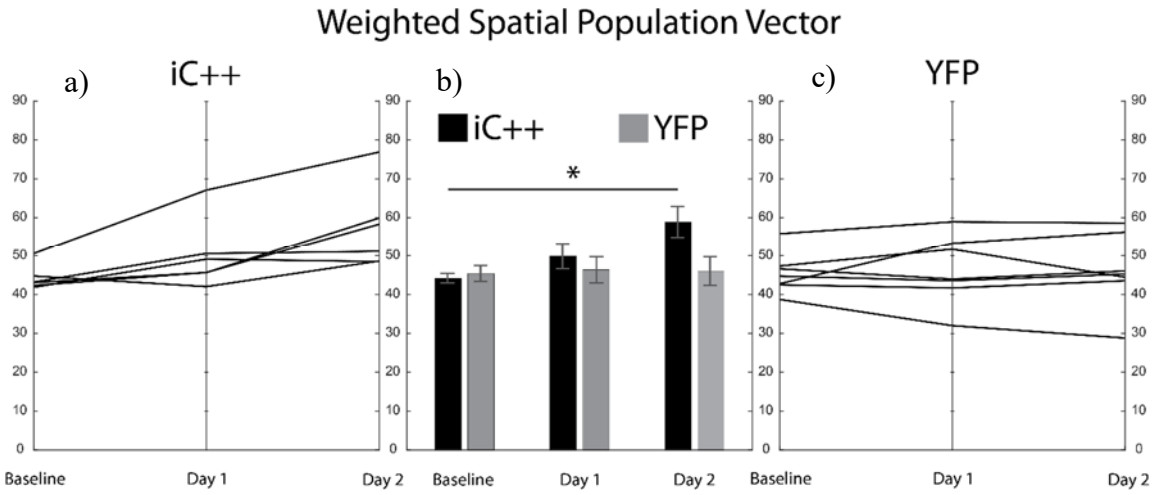

Figure 6-3: Weighted SPV, a) individual values for all iC++ subjects, b) mean values for iC++/ YFP group, c) individual values for all YFP subjects

We can see a significant shift of the weighted spatial population vector towards the NE half of the arena. This indicates a disrupted place field stability in the SW half of the arena, where the dopaminergic VTA neurons were suppressed, and as a result a biased firing distribution (Figure 6-3, Figure 6-4).

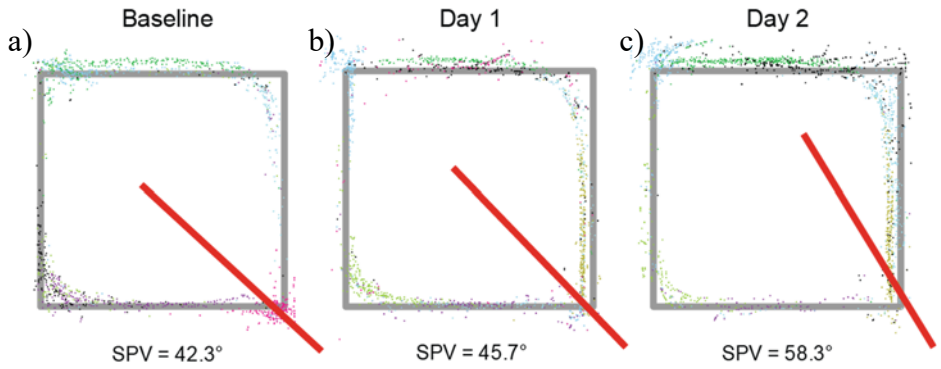

Figure 6-4: Spike map for hippocampal population of rat iC++_2 for a) baseline session, b) after 1 day, c) after 2 days, with SPV represented by red pointer

As we can see in Figure 6-5, the place cells exhibit defined place fields in each session, but the stability of the place fields between the sessions is impaired. This implicates that reason for remapping lies in the reduced ability to transfer this information from the short to the long term memory by long-term potentiation (LTP) (121; 122; 51). Several studies

have shown that LTP in the hippocampus is mediated by dopaminergic projection from the VTA (51; 119).

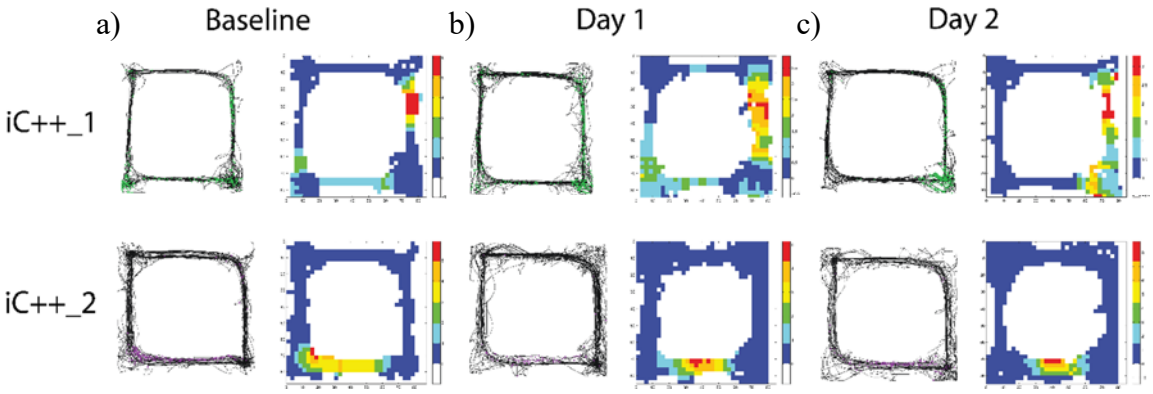

Figure 6-5: Exemplary spike/path and rate map for a) baseline session, b) after 1 day, c) after 2 days

Comparable results have been found in different studies were disrupted place field stability (4) and increased place field remapping (18) has been induced by fear conditioning. It is known that dopaminergic neurons of the VTA react with transient silencing to aversive stimuli (48; 123). In this experiment, the optogenetic suppression of the VTA has several effects. First, silencing of the transient firing of the dopaminergic projections from the VTA via the MFB to the nucleus accumbens (NAc) evokes an aversive behaviour (49; 48). Second, silencing of the dopaminergic projections from the VTA to the hippocampus inhibit the transition from short to long time memory by inhibiting LTP (51; 52; 119) which leads a decreased stability of the place fields due to a high rate of remapping in the SW half of the arena between the sessions. Third, the place cell activity is shifted towards areas with higher (non-suppressed) dopaminergic activity (see: 6.2 Open field recording).

6.4 T-maze

Since the level of illumination was set to an intensity where 50 % of the rats could identify the distal cues and use them for navigation, while 50% just relied on proximal cues. Being able to use both proximal and distal cues will cause a conflict between them (see: 4.10 Continuous T-maze). This resulted in two different navigation strategies. The animals of the preference group relied on the proximal cues for navigation and thus associated the east loop with a reward driven preference while the non-preference group due to a conflict between proximal and distal cues showed no significant preference towards the east or south loop. The preference is here clearly represented by the behaviour of the rat, where a place preference is indicated by an increased number of passes (Figure 6-6).

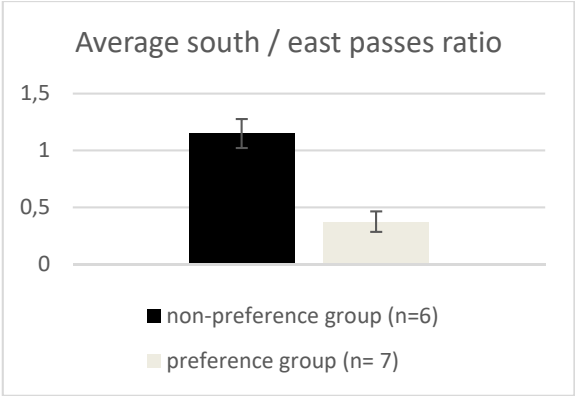

Figure 6-6: Average south/east passes ratio for non-preference and preference group

The symmetry of the sub-fields of each place cell across the midline of the T-maze (see: 4.19 Symmetry method) and evaluated its preferred position which was expressed by the symmetry angle. It can be seen that the preference group showed significantly fewer repetitions than non-preference group (Figure 6-7 a), where a bias of the preferred place field-location toward the preferred loop is in evidence.

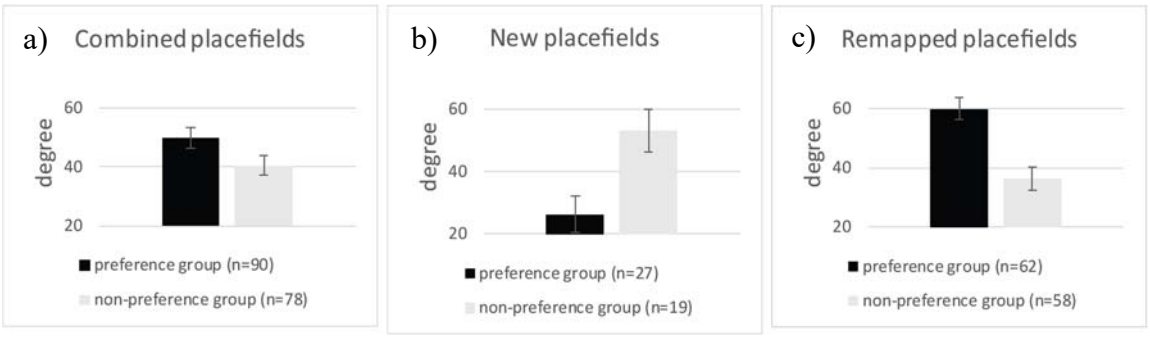

Figure 6-7: Average symmetry angles for a) combined place fields, b) new place fields, c) remapped place fields

As we can see the average symmetry values of the place cells gaining, new place fields behave contrarily. This might be explained by partial remapping or reduced remapping. It is known that different place cells can encode distinct sets of cues (9) and that a significant subpopulation of place cells appear to fire depending on additional factors than just on the pure location (3). If we assume that most of the cells gaining a new field would have exhibited a place field in the north loop of the training arena, and those cells encoding exclusively the location based on the proximal and distal cues, they would rotationally remap according to the rotation of the cues. For the preference group, this would mean the cells encoding proximal cues would keep their positions with respect to the cues. While cells, encoding distal cues, due to the vanishing of the cue, would either unpredictably remap, follow the proximal cues or vanish (35; 124) and thus show a strong bias in the symmetry towards the south quadrant. At the non-preference group, the place fields will rotationally remap according to the encoded cue (124). This will in average

result in a more even distribution of place fields, which result in a higher mean symmetry value (symmetry angle closer to 45°). According to this assumption, cells that gained new place fields carry low information about preferences. As we can see the average symmetry angle of the remapped cells represents better the preference of the rats towards the east loop. As it can be seen in fig, the weighted distribution of the whole population of place cells is biased towards the preferred east loop for the preference group, while as expected the non-preference group shows no remarkable bias.

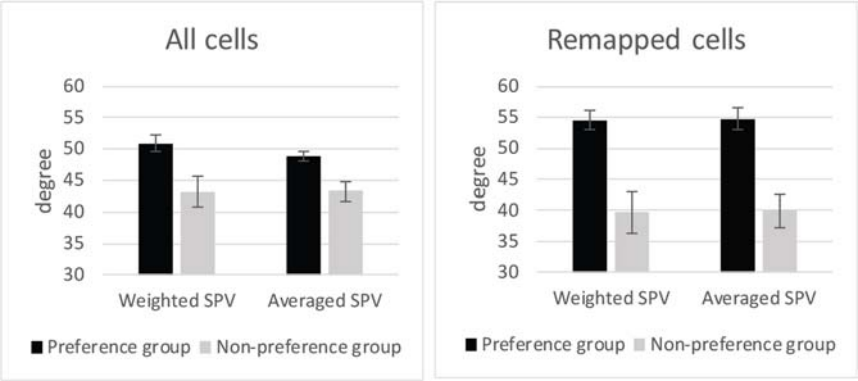

Figure 6-8: weighted and averaged SPV for a) all cells, b) remapped cells

Knowing that place cells can exhibit place fields at places of frequently performed actions (73), the strong correlation between pass ratio and spatial population vector may lead to the assumption that the SPV bias is caused by repeated actions or experiences in the different loops. Since the experiment is designed to be entirely equal between the two loops and no task has to be performed in the loop, the only repeated action is the act of turning toward the east or south half. Other experiments using a continuous T-maze have shown that the firing behaviour of a considerable amount of place cells was affected by this action (20; 125). However, since the place fields of those cells are reported to be located on the stem of the T-maze, they would have biased the SPV towards the midline and not towards one loop. Thus the SPV is correlated to the preference expressed by the ratio of passes between the south and the east loop. It has been shown in various experiments (74; 40; 37; 41) that place fields can be shifted towards a reward or goal location. This links two components of episodic memory together: the what and where. However, this change of firing behaviour in former studies was always done by remapping due to manipulation of the arena or presentation of specific stimuli, or task dependent firing. Here, context-dependent learning leads to a sustainable place preference in a novel environment which is not driven by specific stimuli. The place preference, which is indicated by the rat's behaviour in the arena, is clearly reflected by the firing

distribution of the hippocampal place cell ensemble, represented by the spatial population vector. This clearly shows, that the activity of place cells on a population level exhibit characteristic of episodic-like memory.

7 CONCLUTIONS

In this work, it has been shown that place field remapping can be reliably triggered by frequent stimulation of the dopaminergic projections of the ventral tegmental area. It has been demonstrated that the directionality of that remapping is towards the site of stimulation which indicates dopamine-mediated synaptic plasticity as the underlying mechanism for spatial learning and memory. Congruent to that it was shown that the silencing of dopaminergic projections from the VTA disrupts place field stability and promotes remapping towards locations of higher dopaminergic activity. Finally, it was demonstrated that context-dependent learning results in an experience-dependant place preference in a structural and contextual symmetrical environment, which was encoded on the population level. This proves that hippocampal place cells not only code spatial information but also represent information regarding preferences and expected reward. To my knowledge, this is the first report of episodic-like memory characteristics of place cells.

8 LIST OF LITERATURE

1. *Explicit memory creation during sleep demonstrates a causal role of place cells in navigation.* **De Lavilléon, G., et al.** 18, 2015, Nature Neuroscience, S. 493–495.

2. **Georgopoulos, A., Schwartz, A. und Kettner, R.** Neuronal population coding of movement direction. *Science, 233(4771).* 1986, S. 1416–1419.

3. **Wood, E. R.** Place cells: a framework for episodic memory? [Buchverf.] K. J. Jeffery. [Hrsg.] Oxford Press. *The Neurobiology of Spatial Behaviour.* Oxford : s.n., 2003.

4. *Fear conditioning alters neuron-specific hippocampal place field stability via the basolateral amygdala.* **Donzis, E. J., Rennaker, R. L. und Thompson, L. T.** 1525, 2013, Brain Research, S. 16–25.

5. **Barnes, C. A., et al.** Comparison of spatial and temporal characteristics of neuronal activity in sequential stages of hippocampal processing. *Progress in brain research.* 1990, 83, S. 287–300.

6. *Place units in the hippocampus of the freely moving rat.* **O'Keefe, J.** 51, 1976, Exp Neurol , S. 78–109.

7. **Bostock, E., Muller, R. U. und Kubie, J. L.** Experience-dependent modifications of hippocampal place cell firing. *Hippocampus.* 1991, 1, S. 193–205.

8. **Shapiro, M. L., Tanila, H. und Eichenbbaum, H.** Cues that hippocampal place cells encode: dynamic and hierarchical representation of local and distal stimuli. *Hippocampus.* 1997, 7, S. 624–642.

9. **Tanila, H., Shapiro, M. L. und Eichenbaum, H.** Discordance of spatial representation in ensembles of hippocampal place cells. *Hippocampus.* 1997, 7, S. 613–23.

10. **Lever, C., et al.** Long-term plasticity in hippocampal place-cell representation of environmental geometry. *Nature.* 2002, Bd. 416, 6876, S. 90–4.

11. **Fyhn, M., et al.** Hippocampal remapping and grid realignment in entorhinal cortex. *Nature.* 2007, Bd. 446, (7132, S. 190–4.

12. **Mizumori, S.** Hippocampal place fields: A neural code for episodic memory? *Hippocampus.* 2006, Bd. 9, 16, S. 685–690.

13. **Smith, D. und Mizumori, S.** Hippocampal place cells, context, and episodic memory. *Hippocampus, 16(9).* 2006, S. 716–729.

14. **Smith, D. M. und Mizumori, S. J.** Learning-related development of context-specific neuronal responses to places and events: the hippocampal role in context processing. *J. Neurosci., 26(12).* 2006b, S. 3154-63.

15. *Accumulation of hippocampal place fields at the goal location in an annular watermaze task.* **Hollup, S., et al.** 21, 2001, J Neurosci, S. 1635–44.

16. **Lenck-Santini, P.-P. P., Save, E. und Poucet, B.** Evidence for a relationship between place-cell spatial firing and spatial memory performance. *Hippocampus, 11(4).* 2001, S. 377–90.

17. **Lenck-Santini, P.-P. P., et al.** Relationships between place cell firing fields and navigational decisions by rats. The Journal of neuroscienc : the official journal of the Society for Neuroscience, 22(20), 9035–47. *J. Neurosci. , 22(20).* 2002, S. 9035–47.

18. *Putting fear in its place: remapping of hippocampal place cells during fear conditioning.* **Moita, M. A., et al.** 24, 2004, J. Neurosci., S. 7015–23.

19. **Griffiths, D., Dickinson, A. und Clayton, N.** Episodic memory: what can animals remember about their past? *Trends Cogn Sci, 3(2).* 1999, S. 74–80.

20. **Wood, E. R., et al.** Hippocampal neurons encode information about different types of memory episodes occurring in the same location. *Neuron, 27(3),.* 2000, S. 623–33.

21. **Frank, L. M., Brown, E. N. und Wilson, M.** Trajectory encoding in the hippocampus and entorhinal cortex. *Neuron, 27(1).* 2000, S. 169–78.

22. **Young, B. J., Fox, G. D. und Eichenbaum, H.** Correlates of hippocampal complex-spike cell activity in rats performing a nonspatial radial maze task. *J. Neurosci. 14.* 1994, S. 6553–63.

23. *The dopaminergic mesencephalic projections to the hippocampal formation in the rat.* **Garisbarri, A., Sulli, A. and Packard, M. G.** 21, 1997, pp. 1-22.

24. *Dopaminergic neurons promote hippocampal reactivation and spatial memory persistence.* **McNamara, C., et al.** 17, 2014, Nat Neurosci, S. 1658–1660.

25. **O'Keefe, J. und Dostrovsky, J.** The hippocampus as a spatial map. Preliminary evidence from unit activity in the freely-moving rat. *Brain Research, 34(1).* 1971, S. 171–175.

26. *Dynamics of the hippocampal ensemble code for space.* **Wilson , M. A. und McNaughton, B. L.** 261, 1993, Science, S. 1055–8.

27. *Spatial firing patterns of hippocampal complex-spike cells in a fixed environment.* **Muller, R. U., Kubie, J. L. und Ranck, J.** 7, 1987, J. Neurosci., S. 1935–50.

28. **Thompson,, L. T. und Best, P. J.** Long-term stability of the place-field activity of single units recorded from the dorsal hippocampus of freely behaving rats. *Brain research, 509(2).* 1990, S. 299–308.

29. **Thompson, L. T. und Best, P. J.** Place cells and silent cells in the hippocampus of freely-behaving rats. *J. Neurosci., 9(7).* 1989, S. 2382–90.

30. **O'Keefe, J. und Nadel, L.** *Hippocampus as a Cognitive Map. (Oxford: Clarindon).* Oxford : Clarendon Press, 1978.

31. **O'Keefe, J., et al.** Place cells, navigational accuracy, and the human hippocampus. *Philos. Trans. R. Soc. Lond., B, Biol. Sci., 353(1373).* 1998, S. 1333–40.

32. **O'Keefe, J. und Recce, M.** Phase relationship between hippocampal place units and the EEG theta rhythm. *Hippocampus 3.* 1993, S. 317–30.

33. **O'Keefe, J. und Conway, D. H.** Hippocampal place units in the freely moving rat: why they fire where they fire. *Exp Brain Res., 31(4).* 1978, S. 573-90.

34. **O'Keefe, J. und Speakman, A.** Single unit activity in the rat hippocampus during a spatial memory task. *Exp Brain Res., 68(1).* 1987, S. 1-27.

35. *The effects of changes in the environment on the spatial firing of hippocampal complex-spike cells.* **Muller, R. U. und Kubie, J. L.** 7, 1987, J. Neurosci. 7, S. 1951–68.

36. **Muller, R.** A quarter of a century of place cells. *Neuron 17 .* 1996, S. 813–22.

37. **Hok, V., et al.** Goal-Related Activity in Hippocampal Place Cells. *J. Neurosci., 27(3).* 2007, S. 472– 482.

38. **Hok, V., et al.** Prefrontal Cortex Focally Modulates Hippocampal Place Cell Firing Patterns. *J. Neurosci, 33(8).* 2013, S. 3443–3451.

39. **Rossier, J., et al.** The place preference task: a new tool for studying the relation between behavior and place cell activity in rats. *Behavioral neuroscience, 114(2).* 2000, S. 273–84.

40. *Hippocampal place cells: stereotypy and plasticity.* **Breese, C. R., Hampson, R. E. und Deadwyler, S. A.** 9, 1989, J. Neurosci., S. 1097–111.

41. *The reorganization and reactivation of hippocampal maps predict spatial memory performance.* **Dupret, D., et al.** 13, 2010, Nat. Neurosci., S. 995–1002.

42. **Kobayashi, T., et al.** Contribution of hippocampal place cell activity to learning and formation of goal-directed navigation in rats. *Neuroscience 117.* 2003, S. 1025–35.

43. **Trepel, M.** *Neuroanatomie, 3rd edition.* München Jena : Urban & Fischer, 2003.

44. **Wenzel, J. M., et al.** A role for phasic dopamine release within the nucleus accumbens in encoding aversion: a review of the neurochemical literature. *ACS Chem Neurosci.* 16-26 2015, S. 6.

45. **Routtenberg, A. und Lindy, J.** Effects of availability of rewarding septal and hypothalamic stimulation on bar pressing for food under conditions of deprivation. *J. Comp. Physiol. Psychol. 60.* 1965, S. 150–161.

46. **Carlisle, H. J. und Snyder, E.** The interaction of hypothalamic self-stimulation and temperature regulation. . *Experientia 26 .* 1970, S. 1092–1093.

47. **Carlezon, W. A. und Chartoff, E. H.** Intracranial self-stimulation (ICSS) in rodents to study the neurobiology of motivation. *Nature protocols, 2(11).* 2007, S. 2987–95.

48. **Danjo, T., et al.** Aversive behavior induced by optogenetic inactivation of ventral tegmental area dopamine neurons is mediated by dopamine D2 receptors in the nucleus accumbens. *P Natl Acad Sci Usa.* 6455-60 2014, S. 111.

49. *Input-specific control of reward and aversion in the ventral tegmental area.* **Lammel, S., et al.** 491, 2012, Nature, S. 212–217.

50. *A Unique Population of Ventral Tegmental Area Neurons Inhibits the Lateral Habenula to Promote Reward.* **Stamatakis, A. M., et al.** 80, 2013, Neuron, S. 1039-1053.

51. *The hippocampal-VTA loop: controlling the entry of information into long-term memory.* **Lisman, J. und Grace, A.** 46, 2005, Neuron, S. 703–13.

52. **Ghanbarian, E. und Motamedi, F.** Ventral tegmental area inactivation suppresses the expression of CA1 long term potentiation in anesthetized rat. *PloS one, 8(3).* 2013, S. e58844.

53. **Guru, A., et al.** Making sense of optogenetics. *Int. J. Neuropsychopharmacol., 18(11).* 2015, S. pyv079.

54. **Nagel, G., et al.** Channelrhodopsin-1: a light-gated proton channel in green algae. *Science, 296(5577).* 2002, S. 2395–8.

55. **Nagel, G., Szellas, T. und Huhn, W.** Channelrhodopsin-2, a directly light-gated cation-selective membrane channel. *Proc. Natl. Acad. Sci. USA, 100(24).* 2003, S. 13940-13945.

56. **Lin, J. Y.** A user's guide to channelrhodopsin variants: features, limitations and future developments. *Experimental physiology, 96(1).* 2011, S. 19–25.

57. **Berndt, A., et al.** Structure-guided transformation of channelrhodopsin into a light-activated chloride channel. *Science, 344(6182).* 2014, S. 420–4.

58. **Fenno, L. E., et al.** Targeting cells with single vectors using multiple-feature Boolean logic. *Nature methods, 11(7).* 2014, S. 763–72.

59. **Zhang, F., et al.** Multimodal fast optical interrogation of neural circuitry. *Nature, 446(7136).* 2007, S. 633–639.

60. **Tulving, E.** Episodic and semantic memory. [Buchverf.] E. Tulving und W. Donaldson. [Hrsg.] Academic Press. *Organization of Memory.* New York : s.n., 1972.

61. *General and specific brain regions involved in encoding and retrieval of events: what, where, and when.* **Nyberg, L., et al.** 93, 1996, PNAS , S. 11280–5.

62. **Clayton, N. S., Bussey, T. J. und Dickinson, A.** Can animals recall the past and plan for the future? *Nature reviews. Neuroscience, 4(8).* 2003, S. 685–91.

63. **Clayton, N. S. und Dickinson, A.** Episodic-like memory during cache recovery by scrub jays. *Nature, 395(6699).* 1998, S. 272–274.

64. **Babb, S. J. und Crystal, J. D.** Episodic-like memory in the rat. *Curr. Biol. 16.* 2006, S. 1317–21.

65. **Scoville, W. B. und Mildner , B.** Loss of recent memory after bilateral hippocampal lesions. *J. Neurol. Neurosurg. Psychiatry, 20(1).* 1957, S. 11–21.

66. **Zola-Morgan, S., Squire, L. und Amaral, D.** Human amnesia and the medial temporal region: enduring memory impairment following a bilateral lesion limited to field CA1 of the hippocampus. *J. Neurosci ., 6(10).* 1986, S. 2950-67.

67. **Suddendorf, T. und Corballis, M.** The evolution of foresight: What is mental time travel, and is it unique to humans? *Behavioral and Brain Sciences, 30(03).* 2007, S. 299-313.

68. **Weiler, J., Suchan, B. und Daum, I.** Foreseeing the future: Occurrence probability of imagined future events modulates hippocampal activation. *Hippocampus, 20(6).* 2010, S. 685–690.

69. **Wood, E. R. und Macdonald, S. H.** Effects of interference on olfactory recognition memory in rats with hippocampal lesions. . *Society For Neuroscience Abstracts. 27(1).* 2001, S. 499.

70. **Moser, E., Moser, M. B. und Andersen, P.** Spatial learning impairment parallels the magnitude of dorsal hippocampal lesions, but is hardly present following ventral lesions. *J. Neuroscience, 13(9).* 1993, S. 3916-25.

71. **Kesner, R., Hunsaker, M. und Ziegler, W.** The role of the dorsal CA1 and ventral CA1 in memory for the temporal order of a sequence of odors. *NEUROBIOL LEARN MEM, 93(1).* 2010, S. 111–116. doi:.

72. **O'Keefe, J.** A review of the hippocampal place cells. *Prog Neurobiol., 13(4).* 1979, S. 419-39.

73. **Eichenbaum, H., et al.** The hippocampus, memory, and place cells: is it spatial memory or a memory space? *Neuron 23.* 1999, S. 209–26.

74. *Binding of hippocampal CA1 neural activity to multiple reference frames in a landmark-based navigation task .* **Gothard, K. M., et al.** 16, 1996, J. Neurosci., S. 823-35.

75. **Wood, E. R., Dudchenko, P. A. und Eichenbaum, H.** The global record of memory in hippocampal neuronal activity. *Nature, 397(6720).* 1999, S. 613–6.

76. **Ainge, J. A., et al.** Hippocampal CA1 place cells encode intended destination on a maze with multiple choice points. *J. neurosci., 27(36).* 2007, S. 9769-79.

77. **Ramierez, S., et al.** Creating a false memory in the hippocampus. *Science, 341(6144).* 2013, S. 387–91.

78. **Redondo, R., et al.** Bidirectional switch of the valence associated with a hippocampal contextual memory engram. *Nature, 513(7518).* 2014, S. 426–430.

79. **Shepard, D.** A two-dimensional interpolation function for irregularly-spaced data. *Proceedings of the 1968 23rd ACM national conference .* 1968, S. 517–524.

80. **Fenton, A. A., Csizmadia, G. und Muller, R. U.** Conjoint control of hippocampal place cell firing by two visual stimuli I. The effects of moving the stimuli on firing field positions. *J. Gen. Physiol., 116(2) .* 2000, S. 191-210 .

81. **Muller, R. U. und Kubie, J. L.** The firing of hippocampal place cells predicts the future position of freely moving rats. *J Neurosci., 9(12).* 1989, S. 4101-10.

82. **Hok, V., et al.** Hippocampal Dynamics Predict Interindividual Cognitive Differences in Rats. *J. Neurosci., 32(10).* 2012, S. 3540–3551.

83. **Skaggs, W., et al.** An information-theoretic approach to deciphering the hippocampal code. *Proceeding Advances in Neural Information Processing Systems 5.* 1993, S. 1030-1037.

84. **Fenton, A. A., et al.** Unmasking the CA1 ensemble place code by exposures to small and large environments: more place cells and multiple, irregularly arranged, and expanded place fields in the larger space. *J. Neurosci. 28.* 2008, S. 11250–62.

85. **Colgin, L. L., et al.** Attractor-Map Versus Autoassociation Based Attractor Dynamics in the Hippocampal Network. *Journal of Neurophysiology, 104(1).* 2010, S. 35–50.

86. **Georgopoulos, A. P., Kettner, R. E. und Schwartz, A.** Primate motor cortex and free arm movements to visual targets in three-dimensional space. II. Coding of the direction of movement by a neuronal population. The Journal of neuroscienc : the off. *J. Neurosci., 8(8).* 1988, S. 2928-37.

87. **Leutgeb, J., et al.** Progressive Transformation of Hippocampal Neuronal Representations in “Morphed” Environments. . *Neuron, 48(2).* 2005, S. 345–358.

88. **Leutgeb, S., et al.** Independent codes for spatial and episodic memory in hippocampal neuronal ensembles. *Science, 309(5734).* 2005b, S. 619–23.

89. **Ferbinteanu, J., Shirvalkar, P. und Shapiro, M. L.** Memory modulates journey-dependent coding in the rat hippocampus. *J. Neurosci., 31(25).* 2011, S. 9135–46.

90. **Kennedy, P. J. und Shapiro, M. L.** Motivational states activate distinct hippocampal representations to guide goal-directed behaviors. *Proc. Natl. Acad. Sci. USA, 106(26).* 2009, S. 10805–10.

91. **Bhattacharyya, A.** On a measure of divergence between two multinomial populations. *Sankhyā: the indian journal of statistics, 7(4) .* 1946, S. 401-406.

92. **Aherne, F. J, Thacker, N. A. und Rockett, P. I.** The Bhattacharyya metric as an absolute similarity measure for frequency coded data. *Kybernetika, 34, 4.* 1997, S. 363-368.

93. **Spiers, H., et al.** Place Field Repetition and Purely Local Remapping in a Multicompartment Environment. *Cereb Cortex 25.* 2015, S. 10–25.

94. **Grieves, R. M., et al.** Place field repetition and spatial learning in a multicompartment environment. *Hippocampus 26.* 2016, S. 118–34.

95. **Cantwell, B. J.** *Introduction to symmetry analysis.* Cambridge : Cambridge University Press, 2004.

96. **Kiryati, N. und Gofman, Y.** Detecting symmetry in grey level images: The global optimization approach. *INT J COMPUT VISION, 29(1).* 1998, S. 29–45.

97. **Mamad, O, et al.** Place field assembly distribution encodes episodic-like memory. unpublished.

98. **Witten, I., et al.** Recombinase-Driver Rat Lines: Tools, Techniques, and Optogenetic Application to Dopamine-Mediated Reinforcement. *Neuron 72,.* 2011, S. 721–733.

99. **Tsai, H.-C. C., et al.** Phasic firing in dopaminergic neurons is sufficient for behavioral conditioning. *Science, 324.* 2009, S. 1080–4.

100. **Mamad, O., et al.** Medial septum regulates the hippocampal spatial representation. *Front Behav Neurosci., 30(9).* 2015, S. 166.

101. **Dragoi, G., Harris, K. und Buzsáki, G.** Place representation within hippocampal networks is modified by long-term potentiation. *Neuron 39.* 2003, S. 843–53.

102. **Tsao, A., Moser, M. B. und Moser, E. I.** Traces of experience in the lateral entorhinal cortex. *Current biology, 23.* 2013, S. 399-405.

103. **Tsanov, M., et al.** Theta-modulated head direction cells in the rat anterior thalamus. *J. Neurosci. 31.* 2011, S. 9489–502.

104. **Passino, E., et al.** Genetic approach to variability of memory systems: analysis of place vs. response learning and fos-related expression in hippocampal and striatal areas of C57BL/6 and DBA/2 mice. *Hippocampus 12.* 2002, S. 63–75.

105. **Gaffan, E. A., Bannerman, D. M. und Healey, A. N.** Learning associations between places and visual cues without learning to navigate: neither fornix nor entorhinal cortex is required. *Hippocampus 13.* 2003, S. 445–60.

106. **Navratilova, Z., et al.** Experience-dependent firing rate remapping generates directional selectivity in hippocampal place cells. *Front Neural Circuits 6.* 2012, S. 6.

107. **Brun, V. H., et al.** Place Cells and Place Recognition Maintained by Direct Entorhinal-Hippocampal Circuitry. *Science, 296(5576).* 2002, S. 2243–2246.

108. **Quirk, G., Muller, R. und Kubie, J.** The firing of hippocampal place cells in the dark depends on the rat's recent experience. *J. Neurosci., 10.* 1990, S. 2008–17.

109. **Sharp, P., Green, C., 1994., Sharp, P. und Green, C.** Spatial correlates of firing patterns of single cells in the subiculum of the freely moving rat. *J. Neurosci., 14.* 1994, S. 2339–56.

110. **MathWorks, The.** Corrcoef. [Online] 1994. [Zitat vom: 8. Aug 2016.] http://uk.mathworks.com/help/matlab/ref/corrcoef.html.

111. **Gross, D.** schwerpunkt . *Formeln und Aufgaben zur Technischen Mechanik 1.* 10th. s.l. : Springer-Verlag Berlin Heidelberg, 2011, S. 32-33.

112. **Kazakos, D.** The Bhattacharyya distance and detection between Markov chains. *IEEE Transactions on Information Theory, 24(6).* 1978, S. 747–754.

113. **Fibiger, H., et al.** The role of dopamine in intracranial self-stimulation of the ventral tegmental area. *J. Neurosci., 7, 3888–96.* 1987, S. 3888–96.

114. **Creed, M. C, Ntamati, N. R. und Tan,, K. R.** VTA GABA neurons modulate specific learning behaviors through the control of dopamine and cholinergic systems. . *Front Behav Neurosci 8.* 2014, S. 8.

115. **Foster, D. J. und Wilson, M. A.** Reverse replay of behavioural sequences in hippocampal place cells during the awake state. *Nature 440.* 2006, S. 680–3.

116. *Neural Network Model of Forward Shift of CA1 Place Fields Towards Reward Location.* **Ponzi, A.** [Hrsg.] M. Ishikawa. Kitakyushu : Springer-Verlag Berlin Heidelberg, 2008. Neural Information Processing: 14th International Conference, ICONIP 2007. S. 309–316.

117. *Long-term potentiation and the mechanisms of memory. .* **Izquierdo, I.** 30, 1993, Drug Development Research, S. 1–17.

118. *Storage of spatial information by the maintenance mechanism of LTP.* **Pastalkova, E., et al.** 313, 2006, Science, S. 1141–4.

119. **Rosen, Z.B.** Dopaminergic control of hippocampal neural circuitry. Columbia University, New York City. New York : PhD thesis, Columbia University, 2013.

120. **Granado, N., et al.** D1 but not D5 Dopamine Receptors Are Critical for LTP, Spatial Learning, and LTP-Induced arc and zif268 Expression in the Hippocampus. *Cereb Cortex 18.* 2008, S. 1–12.

121. **Agnihotri, N. T. und Hawkins, R. D.** The long-term stability of new hippocampal place fields requires new protein synthesis. . *Proc. Natl. Acad. Sci. U.S.A, 101.* 2004, S. 3656–3661.

122. **Knierim, J. J.** Hippocampal remapping: implikations for spatial learning and navigation. [Buchverf.] K. J. Jeffery. *The Neurobiology of Spatial Behaviour.* Oxford : Oxford Press, 2003.

123. **Tan, K., et al.** GABA neurons of the VTA drive conditioned place aversion. *Neuron 73.* 2012, S. 1173–83.

124. **Knierim, J.** Dynamic interactions between local surface cues, distal landmarks, and intrinsic circuitry in hippocampal place cells. *J. Neurosci., 22.* 2002, S. 6254–64.

125. **Lee, I., Rao, G., Knierim, J.,.** A Double Dissociation between Hippocampal Subfields Differential Time Course of CA3 and CA1 Place Cells for Processing Changed Environments. *Neuron.* 2004, 42, S. 803–815.